UNIVERSIDADE FEDERAL DO RIO GRANDE DO SUL

INSTITUTO DE CIÊNCIAS BÁSICAS DA SAÚDE

DEPARTAMENTO DE FISIOLOGIA

PROGRAMA DE PÓS-GRADUAÇÃO EM CIÊNCIAS BIOLÓGICAS: NEUROCIÊNCIAS

EFEITO DA SECÇÃO DO NERVO ISQUIÁTICO SOBRE PARÂMETROS ULTRAESTRUTURAL, HISTOQUÍMICO, IMUNOISTOQUÍMICO E DE CAPTAÇÃO DE ANÁLOGOS DA GLICOSE EM GÂNGLIO DA RAIZ DORSAL DE RÃS *Lithobates catesbianus*

TESE DE DOUTORADO

FABIANA RIGON

PORTO ALEGRE, 2013

EFEITO DA SECÇÃO DO NERVO ISQUIÁTICO SOBRE PARÂMETROS ULTRAESTRUTURAL, HISTOQUÍMICO, IMUNOISTOQUÍMICO E DE CAPTAÇÃO DE ANÁLOGOS DA GLICOSE EM GÂNGLIO DA RAIZ DORSAL DE RÃS *Lithobates catesbianus*

FABIANA RIGON

TESE SUBMETIDA AO PROGRAMA DE PÓS-GRADUAÇÃO EM CIÊNCIAS BIOLÓGICAS: NEUROCIÊNCIAS, ICBS, UNIVERSIDADE FEDERAL DO RIO GRANE DO SUL, COMO REQUISITO PARCIAL À OBTENÇÃO DO GRAU DE DOUTOR EM NEUROCIÊNCIAS.

ORIENTADORA: PROFA. DRA. WANIA APARECIDA PARTATA
CO-ORIENTADORA: PROFA. DRA. MARIA CRISTINA FACCIONI-HEUSER

PORTO ALEGRE, RS, 2013

Dedico esse trabalho a minha

mãe Maria e ao meu pai Danilo.

AGRADECIMENTOS

À profa. Dra. Wania Aparecida Partata, minha orientadora, pela acolhida em seu laboratório, pelo incentivo, conselhos, apoio e por sua competência que possibilitaram meu aperfeiçoamento e enriquecimento profissional.

À profa. Dra. Maria Cristina Faccioni-Heuser, co-orientadora, por suas sugestões, amizade, generosidade e sabedoria.

Ao meu esposo Alexandre Futterleib pelo seu carinho, compreensão e companheirismo.

À colega/amiga "Tuti" pelas longas histórias, desabafos, conselhos, saídas e festas.....por ser a responsável de eu estar hoje com meu grande companheiro e ser a minha "dinda".

Aos colegas/amigos do laboratório, por todos os momentos de alegria e tristeza e pelas histórias regadas à café passado na hora e comidinhas da tia Ritinha.

À tia Ritinha que não me deixou passar fome.

À Christiane Lopes e à Moema Queiroz por todo auxílio prestado.

Ao Centro de Microscopia Eletrônica da UFRGS pela utilização do microscópio.

À coordenadora do Curso de Fisioterapia Jucélia Fátima da Silva Güths pelo seu apoio e compreensão.

Muito Obrigada

Quando me amei de verdade, compreendi que em qualquer circunstância, eu estava no lugar certo, na hora certa, no momento exato.
E então, pude relaxar.
Hoje sei que isso tem nome.... Auto-estima.
Quando me amei de verdade, pude perceber que minha angústia, meu sofrimento emocional, não passa de um sinal de que estou indo contra minhas verdades.
Hoje sei que isso é....Autenticidade.
Quando me amei de verdade, parei de desejar que a minha vida fosse diferente e comecei a ver que tudo o que acontece contribui para o meu crescimento.
Hoje chamo isso de.... Amadurecimento.
Quando me amei de verdade, comecei a perceber como é ofensivo tentar forçar alguma situação ou alguém apenas para realizar aquilo que desejo, mesmo sabendo que não é o momento ou a pessoa não está preparada, inclusive eu mesmo.
Hoje sei que o nome disso é.... Respeito.
Quando me amei de verdade comecei a me livrar de tudo que não fosse saudável... Pessoas, tarefas, tudo e qualquer coisa que me pusesse para baixo. De início minha razão chamou essa atitude de egoísmo.
Hoje sei que se chama.... Amor-próprio.
Quando me amei de verdade, deixei de temer o meu tempo livre e desisti de fazer grandes planos, abandonei os projetos megalômanos de futuro. .
Hoje faço o que acho certo, o que gosto, quando quero e no meu próprio ritmo.
Hoje sei que isso é... Simplicidade.
Quando me amei de verdade, desisti de querer sempre ter razão e, com isso, errei muitas menos vezes.
Hoje descobri a.... Humildade.
Quando me amei de verdade, desisti de ficar revivendo o passado e de preocupar com o futuro. Agora, me mantenho no presente, que é onde a vida acontece.
Hoje vivo um dia de cada vez. Isso é.... Plenitude.
Quando me amei de verdade, percebi que minha mente pode me atormentar e me decepcionar. Mas quando a coloco a serviço do meu coração, ela se torna uma grande e valiosa aliada.
Tudo isso é.... Saber viver!!!

Charles Chaplin

SUMÁRIO

APRESENTAÇÃO

Esta tese é o resultado da investigação do efeito da secção do nervo isquiático sobre parâmetros ultraestrutural, histoquímico, imunoistoquímico e de captação de análogos da glicose em gânglio da raiz dorsal de rãs *Lithobates catesbianus*. A tese está estruturada em seis capítulos, onde inicialmente se apresenta a introdução ao tema, que está organizada em cinco subitens de referencial teórico que abordam os achados relativos ao tema, provenientes da literatura científica atual. Em seguida, é apresentado o objetivo do estudo, dividido em dois subitens. No primeiro é mostrado o objetivo geral da tese e no segundo os objetivos específicos. No capítulo Material e Métodos e Resultados são apresentados três artigos científicos, que mostram os materiais e métodos usados e os resultados obtidos nos estudos. O primeiro artigo apresenta o efeito da secção do nervo isquiático sobre a ultraestrutura, a reação da nicotinamida adenina dinucleotídeo fosfato-diaforase (NADPH-diaforase) e a imunoistoquímica à serotonina, tirosina hidroxilase, c-Fos e transportadores de glicose dos tipos 1 e 3 no gânglio da raiz dorsal (DRG) de rãs *Rana catesbeiana*, que foi recentemente publicado no periódico *Brazilian Journal of Medical and Biological Research*. Os resultados detalhados da ultraestrutura, da reação à NADPH-diaforase e da imunoistoquímica à serotonina, tirosina hidroxilase e transportadores de glicose dos tipos 1 e 3 no DRG de rãs *Lithobates catesbianus* são mostrados no segundo artigo, que está neste momento sendo analisado pelo corpo editorial de um periódico da área. O terceiro artigo apresenta o efeito da secção do nervo isquiático sobre a captação de análogos da glicose e oxidação de lactato no DRG rãs *Lithobates catesbianus*, que foi aceito para publicação no periódico *Braziliam Journal of Biology*. No capítulo Discussão, os principais resultados dos três artigos científicos são discutidos em conjunto, amparados por achados da literatura. No quarto capítulo são apresentadas as conclusões deste trabalho de

doutorado, juntamente com as perspectivas de futuros estudos sobre o tema da tese. No último capítulo encontram-se as referências bibliográficas dos textos científicos consultados para a redação dos capítulos Introdução e Discussão. As referências bibliográficas dos artigos científicos são apresentadas ao final de cada trabalho.

RESUMO

As rãs são utilizadas como modelos experimentais em diferentes situações experimentais. Uma delas é o estudo dos efeitos da seção do nervo isquiático (SNI) sobre o tecido nervoso. Essa ampla utilização desses animais como modelos experimentais justifica a realização de estudos que visam o conhecimento morfofuncional de seus tecidos.

Inúmeros estudos mostram que, assim como nos mamíferos, o principal substrato energético no tecido nervoso de rãs é a glicose. Porém, é desconhecida a distribuição dos transportadores de glicose no tecido nervoso de rãs, bem como se a SNI altera esse transporte. Outra questão em aberto é se o lactato, cuja concentração está aumentada no plasma de rãs durante períodos de hibernação e após atividades motoras, é usado como substrato energético pelo tecido nervoso, o que está demonstrado em outras espécies de vertebrados.

É desconhecida ainda no gânglio da raiz dorsal (GRD) de rãs a distribuição e os efeitos da SNT sobre a reação à nicotinamida adenina dinucleotídeo fosfato diaforase (NADPH-diaforase), enzima considerada equivalente a óxido nítrico sintase, responsável pela síntese de óxido nítrico, e a reação ao ácido periódico-reativo de Schiff (PAS), que indica a presença de mucopolissarídeos, incluindo o glicogênio, uma importante reserva energética no tecido nervoso de rãs. Desconhece-se também a distribuição e os efeitos da SNT sobre a imunorreatividade à serotonina, importante molécula com função neurotransmissora e/ou moduladora no sistema nervoso, tirosina hidroxilase, enzima limitante na síntese de catecolaminas, moléculas com diversos papéis fisiológicos, incluindo ação neurotransmissora e/ou neuromoduladora no tecido nervoso, e c-Fos, proteína considerada marcadora de ativação neural por estimulação nociva.

Outras questões ainda em aberto são os efeitos da SNT sobre: a captação do análogo da glicose 1-[^{14}C] 2-deoxi-D-glicose (^{14}C-2-DG) e concentração plasmática de glicose e lactato; se os tipos II e III de células gliais satélites (CGSs), recentemente descritas no GRD de coelho, estão presentes nesse gânglio de rãs; e os efeitos da SNT sobre a ultraestrutura de CGSs e neurônios do GRD. Assim, o objetivo dessa tese foi determinar: 1) a ultraestrutura de neurônios e CGSs; 2) a distribuição das reações à NADPH-diaforase e PAS, e a imunoistoquímica à serotonina, tirosina hidroxilase, c-Fos e transportadores de glicose tipo 1 e 3; e 3) a captação de ^{14}C-2-DG, na presença e ausência de lactato, em GRD de rãs *Lithobates catesbianus* com e sem SNI. A escolha pelos transportadores de glicose tipos 1 e 3 foi pelo fato de ocorrerem na membrana de endotélio, células gliais e de neurônios.

Para a realização do estudo inicialmente 12 rãs *Lithobates catesbianus*, adultas, machos, com peso de 100-200g, que não sofreram qualquer manipulação cirúrgica foram mortas por decapitação e os gânglios das raízes dorsais (GRDs) do nervo isquiático retirados e preparados para análises ultraestrutural, histoquímica à NADPH-diaforase e PAS, e imunoistoquímica à serotonina, tirosina hidroxilase e transportadores de glicose dos tipos 1 e 3. Feito isso, 18 outras rãs, nas mesmas condições físicas, foram divididas em três grupos experimentais (n=6/grupo): controle (rãs que não sofreram

qualquer manipulação cirúrgica), sham (rãs onde foram efetuados apenas os procedimentos para isolamento do nervo isquiático) e SNI (rãs que tiveram o nervo isquiático direito totalmente seccionado em seu tronco comum). Esses animais foram mortos três dias após a intervenção cirúrgica e seus GRDs do nervo isquiático usados para demonstrar os efeitos da secção nervosa sobre a ultraestrutura, a reação à NADPH-diaforase, e a imunoistoquímica à serotonina, tirosina hidroxilase, c-Fos e transportadores de glicose dos tipos 1 e 3 no GRD. Outros 20 animais, divididos nos mesmos grupos experimentais, foram usados para demonstrar os efeitos da SNI sobre a captação de ^{14}C-2-DG, na presença ou ausência de lactato, e a taxa de produção de $^{14}CO_2$ a partir de ^{14}C-L-lactato e de ^{14}C-glicose no GRD. Essas rãs foram usadas ainda para demonstrar os efeitos da denervação periférica sobre a concentração plasmática de glicose e lactato.

Nossos resultados mostraram que os neurônios sensoriais do GRD de rã *Lithobates catesbianus* tiveram distribuição, diâmetro e morfologia que foi similar àquela descrita para essas células em gânglio de mamíferos. As CGSs apresentaram morfologia similar àquela descrita para essas células em gânglios de outras espécies de vertebrados. As células dos tipos II e III, observadas no GRD de coelho, não ocorreram no GRD de *Lithobates catesbianus*. O padrão de atividade à NADPH-diaforase e a distribuição da imunorreatividade à serotonina, tirosina hidroxilase e Glut 1 e 3 foram também similares ao descrito em mamíferos. Pela primeira vez foi demonstrada, em anfíbios, a presença de reação à NADPH-diaforase em CGCs do GRD. A captação de ^{14}C-2-DG foi reduzida quando o lactato foi acrescentado ao meio de incubação. As alterações induzidas pela SNI foram também similares àquelas descritas nos mamíferos. Houve acréscimo no número de mitocôndrias, retículo endoplasmático, ribossomas e filamentos no citoplasma das CGSs, mais neurônios e CGCs com reação positiva à NADPH-diaforase, um maior número de prolongamentos imunorreativos à tirosina hidroxilase em torno de somas de neurônios sensoriais, e mais núcleos neuronais imunorreativos a c-Fos. Nenhuma alteração ocorreu na imunorreatividade a serotonina e transportadores de glicose. Houve aumento na captação de ^{14}C-2-DG, que foi reduzido quando o lactato foi acrescentado ao meio de incubação. Porém, a formação de $^{14}CO_2$ a partir de ^{14}C-L-lactato e de ^{14}C-glicose não alterou nessas condições. Todavia, diferentemente dos mamíferos, a SNI não provocou mudança no número de CGCs no GRD, mostrando uma peculiaridade na resposta das rãs à SNI.

Assim, nosso estudo reforça o uso de rãs como modelo experimental para estudo dos efeitos da SNI, um modelo de dor fantasma, sobre o tecido nervoso. Porém, dada a diferença peculiar ocorrida no GRD de rãs com SNI, é evidente a necessidade de mais conhecimento dos efeitos dessa situação experimental nesses animais.

Palavras-chave: Axotomia, Histoquímica, Imunorreatividade, NADPH-diaphorase, Serotonina, Tirosina Hidroxilase, 1-[^{14}C] 2-deoxi-D-glicose, 3-O-[^{14}C] metil-D-glicose.

ABSTRACT

Frogs have been used as experimental models in different experimental situations. One of these is the study of the effects of the sciatic nerve transection (SNT) on the nerve tissue. The wide use of these animals as experimental models justifies the studies aimed at morphofunctionally understanding of their tissues.

Numerous studies have shown that glucose is the main energy substrate in the nerve tissue of frogs as well as in mammals. However, the distribution of glucose transporters in the nerve tissue of frogs is unknown as well as whether SNT alters such transportation. Another unanswered question is whether the lactate, whose concentration is increased in the frog plasma during hibernation periods and after motor activities, is used as an energy substrate by the nerve tissue, which has been demonstrated in other vertebrate species.

In the dorsal root ganglion (DRG) cells of frogs are still unknown the distribution and effects of SNT on the reaction of nicotinamide adenine dinucleotide phosphate diaphorase (NADPH-diaphorase), an enzyme that is considered equivalent to nitric oxide synthase, responsible for the synthesis of nitric oxide, and on the reaction of periodic acid-Schiff (PAS), which indicates the presence of mucopolysaccharides, including glycogen, an important energy reserve in frog nerve tissue. Moreover, the distribution and effects of SNT on immunoreactivity to serotonin, an important molecule that functions as a neurotransmitter and / or neuromodulator in the nervous system, tyrosine hydroxylase, the rate-limiting enzyme in catecholamine biosynthesis, molecules with various physiological roles, including neurotransmitter and / or neuromodulator action in the nerve tissue, and c-Fos, a protein that is regarded as a marker of neuronal activation by noxious stimulation are also unknown.

Other questions regarding is the effect of SNT on the uptake of glucose analogue *2*-Deoxy-D-glucose-1-14C (^{14}C-2-DG) and glucose and lactate concentration plasma; whether the types II and III of satellite glial cells (SGCs), recently described in rabbit DRG, are present in this ganglion of frogs; and the effects of SNT on the ultrastructure of SGCs and DRG neurons remain unanswered as well. Thus, this thesis aimed to determine: 1) the ultrastructure of neurons and SGCs; 2) the distribution of NADPH-diaphorase and PAS reaction, and immunohistochemistry for serotonin, tyrosine hydroxylase, c-Fos and glucose transporters types 1 and 3; and 3) the uptake of 2-DG-14C, in the presence and absence of lactate, in DRG of frogs, *Lithobates catesbianus*, with and without SNT. Glucose transporters types 1 and 3 were chosen because they occur in the membrane of endothelial cells, glial cells and neurons.

Initially, 12 adult male frogs, *Lithobates catesbianus*, weighing 100-200g, not having undergone any previous surgical manipulation, were killed by decapitation. The DRGs of the sciatic nerve were removed and prepared for ultrastructural analysis, histochemistry of NADPH-diaphorase and PAS, and immunohistochemistry for serotonin, tyrosine hydroxylase and glucose transporters types 1 and 3. After that, 18 other frogs in the same physical conditions were divided into three experimental groups (n = 6/group): control group (frogs not subjected to any surgical manipulation), sham

(frogs in which only surgical procedures for isolating the sciatic nerve were performed), and SNT (frogs in which the right sciatic nerve was completely transected). These animals were killed three days after the procedure, and their sciatic nerve DRGs used to demonstrate the effects of nerve transection on the ultrastructure, NADPH-diaphorase reaction, and immunohistochemical serotonin, tyrosine hydroxylase, c-Fos and glucose transporters types 1 and 3 in the DRG. Other 20 animals, divided into the same experimental groups, were used to demonstrate the effects of SNI on the uptake of ^{14}C-2-DG in the presence or absence of lactate, the production rate of $^{14}CO_2$ from ^{14}C-L-lactate and ^{14}C-glucose in the DRG. These frogs were used to further demonstrate the effects of peripheral denervation on plasma glucose and lactate levels.

Our results have demonstrated that sensory neurons of bullfrog, *Lithobates catesbianus*, DRG showed distribution, diameter and morphology similar to those described for these ganglion cells in mammals. The CGSs showed morphology similar to that described for these cells in the lymph nodes of other vertebrate species. Cells types II and III, observed in rabbit DRG did not occur in the *Lithobates catesbianus* DRG. The pattern of NADPH-diaphorase activity and distribution of immunoreactivity of serotonin, tyrosine hydroxylase and Glut 1 and 3 were also similar to those described in mammals. For the first time, it has been demonstrated the presence of NADPH-diaphorase reaction on SGCs of DRG in amphibians. The uptake of ^{14}C-2-DG was reduced when lactate was added to the incubation medium. SNT-induced changes were also similar to those ones described in mammals. There was an increase in the number of mitochondria, endoplasmic reticulum, ribosomes and filaments in the SGCs cytoplasm; more neurons and SGCs with positive reaction to NADPH-diaphorase; a greater number of tyrosine hydroxylase immunoreactive extensions around body sensory neurons; and more c-Fos immunoreactivity in neuronal nuclei. No changes occurred in serotonin immunoreactivity and glucose transporters. There was an increase in the uptake of ^{14}C-2-DG, which was reduced when lactate was added to the incubation medium. However, the formation of ^{14}C-2-DG from ^{14C}-L-lactato and glucose did not change under these conditions. Unlike mammals, SNT caused no change in the number of SGCs in DRG, showing a peculiarity in the response of frogs to SNT.

Therefore, our study supports the use of frogs as an experimental model to study the effects of SNT, a model of phantom pain on the nerve tissue. However, given the peculiar differences occurred in the DRG of frogs with SNT, it is clearly necessary to carry out further studies to better understand the effects of an experimental situation like this in such animals.

Keywords: Axotomy, Histochemistry, Immunoreactivity, NADPH-diaphorase, Serotonin, Tyrosine Hydroxylase, 1-[^{14}C] 2-deoxy-D-glucose, 3-O-[^{14}C] methyl-D-glucose.

LISTA DE ABREVIATURAS

GLUT - Transportadores de glicose

GRDs - Gânglios das raízes dorsais

GRD - Gânglio da raiz dorsal

NADPH-diaforase - nicotinamida adenina dinucleotídeo fosfato-diaforase

CGSs - Células gliais Satélite

CGS - Célula glial satélite

RER - Retículo endoplasmático rugoso

SNI - Secção do nervo isquiático (do inglês, *Sciatic nerve transection* - SNT)

^{14}C-2-DG - 1-[^{14}C] 2-deoxi-D-glicose

^{14}C-3-OMG - 3-O-[^{14}C] metil-D-glicose

5-HT - serotonina

TH - Tirosina hidroxilase

LISTA DE FIGURAS

LISTA DE FIGURAS DO ARTIGO 1

LISTA DE FIGURAS DO ARTIGO 2

LISTA DE FIGURAS DO ARTIGO 3

LISTA DE TABELAS

LISTA DE TABELAS DO ARTIGO 3

1. INTRODUÇÃO

1.1. Características gerais dos anfíbios

Quase todos os dados da Fisiologia Animal, e a maior parte do conhecimento da Fisiologia Humana, são derivados de estudos com animais de experimentação usados para responder questões específicas sobre como funcionam os processos fisiológicos. Inúmeros exemplos na literatura mostram que a identificação de similaridades e diferenças de estrutura e função entre as espécies permite constatar que algumas delas, de acordo com certas peculiaridades, podem servir como modelo ideal para o estudo de processos fisiológicos básicos. Assim, são muitas as contribuições da Fisiologia Animal na medicina, pois distintas espécies animais podem ser utilizadas como modelos no estudo de doenças específicas. Estes modelos permitem uma diversidade de experimentos que foram previamente apenas imaginados. O uso inteligente e perceptivo da informação proveniente desses modelos animais depende do entendimento de processos fisiológicos básicos fundamentais dos mesmos.

Os anfíbios são utilizados em uma grande variedade de estudos científicos. A classe *Anfibia* compreende atualmente aproximadamente 4550 espécies. Destas 390 são salamandras, ordem Caudata (Urodela); 163 são cobras-cegas, ordem Gymnofiona (Apoda); e em torno de 4000 são rãs e sapos, ordem Anura (Salientia) (Stebbins e Cohen, 1997). Em muitos locais do mundo, as rãs constituem parte importante da alimentação, sendo que em algumas sociedades primitivas e pobres elas constituem uma das principais fontes de proteína animal. Além desta importância na alimentação, milhões de estudantes de nível superior adquirem muitos de seus conhecimentos em anatomia e fisiologia de vertebrados utilizando como modelo as rãs. Estes animais também têm sido empregados em pesquisas, sendo que sua utilização muito contribuiu e continua contribuindo amplamente para o avanço da ciência nas áreas de embriologia,

endocrinologia, fisiologia, bioquímica, farmacologia, neurociências e genética (Koskela e Pasanen, 1975; Stebbins e Cohen, 1997; Kiss et al., 2009; Voituron et al., 2009).

Esta ampla utilização dos anfíbios, principalmente na área científica, justifica a realização de estudos que visam o conhecimento morfofuncional dos tecidos desses animais. Uma espécie de anfíbio muito empregado como modelo experimental é a rã *Lithobates catesbianus*[1], conhecida como rã touro. Este anfíbio aquático, resistente às baixas temperaturas, é típico da região norte dos Estados Unidos, mas que se adaptou às condições climáticas do Brasil, sendo o espécime encontrado em criadouros locais (Stebbins e Cohen, 1997; Rocha e Branco, 1998).

Uma característica dos anfíbios é sua grande distribuição geográfica. Esses animais são encontrados em uma diversidade de regiões, desde áreas desérticas até os círculos polares (Stebbins e Cohen, 1997). Para se adaptar a esta vasta distribuição, diferentes estratégias foram desenvolvidas, como por exemplo, a aquisição de dois estados funcionais durante o ano nos climas temperados, os quais são referidos como ativo (verão e primavera) e inativo (outono e inverno) (Mizell, 1965; Scapin e Giuseppe, 1993; 1994). Esta estratégia de sobrevivência decorre do efeito da temperatura e da luminosidades sobre a atividade e processos metabólicos, os quais visam proporcionar aos animais plasticidade fisiológica e metabólica para sua sobrevivência (Smith, 1952; Mizell, 1965; Pasanen e Koskela, 1974; Hermes-Lima e Storey, 1998).

O metabolismo energético no tecido nervoso de vertebrados é muito ativo, sendo a glicose o principal substrato (Larrabee, 1987; 1996; Bouzier-Sore et al., 2006; Pellerin e Magistreti, 2011; Du et al., 2012). Em Rodentia, sete tipos de transportadores de glicose (GLUT, sigla do inglês *glucose transporter*), denominados GLUT1-5, 7 and 8),

---

De acordo com Frost et al. (2006), o nome da rã *Rana catesbeiana* mudou para *Lithobates catesbianus* (para consulta, ver Bulletin of the American Museum of Natural History, No. 297)

são os responsáveis pela entrada, por difusão facilitada, da glicose para o interior de células do tecido nervoso. Os principais tipos nesse tecido são GLUT-1 e GLUT-3, que se localizam nas membranas de células endoteliais, gliais e neurônios. Estudos mostram que a densidade destes transportadores é alterada de acordo com a demanda energética do tecido (Stark el al., 2000; Duelli e Kuschinsky, 2001; Choeiri et al., 2002; Tabernero et al., 2006; Devraj, 2011). Porém, é desconhecida a distribuição dos transportadores de glicose no tecido nervoso de rãs, animais que passam por dois estados funcionais diferentes durante o ano. Desconhece-se também o padrão de captação da glicose no tecido nervoso de anfíbios, embora o glicogênio seja uma importante reserva energética no sistema nervoso de rãs (Yamamoto, 1963; Hunt e Nelson, 1965; Berthold, 1966; Gleeson, 1991).

Outra molécula usada como substrato energético no tecido nervoso de vertebrados é o lactato (Larrabee 1996; Chih et al., 2001; Bouzier-Sore et al., 2006; Ghandi et al., 2009; Dienel, 2012). Neste tecido de aves e mamíferos, o lactato parece constituir um dos substratos energéticos preferenciais em rotas metabólicas oxidativas (Larrabee, 1980; 1982; 1985; 1987; 1995; 1996; Bouzie-Sore et al., 2003a,b; 2006; Pellerin e Magistretti, 2011). É sabido que as rãs acumulam altas concentrações de lactato durante períodos de hibernação e após atividades motoras (Warren e Jackson, 2005). Assim, pode-se pensar que o lactato pode ser um dos substratos energéticos para o tecido nervoso de rãs, o que ainda não foi demonstrado nesses animais.

1.2. Características gerais do gânglio da raiz dorsal de anfíbios

Assim como em mamíferos, os axônios dos nervos espinais de anfíbios possuem ou não bainha de mielina. Os corpos neuronais de onde emergem esses axônios estão

localizados nos gânglios das raízes dorsais (GRDs) (Beccari, 1943; Butler e Hodos, 1996; Kardong, 1997). De acordo com a morfologia neuronal, a velocidade de condução e a latência de resposta, as fibras aferentes dos nervos periféricos de anfíbios foram classificadas em três tipos: 1) as chamadas fibras do tipo A, que são fibras de grosso calibre e com bainha de mielina; 2) as chamadas fibras do tipo B, que são fibras pouco espessas e com bainha de mielina; e 3) as chamadas fibras do tipo C, as fibras finas não mielinizadas (Stevens, 2004). Assim como em mamíferos, as fibras do tipo B e C estão envolvidas com a codificação e transmissão de estímulos nocivos (Hamamoto e Simone, 2003; Garry et al., 2004; Stevens, 2004).

Os somas neuronais nos GRDs são classificados em grandes e pequenos. Os neurônios grandes normalmente se apresentam claros nas colorações de rotina, dão origem a axônios mielinizados e são chamados neurônios A. Os neurônios pequenos geralmente se apresentam escuros nas colorações histológicas rotineiras, seus axônios são mielinizados e amielínicos e são denominados neurônios B (Maruhashi et al., 1952; Yamamoto, 1963; Berthold, 1966; Hanani, 2005). Contudo, o emprego de técnicas histoquímicas, imunoistoquímicas e eletrofisiológicas tem identificado diferentes subpopulações de neurônios no GRD de rãs (Berrios et al., 2008).

Ultraestruturalmente, os somas neuronais localizados no GRD de rãs estão envolvidos por células gliais chamadas células gliais satélites (CGSs) (Pannese, 1981; Hanani, 2005). Nesse gânglio, as CGSs se dispõem em torno dos somas neuronais em um arranjo similar àquele observado nos mamíferos. Aí, cada neurônio ganglionar, juntamente com o segmento inicial de seu axônio, está envolvido por uma camada de células satélites, sendo este um conjunto individualizado, separado do conjunto adjacente por tecido conjuntivo (Pannese, 1981; Matsumo e Rosenbluth, 1986; Pfeifer et al., 1995; Hanani, 2005; Huang et al., 2005; Hanani, 2010a).

Em mamíferos, está demonstrado que a distância entre as membranas neuronal e da CGS é de aproximadamente 20 nm (Pannese, 1981). Os neurônios enviam numerosos prolongamentos citoplasmáticos, similares a microvilosidades, em direção às CGSs, muitos dos quais se aproximam de invaginações e prolongamentos citoplasmáticos que partem de CGSs (Pannese, 2003). Essa característica sugere intensa comunicação entre CGSs e neurônios. Segundo alguns autores, a CGS, por sua disposição em relação ao neurônio, poderia controlar o fluxo de substâncias químicas para o espaço extracelular neuronal. Além disso, ela estaria apta a atender às demandas energéticas do neurônio (Pannese, 1981;2003; Hanani, 2005). Contudo, permanece ainda especulativo o papel funcional das CGSs.

Os estudos ultra-estruturais de gânglios sensoriais de diversas espécies de vertebrados, incluindo gânglio simpático de rãs, mostraram que cada CGS possui um núcleo ovóide, com muitos grumos localizados centralmente e a cromatina formando uma banda periférica. No citoplasma são encontradas todas as estruturas características de uma célula animal. É comum a ocorrência de grânulos de glicogênio e inclusões lipídicas (Pannese 1964; Leech, 1967; Pannese, 1981; Matsumoto e Rosenbluth, 1986). Estudos quantitativos em diferentes espécies de animais demonstraram que o número de CGSs, por soma neuronal, aumenta em proporção ao volume neuronal, o que favorece o provável papel de apoio metabólico ao neurônio dessa célula (Ledda et al., 2004; Ohtori et al., 2004; Dublin e Hanani, 2007). Em lagartos, a média de CGSs por soma neuronal é de três células gliais por corpo neuronal. Em camundongos esse número chega a cinco. Em ratos, o número de CGSs para cada neurônio é oito, enquanto ele chega a dez em coelho. Ainda não se conhece essa relação nos anfíbios. Como a diferença no número de CGSs por corpo neuronal provavelmente decorre da demanda metabólica do

tecido nervoso de cada espécie (Ledda et al., 2004), é interessante o conhecimento dessa relação em distintas espécies de vertebrados, inclusive nos anfíbios.

Siemionow et al. (2006) relataram a presença de três tipos de CGSs no GRD de coelhos. De acordo com a morfologia, essas células foram denominadas de Tipo I, II e III. As CGSs do tipo I foram descritas como CGSs típicas, sendo as mais numerosas e representando 55,8% do total das células analisadas. Estas células tinham núcleo de formato fusiforme, heterocromatina densa e poucas fendas na membrana nuclear. O citoplasma se apresentava com mitocôndrias dispersas ou agrupadas, de formato alongado ou arredondado contendo grânulos densos nas cristas mitocondriais. Foram observados ainda complexo de Golgi, retículo endoplasmático rugoso (RER) e numerosas vesículas de diâmetros variados com material de baixa densidade no seu interior, as quais estavam localizadas próximas à membrana plasmática. O espaço entre a CGS e o neurônio tinha aproximadamente 15 a 20 µm. As CGSs do tipo II, as quais totalizaram 4% do total das células satélites analisadas, foram observadas sempre próximas de neurônios e, até o momento, não foram descritas em outras espécies. Esse tipo de CGS possuía muitas projeções emergindo de seu citoplasma, as quais formavam múltiplas camadas sobrepostas que deixavam isolado o núcleo dessa célula. Essa quantidade de camadas tornava difícil a determinação do término do citoplasma da célula glial e o início da membrana neuronal. O núcleo da CGS tipo II foi o maior dos diferentes tipos dessas células. As células do tipo III representaram 39,7% do total de células satélites observadas. Este tipo tinha como característica a presença de um espaço entre a CGS e o neurônio preenchido por substância fundamental. Estas células envolviam parcial ou completamente o segmento inicial dos axônios neurônais do GRD. Até o momento, não há estudos relatando a presença das CGSs do tipo II e III em outras espécies de animais, incluindo as rãs.

Uma característica do tecido nervoso de rãs é a presença de reação positiva a diversas técnicas histoquímicas. Aqui será citada a reação positiva à enzima nicotinamida adenina dinucleotídeo fosfato (NADPH-diaforase) (Crowe et al., 1995; Cristino et al., 2004), por ser essa reação usada no presente estudo. A NADPH-diaforase é considerada equivalente à enzima óxido nítrico sintase, responsável pela síntese de óxido nítrico (Hope et al., 1991). Em mamíferos, o óxido nítrico desempenha diversos papéis, inclusive na nocicepção (Cury et al., 2011), processo onde estímulos térmicos, mecânicos e químicos intensos são detectados por uma subpopulação de fibras nervosas periféricas denominadas nociceptores (Basbaum et al., 2009; Von Hehn et al., 2012). Contudo, ainda se desconhece a distribuição da NADPH-diaforase no GRD de rãs *Rana catesbeiana*, espécie muito usada como modelo em distintas situações experimentais.

Foi demonstrado que células do GRD de rãs respondem à serotonina, substância química que desempenha diversas funções fisiológicas, dentre elas a de neurotransmissão e/ou neuromodulação (Lesch e Waider, 2012). Em rãs, a serotonina exerceu efeito despolarizante quando aplicada diretamente no GRD ou em fibras aferentes primárias (Holz e Anderson, 1984; Philippi et al., 1995). O mesmo efeito despolarizante ocorreu quando noradrenalina, uma das catecolaminas com diversos papéis fisiológicos, incluindo ação neurotransmissora e/ou neuromoduladora (Ko e Strafella, 2012; Tolleson e Claassen, 2012), foi aplicada em neurônios isolados de GRD de sapos (Chen et al., 1993). Porém, assim como ocorre com a NADPH-diaforase, se desconhece o padrão de distribuição da imunorreatividade à serotonina e às catecolaminas no GRD de rãs.

1.3. Efeito da lesão nervosa periférica sobre células do GRD

Existe na literatura uma vasta quantidade de trabalhos mostrando que a secção do nervo isquiático[1] (SNI, sigla do inglês *sciatic nerve transection* - SNT), um modelo para o estudo da dor fantasma, a dor decorrente da amputação de membros, provoca alterações nas células do GRD de distintas espécies de vertebrados, inclusive em gânglio simpático de rãs (Hunt e Nelson, 1965; Humbertson et al., 1969; Pannese, 1981; Shinder et al., 1999; Hanani, 2005; Li et al., 2013). Esse modelo de dor fantasma foi desenvolvido por Wall e colaboradores em 1979 (Figura 1). Em mamíferos, as alterações iniciam no 1º dia após a lesão nervosa periférica, apresentando um pico no 6º dia, e retornando aos números iniciais no 18º dia (Humbertson et al., 1969).

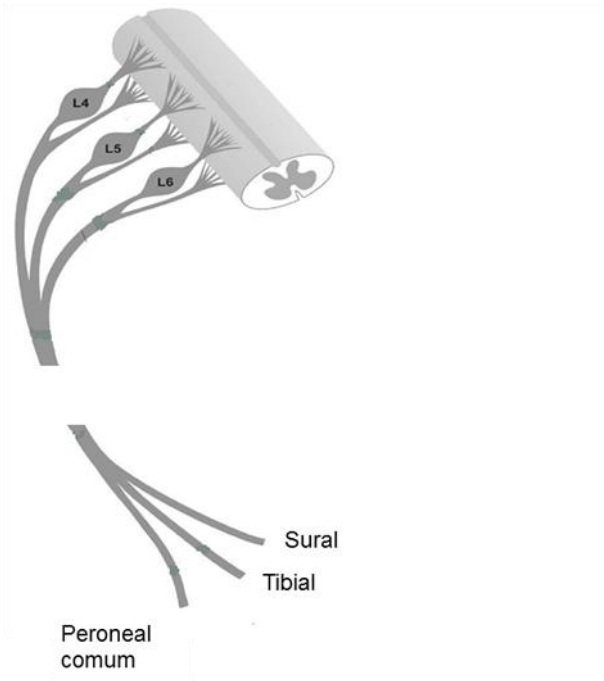

Figura 1. Esquema de um segmento da medula espinal ilustrando a formação do nervo isquiático pela união das raízes dorsais e ventrais da medula espinal. Nas raízes dorsais estão mostrados os gânglios das raízes dorsais (L4, L5 e L6) do nervo isquiático. Está mostrado também as três divisões do nervo isquiático: nervos tibial, sural e peroneal comum. No tronco comum do nervo isquiático é mostrado a secção desse nervo pela descontinuidade do mesmo (Modificado de Klusáková e Dubový, 2009).

As modificações nos somas de células do GRD devido à SNI são diversas, desde alterações estruturais e moleculares, e mudanças metabólicas (Li et al., 2013). Dentre

[1]Isquiático é a nova denominação em substituição ao termo "ciático", conforme última edição da Terminologia Anatomica elaborada pelo *Federative Committee on Anatomical Terminology* (FCAT).

essa diversidade de mudanças, pode-se citar a redução no número de neurônios nesses gânglio (Oliveira, 2001; Yun e Jakobsen, 2010). Segundo Hart el al. (2002), os primeiros sinais de morte neuronal estão presentes 24 horas após a lesão nervosa periférica. Doze semanas após a lesão, são encontrados neurônios com citoplasma vacuolizado. A membrana plasmática dessas células não apresenta sinais de alterações estruturais. O núcleo da célula está deslocado da região central e se apresenta com condensação e deslocamento irregular da cromatina. É comum a presença de invaginações na membrana nuclear. No citoplasma se encontra mitocôndrias vacuolizadas. O RER e o complexo de Golgi frequentemente se apresentam dilatados (Leech, 1967; Hart et al., 2002; Atlasi et al., 2009). Contudo, as alterações estruturais não se limitam aos neurônios, ocorrendo também em CGSs. Após a SNI, diversos estudos relataram aumento no número dessas células (Hunt e Nelson, 1965; Humbertson et al., 1969; Pannese, 1981; Shinder et al., 1999; Hanani, 2005; 2010b). De acordo com Shinder et al. (1999), a hiperplasia das CGSs determina ao conjunto neurônio-células gliais uma aparência que lembra "as camadas de uma cebola". Especula-se que a hiperplasia das células satélites, ao reduzir o espaço extracelular, poderia diminuir o acesso de substâncias químicas ao meio extracelular dos neurônios (Hanani, 2005). Porém, elas estariam aptas para melhor atender às demandas energéticas neuronais (Pannese, 1981). A SNI também ocasiona aumento no número de expansões lamelares que emergem das CGSs, as quais se distribuem pelo tecido conjuntivo. Nessas expansões se observa a presença de mitocôndria, polissomas, RER e filamentos (Hanani et al., 2002; Pannese et al., 2003).

Além das mudanças estruturais, a SNI provoca também alterações funcionais nas células do GRD. A seguir, serão citadas algumas dessas mudanças, todas relacionadas com moléculas de interesse no contexto deste trabalho. Em mamíferos, Hansen et al.

(2011) mostraram que a deficiência de transportadores de serotonina ocasiona melhora nos sintomas de alodinia (resposta dolorosa a estímulos considerados inócuos) e hiperalgesia (aumento da sensação dolorosa a estímulos potencialmente nocivos), eventos comumente observados após lesão em nervos periféricos (Cheng e Ji, 2008; Basbaum et al., 2009; Nickel et al., 2012; Von Hehn et al., 2012). A imunorreatividade a tirosina hidroxilase (TH), a enzima limitante na síntese de catecolaminas, a qual catalisa a conversão de L-tirosina a dopamina que será posteriormente convertida em noradrenalina e adrenalina, é aumentada após SNI (Ma e Bisby, 1999; Hu e McLachlan, 2001; 2003). Esta condição experimental também provocou acréscimo na expressão de c-Fos, proteína considerada marcadora de ativação neural por estimulação nociva (Soares et al., 2001). Ainda, a SNI ocasiona aumento no número de somas neuronais positivos à NADPH-diaforase no GRD (Keilhoff et al., 2003; Lukácová et al., 2003).

A lesão em nervos periféricos também modifica parâmetros metabólicos nos mamíferos. Nessa situação experimental foi demonstrada redução na imunorreatividade ao GLUT-1 em estruturas do sistema nervoso central e periférico (Stark et al., 2000). A compressão no nervo isquiático provocou acréscimo na utilização de glicose nos cornos ventral e dorsal da medula espinal de rato (Price et al., 1991). A secção nos nervos facial e hipoglosso aumentou a utilização desse substrato energético nos núcleos motores desses nervos cranianos (Kreutzberg e Emmerst, 1980). Resultado similar foi observado após lesão na cóclea, o que ocasionou acréscimo na captação do análogo da glicose 1-[^{14}C] 2-deoxi-D-glicose (^{14}C-2-DG) nas regiões envolvidas com o processamento da informação auditiva (Ahn et al., 2004).

Uma consequência da lesão em axônios de nervos periféricos é o aumento na liberação de glutamato no corno dorsal da medula espinal, região de entrada dessas fibras aferentes (Klusáková e Dubový, 2009). Um aumento no número de

transportadores de glutamato do tipo 2 ocorreu nas fibras do nervo isquiático após a secção do mesmo (Brumovsky et al., 2007). Está demonstrado que em situações experimentais onde há acréscimo na concentração de glutamato ocorre também aumento no lactato, que pode ser usado como substrato energético pelas células neurais (Schurr et al., 1999; Schurr e Payne, 2007; Barros e Deitmer, 2010; Schurr e Gozal, 2012). Esta pode ser a situação no GRD após a SNI. Todavia, essa questão permanece em aberto.

Como já mencionado, os estudos citados acima foram realizados, em sua maioria, em mamíferos. Contudo, as rãs vem sendo utilizadas como modelo experimental em estudos de nocicepção (Stevens, 2004; Stevens et al., 2007; 2009; Chen et al., 2011; Coble et al., 2011; Ohkita et al., 2012; Saito et al., 2012), inclusive em estudos com SNI (Partata et al., 2002; Guedes et al., 2004a, b). De acordo com Stevens (2004), o uso desses animais na pesquisa sobre nocicepção permite uma abordagem filogenética do tema. Permite ainda o uso de um sistema nervoso com organização mais simples do que a de um mamífero, além de vantagens econômicas, tanto pela facilidade na manutenção dos animais como pelo menor preço dos mesmos. Porém, os estudos com rãs mostraram que as alterações morfofuncionais no tecido nervoso desses animais com SNI são, em parte, similares àquelas observadas nos mamíferos (Partata et al., 2002; Guedes et al., 2004a, b; Schaible e Richter, 2004; Nickel et al., 2012). Todavia, outras foram peculiares a esses animais. Apenas em rãs a SNI provocou aumento na imunorreatividade ao neuropeptídeo Y nos somas neuronais do GRD ipsilateral e contralateral à lesão nervosa periférica, enquanto em ratos o acréscimo ocorreu somente no GRD ipsilateral à lesão (Guedes et al., 2004b). Em rãs, a SNI também provocou redução na imunorreatividade ao peptídeo substância P no corno dorsal da medula espinal. Porém, o retorno da imunorreatididade foi mais rápido em rãs do que em mamíferos (Partata et al., 2002).

1.4. Considerações finais

A presença de similaridades nas respostas de rãs à SNI fortalece o uso desses animais como modelos experimentais para o estudo dos efeitos da lesão nervosa periférica sobre o tecido nervoso, tema que ainda possui muitas questões em aberto. É certo que o entendimento dos efeitos da SNI sobre o tecido nervoso proporcionará o desenvolvimento de melhores abordagens para o tratamento da dor fantasma, condição dolorosa difícil de ser tratada. Porém, dada às peculiaridades em muitas das respostas patofisiológicas de rãs torna-se evidente a necessidade de realização de estudos complementares para melhor compreensão dos efeitos de uma lesão nervosa periférica sobre o tecido nervoso de rãs. O conhecimento dessas diferenças indiscutivelmente permitirá um melhor entendimento das respostas fisiológicas desses animais em uma condição dolorosa, o que, sem dúvida, reforçará o emprego dos mesmos como modelos experimentais para o estudo dos mecanismos envolvidos na codificação e transmissão da informação nociceptiva. O emprego de rãs como modelos experimentais em uma condição dolorosa também oferecerá subsídios ao entendimento evolutivo dessa resposta, já que os anfíbios foram os primeiros vertebrados terrestres. Assim, com o intuito de ampliar o conhecimento dos efeitos peculiares da SNI sobre o tecido nervoso de rãs, e fortalecer o uso desses animais como modelos experimentais para o estudo da nocicepção, o presente estudo demonstrou o efeito da SNI, que simula um quadro de dor fantasma, sobre parâmetros ultraestrutural, histoquímico, imunoistoquímico e de captação de análogos da glicose em gânglio da raiz dorsal de rãs *Lithobates catesbianus*.

2. OBJETIVOS

2.1 OBJETIVO GERAL

O objetivo geral do presente trabalho foi determinar: 1) a ultraestrutura de neurônios e CGSs, 2) a histoquímica e imunoistoquímica de algumas moléculas com papel importante na neurotransmissão neural, e 3) a captação de ^{14}C-2-DG, análogo da glicose, na presença e ausência de lactato, em GRD de rãs *Lithobates catesbianus* submetidas à SNI. Para isso os experimentos foram realizados 3 dias após a lesão e como controle foram utilizadas rãs sem qualquer manipulação cirúrgica.

2.2 OBJETIVOS ESPECÍFICOS

- Determinar a ultraestrutura de neurônios e CGSs do GRD de rãs sem qualquer manipulação no nervo isquiático e submetidas à manipulação e à secção nesse nervo, realizando as determinações 3 dias após a cirurgia;
- Determinar a distribuição da imunorreatividade à c-Fos, serotonina, tirosina hidroxilase, GLUT-1 e GLUT-3 no GRD de rãs sem qualquer manipulação no nervo isquiático e submetidas à manipulação e à secção nesse nervo, realizando as determinações 3 dias após a cirurgia;
- Determinar a distribuição das reações à NADPH-diaforase e ao ácido periódico-reativo de Schiff (PAS) no GRD de rãs sem qualquer manipulação no nervo isquiático e submetidas à manipulação e à secção nesse nervo, realizando as determinações 3 dias após a cirurgia;
- Determinar a captação de ^{14}C-2-DG, na presença ou ausência de lactato, no GRD de rãs sem qualquer manipulação no nervo isquiático e submetidas à manipulação e à secção nesse nervo, realizando as determinações 3 dias após a cirurgia;

- Determinar a taxa de produção de $^{14}CO_2$ a partir de ^{14}C-L-lactato e de ^{14}C-glicose no GRD de rãs sem qualquer manipulação no nervo isquiático e submetidas à manipulação e à secção nesse nervo 3 dias após a cirurgia;
- Determinar os efeitos da SNI sobre a concentração plasmática de glicose e lactato em rãs sem qualquer manipulação no nervo isquiático e submetidas à manipulação e à secção nesse nervo, realizando as determinações 3 dias após a cirurgia.

3. MATERIAL E MÉTODOS

E RESULTADOS

3.1. Artigo submetido à revista Tissue & cell

Ultrastructure, NADPH-diaphorase reaction, and serotonin-, tyrosine hydroxylase-, and glucose transporters 1 and 3-like immunoreactivities in frog dorsal root ganglia

Fabiana Rigon[a], Vanusa B. Auler[a], Lidiane Dal Bosco[a], Maria C. Faccioni-Heuser[b,c], Wania. A. Partata[a,*]

[a]*Laboratório de Neurobiologia Comparada; Departamento de Fisiologia, Instituto de Ciências Básicas da Saúde (ICBS), Universidade Federal do Rio Grande do Sul, Porto Alegre 90050170, RS, Brazil*

[b]*Laboratório de Histofisiologia Comparada, Depto Ciências morfológicas, ICBS, Universidade Federal do Rio Grande do Sul, Porto Alegre 90050170, RS, Brazil*

[c]*Centro de Microscopia Eletrônica, Universidade Federal do Rio Grande do Sul, Porto Alegre 90050170, RS, Brazil*

Running Title: Structure of frog dorsal root ganglion

Keywords: Immunoreactivity; NADPH-diaphorase; Tyrosine Hydroxylase; Serotonin

Acknowledgments: This study was supported by grants from Fundação de Amparo à Pesquisa do Estado do Rio Grande do Sul (FAPERGS) and Conselho Nacional de Desenvolvimento Científico e Tecnológico (CNPq).

*Corresponding author at: Laboratório de Neurobiologia Comparada; Departamento de Fisiologia, Instituto de Ciências Básicas da Saúde, Universidade Federal do Rio Grande do Sul, Rua Sarmento Leite, 500, 90050-170, Porto Alegre, RS, Brazil. Tel.: + 55 51 3308 3305; fax: + 55 51 3308 3166 *E-mail address*: partataw@gmail.com (W.A. Partata)

ABSTRACT

Amphibian dorsal root ganglia (DRG) cells contain glycogen, show reactivity to nicotinamide adenine dinucleotide phosphate diaphorase (NADPH-diaphorase), respond to application of serotonin and catecholamine, and have one type of satellite glial cell (SGC), according to previous descriptions. Recently a new type of SGC was identified in rabbit DRG. To investigate whether this new SGC type occurs in frog DRG and to determine the pattern of immunoreactivity to glucose transporters (Glut) types 1 and 3, tyrosine hydroxylase and serotonin, as well as NADPH-diaphorase and Hotchkiss' PAS (periodic acid-Schiff) reactions, dorsal root ganglia were excised from 12 adults of the bullfrog *Rana catesbeiana*, prepared, sectioned and analyzed under transmission electron and light microscopy. The neuronal and SGC ultrastructure displayed typical characteristics. The new type of SGC was not found. Glut-1-like immunoreactivity occurred in the SGC and blood vessels, while Glut-3 was found in medium-diameter neurons. The tyrosine hydroxylase-like immunoreaction was located predominantly around neurons and SGC, while serotonin occurred in a few medium-diameter neurons. The NADPH-diaphorase reaction was intense in SGC and medium and small neurons, but weak in large neurons. The PAS reaction was moderate in neurons but strong in SGC. These results concord with previous ultrastructural descriptions of amphibian DRG, and show the functional similarity between frog and rodent DRG.

1. Introduction

The amphibian spinal cord and ganglion have been frequently used as a model in physiological and pharmacological studies (Partata et al., 2002; Guedes et al., 2004a;b; Stevens, 2004; Guo et al., 2011; Kaeser et al., 2011; Ohkita et al., 2012). In these animals, as in mammals, the dorsal root ganglia (DRG) are composed of three classes of neurons, which are distinguished according to their morphology and function. A recent study identified six distinct subpopulations of neurons in frog DRG, based on neuron morphology and size in light microscopy (Berrios et al., 2008). In DRG, in addition to neurons, myelinated and unmyelinated fibers, macrophages and fibroblasts, and satellite glial cells (SGCs) also constitute the resident components (Yamamoto, 1963; Pannese, 1981; Jhaveri and Frank, 1983; Szèkely and Antal, 1984; Baluk, 1986; Ten Donkelaar, 1998). Various roles such as protective, trophic and secretory functions have been assigned to SGCs, and their morphology has been studied in detail in some vertebrate species, including frogs (Yamamoto, 1963; Baluk, 1986; Pannese, 1981; 2010; Hanani, 2005; 2010). A previous study described a new type of support cell in rabbit DRG (Siemionow et al., 2006). According to the authors, this new type represents a different cell line or a highly adapted cell with specific functional capacities that differ from those of a typical satellite cell. It is unknown if this new type is present in frog DRG.

Frog DRG neurons also show reactivity to nicotinamide adenine dinucleotide phosphate diaphorase (NADPH-diaphorase) (Cristino et al., 2004; Crowe et al., 1995), but we are unaware of any report on the distribution of this reaction in DRG from bullfrog. Frog DRG cells respond to application of serotonin (Holz and Anderson, 1984; Philippi et al., 1995) and catecholamine (Cheng et al., 1993). No report, however, was

found on the pattern of serotonin and tyrosine hydroxylase immunoreactivity in frog DRG.

Energy metabolism is very active in frog nervous tissue, with glucose as the obligatory energy substrate (Larrabee, 1987; 1996), although glycogen forms a limited energy store (Yamamoto, 1963; Hunt and Nelson, 1965; Gleeson, 1991). In rodents, a family of seven facilitative glucose transporters (Glut-1-5, 7 and 8) mediates the cellular uptake of glucose. The main types found in the brain are Glut-1 and Glut-3, which are located in the membranes of endothelial cells, astrocytes and neurons, and their densities are well adjusted to changes in local energy demand (Duelli and Kuschinsky, 2001; Choeiri et al., 2002). In frog DRG, however, the distribution of these glucose transporters is unknown.

In order to elucidate the ultrstructure and patterns of metabolic substances in bullfrog DRG cells, we used transmission electron microscopy to reveal the ultrastructure of these cells, especially SGCs. In addition, we used light microscopy to demonstrate the pattern of Glut-1- and 3-, serotonin- and tyrosine hydroxylase-like immunoreactivities, and the distribution of the NADPH-diaphorase and Hotchkiss' PAS (periodic acid-Schiff reaction) reactions.

2. Materials and methods

2.1. Animals

Twelve adult male frogs *Rana catesbeiana*, weighing 100-200g, were obtained from RANASUL (Imbé, RS) in summer and autumn. Upon arrival at the laboratory they were housed in cages with water and kept under natural conditions of temperature and

photoperiod. The animals were fed *ad libitum* with specific food and acclimated to laboratory conditions for at least 2 weeks before being used. The experimental protocol followed the NIH *Guide for the Care and Use of Laboratory Animals* (NIH publication 85-23 revised 1985). All efforts were made to minimize the number of animals used and their suffering.

2.2. Transmission Electron Microscopy

After acclimation the frogs were killed by decapitation and their bilateral DRG of the sciatic nerve were dissected out within 3 minutes. The ganglia were fixed immediately by immersion in a solution containing 2% paraformaldehyde and 1.5% glutaraldehyde (Sigma, USA) diluted in 0.1M phosphate buffer pH 7.3 (PB) for 1h. The material was washed in the same buffer solution and postfixed in 1% osmium tetroxide (Sigma, USA) diluted in PB for 1h at room temperature. After this, the sections were washed in PB and subsequently dehydrated through an ascending series of acetone, and then embedded in Araldite (Durcupan, Fluka, Switzerland). Semithin sections (1 μm) were obtained using an ultramicrotome (MT 6000=XL, USA) with a diamond knife (Diatome - Switzerland) and stained with 1% toluidine blue for examination under a light microscope. The ultrathin sections (70 nm) were cut with the same ultramicrotome using a diamond knife (Drukker – Netherlands). These sections were stained with 2% uranyl acetate (Merck, Germany) followed by 1% lead citrate and examined with a JEM 120 EX II electron microscope (Centro de Microscopia Eletrônica, Universidade Federal do Rio Grande do Sul).

2.3. Histochemistry and Immunohistochemistry

Glycogen was detected according to Hotchkiss' PAS (periodic acid-Schiff reaction) technique. Ten frogs were decapitated, and the DRG were dissected and sectioned (10 μm). The sections were mounted on gelatinized slides to dry. After hydration in water, the sections were placed in a solution of 0.5% periodic acid for 10 min. After being washed in destilled water, the sections were incubated at room temperature for 30 min in Schiff reagent (1 g basic fuchsin in 200 mL water) and then were washed three times in a sulfur solution prepared with 10 mL HCl, 10 mL sodium bisulfite and 180 mL water. The sections were rinsed in water for 5 min, dehydrated in an ethanol series, cleared and covered with Entellan (Merck). For control, some sections were treated with saliva for 1 h at 37^{o} C before PAS staining.

For NADPH-diaphorase and immunohistochemical procedure the frogs were descerebrated and after a brief saline flush were intracardially perfused with 4% paraformaldehyde in 0.1 M phosphate buffer, pH 7.4 (PB). The DRG were quickly dissected out, immersed in the same fixative solution for 4 h and then cryoprotected in 15 and 30% sucrose solutions in phosphate buffer at 4^{o} C. Coronal serial sections (50 μm) were obtained on cryostat and collected in cold phosphate buffered saline (PBS).

For NADPH-diaphorase procedure free-floating sections were treated with 10 mL PB containing 12 μL Triton X-100 for 10 min and transferred to fresh NADPH-diaphorase medium containing 0.5 mg/ml β-NADPH, 0.2 mg/mL nitro blue tetrazolium and 0.2 M PB containing 12 μL Triton X-100. After pre-incubation at room temperature for 5 min under continuous shaking, they were incubated at 37 ºC for 4 h. The reaction was stopped by the addition of excess 0.1 M PB. Control sections were incubated in a reaction medium without substrate.

For immunohistochemistry the sections were treated with 3% hydrogen peroxide in 10% methanol for 30 min, washed with PBS for further 30 min and incubated for 30

min in 3% normal goat serum in PBS containing 0.4% Triton X-100 (PBS-T). The sections were incubated overnight with gentle agitation at 4^{o} C with primary antibody [Glut1, polyclonal antibody that recognizes ~42-45 kDa protein, diluted 1:1000 (Sigma); Glut3, polyclonal antibody that recognizes C-terminal sequence of the protein, diluted 1:1000 (Sigma); serotonin, polyclonal antibody, diluted 1:1200 (Sigma); tyrosine hydroxylase, polyclonal antibody, diluted 1:1000 (Sigma)]. The primary antibody was then removed and the sections washed in PBS-T for 30 min. Then the sections were immersed in a secondary (anti-IgG, Sigma), diluted 1:50 in PBS-T, for 2 h at room temperature with gentle agitation. After washing with PBS-T for 30 min a soluble complex of horseradish peroxidise rabbit anti-horseradish peroxidise diluted 1:500 was applied for 2 h at room temperature. The samples were then washed in PBS, incubated in a solution of 3,3'-diaminobenzidine tetrahydrochoride (60 mg/100 mL, Sigma) and 0.005% v/v hydrogen peroxide in PBS. Specific immunostaining was abolished when the primary antibody was omitted from the staining sequence.

After NADPH-diaphorase and immunohistochemical procedures, the sections were mounted onto gelatinized slides, dehydrated in an ethanol series, cleared, covered with Entellan (Merck) and examined and photographed with Nikon Optiphot-2 microscopy equipped with a Nikon FX-35DX camera.

3. Results

In light microscopy, the frog DRG showed a typical morphology. Neurons with small (10 µm), medium (30 µm) and large (55 µm) diameters were present. The large neurons were usually located in the ganglion cortex, while the medium and small cells were located at the center. The nerve-cell body was surrounded by one or more SGCs.

Ultrastructurally, sensory neurons showed the morphometry typically described for these cells. Some of them exhibited electron-dense cytoplasm and others showed intermediate electron densities. Neuronal cell bodies and the initial segment of the axon were completely ensheathed by SGCs. Sometimes only a thin ring of cytoplasm of SGC was observed around the soma of the sensory neuron. SGCs also showed the typical morphometry of these cells; they were fusiform and were separated from adjacent neurons by a space of around 20 nm. This space commonly contained lamellar cytoplasmic expansions of the SGC (Fig. 1A, B) and neuronal projections (Fig. 1A). The lamellar expansions were numerous and irregularly shaped (Fig. 1B, C).

No different electron densities of nuclei and cytoplasm of the SGCs were found. The plasmatic membrane of these cells was around 10-12 nm thick. Their nucleus showed a characteristic chromatin condensation, with heterochromatin attached to the nuclear membrane (Fig. 2A). When visible, the nucleolus was centrally located. Mitochondria (Fig. 2B), Golgi complex and rough endoplasmic reticulum (RER) could be observed near the nucleus. Mitochondria clusters were found dispersed through the cytoplasm, but this was not a frequent feature. The Golgi complex was not abundant in SGC cytoplasm. This organelle usually appeared with 4-6 flattened cisternae associated with a few vesicles with different electron densities, that were separate from or adjacent to the cisternae (Fig. 2B). RER was a common structure, with its usual features. Some lysosomes and round clear vesicles were also found (Fig. 2B, D); the vesicles had different sizes and often showed amorphous content. Many ribosomes (15 nm diameter), free or in clusters, and intermediate filaments (8-10 nm diameter) were observed both adjacent to the nucleus and scattered through the cytoplasm (Fig. 2C, D). Lipid (Fig. 2E) and glycogen droplets was also found in SGC cytoplasm.

The Hotchkiss' PAS reaction was moderate in the sensory neurons, but strong in SGC (Fig. 3A). While this positive reaction disappeared in neuronal cytoplasm after saliva treatment, it was still found in SGCs. A strong NADPH-diaphorase reaction occurred in medium and small neurons, primarily in the former. A weak NADPH-diaphorase reaction was observed in large neurons. SGC showed strong NADPH-diaphorase staining, regardless of whether these cells surrounded positive large, medium or small neurons (Fig. 3B).

DRG cells were immunopositive for all antibodies, although the pattern of immunostaining was different for each molecule. Very few medium and small sensory neurons showed serotonin-like immunoreactivity (Fig. 4A). This immunoreaction was always moderate. SGCs did not show serotonin-like immunoreactivity. Tyrosine hydroxylase-like immunoreactivity occurred around small, medium and large neurons (Fig. 4B). These formations were not common in frog DRG. A few immunoreactive neurons were observed throughout the DRG. Tyrosine hydroxylase-like immunoreactivity was also found surrounding the SGCs. Glut3-like immunoreactivity was found in sensory neurons, which were moderately stained for this antibody (Fig. 4C). These neurons were predominantly medium-sized. No immunoreaction was found in SGCs. No vascular Glut3 staining was observed. Moderate Glut1-like immunoreactivity was found in the capsule of the DRG and in blood vessels. No labeling could be detected in the neurons, but moderate labeling was found in SGCs (Fig. 4D).

4. Discussion

The present investigation demonstrated that the new type of SGC, recently described in rabbit DRG (Siemionow et al., 2006), was not found in bullfrog DRG. The

distribution patterns of PAS and NADPH-diaphorase reactions and Glut1- and 3-, tyrosine hydroxylase- and serotonin-like immunoreactivities were similar to that described for mammals, including a positive NADPH-diaphorase reaction in SGCs from frog DRG.

Structurally, the nerve-cell bodies from bullfrog DRG showed a distribution similar to that described for autonomic ganglia of frogs (Yamamoto, 1963; Baluk, 1986) and spinal ganglia of other vertebrate species (Siemionow et al., 2006; Arkhipova et al., 2010; Pannese, 1981; 2010; Hanani, 2005; 2010). With respect to size, the frog DRG neurons fit the three general classes described for amphibians: large, medium and small (Maruhashi et al., 1952; Yamamoto, 1963). The fixation of the ganglia probably prevented identification of the six classes of neurons that were recently described for this tissue (Berrios et al., 2008). Each nerve-cell body was usually enveloped by a SGC sheath, distinctly separated from sheaths encircling adjacent neurons by connective tissue. SGCs displayed the typical morphometry attributed to these cells (Matsumoto and Rosenbluth, 1986; Siemionow et al., 2006; Arkhipova et al., 2010; Pannese, 1981; 2010; Hanani, 2005; 2010). Thus, our observations are in agreement with the morphological type of SGC described in other studies with frog species (Yamamoto, 1963; Pannese, 1981; Baluk, 1986).

The positive reaction to NADPH-diaphorase in SGCs may indicate the synthesis of nitric oxide by this cell. NADPH-diaphorase is a nitric oxide synthase, the enzyme responsible for nitric oxide synthesis (Hope et al., 1991), and the simple histochemical technique of NADPH-diaphorase is an indication of the cellular localization of nitric oxide synthase. This is the first demonstration of this reaction in SGCs from amphibians. Recently, the NADPH-diaphorase reaction was demonstrated in SGCs from rat DRG (Nascimento et al., 2008). It has been suggested that in these animals the

effects of nitric oxide are mediated by the collaboration between neurons and SGC (Thippeswamy and Morris, 2002; Nascimento et al., 2008). This collaboration may be occurring in frog DRG, since the neurons also stained for NADPH-diaphorase and many of them were close to positive SGC. The presence of the NADPH-diaphorase reaction in neurons from frog DRG was also described by other authors (Crowe et al., 1995; Philippi et al., 1995; Cristino et al., 2004), although none of them mentioned SGC.

Since Hotchkiss' PAS reaction is used to show glycogen distribution, the moderate reaction found in nerve-cell bodies may be due to the low glycogen content. Energy reserves fluctuate seasonally in amphibians, and sequential deposition of lipid and carbohydrate stores occurs throughout summer and autumn, with fat being deposited earlier than liver glycogen (Boutilier et al., 1997). Our study was performed with frogs collected mostly in autumn, which may explain the lipid droplets present in the SGC cytoplasm and the moderate PAS reaction in DRG cells. The presence of energy substrates in SGC cytoplasm reinforces its role as a metabolic support for neurons.

Immunoreactivity for tyrosine hydroxylase, the rate-limiting enzyme that converts tyrosine to catecholamines, which are neurotransmitters and/or hormones in the periphery and in the central nervous system, was similar to results reported for rodents (Brumovsky et al., 2006; Li et al., 2011; Xia et al, 2011). The result for serotonin was also similar to that described in rodents (Delree et al., 1992). The functional significance of these findings is not yet understood and needs to be analyzed. It would be interesting to investigate if the immunoreactive neurons fall in the classical "peptidergic" or "non-peptidergic" categories. Research into this question is under way in our laboratory.

In conclusion, the new type of SGC described in rabbit DRG was not found in frog DRG. This may indicate an evolutionary difference, but further ultrastructural studies with other vertebrate species are necessary to clarify this hypothesis. This study provided the first demonstration of a positive NADPH-diaphorase reaction in SGCs from frog DRG. Since these results were similar to that found in rodents, it may indicate the early evolutionary appearance of this reaction in SGCs from vertebrates. Similarities were also found in the pattern of PAS and NADPH-diaphorase reactions and Glut1- and 3-, tyrosine hydroxylase- and serotonin-like immunoreactivities. Thus, our study concord with previous ultrastructural descriptions of amphibian DRG and show the functional similarity between frog and rodent DRG.

Conflict of interest

The authors declare that there are no conflicts of interest.

References

Arkhipova, S.S., Raginov, L.S., Mukhitov, A.R., Chelyshey, Y.A., 2010. Satellite cells of sensory neurons after various types of sciatic nerve trauma in the rat. Neurosci. Behav. Physiol. 40, 609-614.

Bałuk, P., 1986. Scanning electron microscopic studies of bullfrog sympathetic neurons exposed by enzymatic removal of connective tissue elements and satellite cells. J. Neurocytol. 15(1), 85-95.

Berrios, I., Castro, C., Kuffer, D.P., 2008. Visualization of six unique morphological subpopulations of adult frog dorsal root ganglion neurons at the light microscopic level. P. R. Health Sci. J. 27(1), 55-59.

Boutilier, R.G., Donohoe, P.H., Tattersall, G.J., West, T.G., 1997. Hypometabolic homeostasis in overwintering aquatic amphibians. J. Exp. Biol. 200, 387-400.

Brumovsky, P., Villar, M.J., Hökfelt, T., 2006. Tyrosine hydroxylase is expressed in a subpopulation of small dorsal root ganglion neurons in the adult mouse. Exp. Neurol. 200(1), 153-165.

Choeiri, C., Staines, W., Messier, C., 2002. Immunohistochemical localization and quantification of glucose transporters in the mouse brain. Neuroscience 111, 19-34.

Cristino, L., Florenzano, F., Bentivoglio, M., Guglielmotti, V., 2004. Nitric oxide synthase expression and cell changes in dorsal root ganglia and spinal dorsal horn of developing and adult *Rana esculenta* indicate a role of nitric oxide in limb metamorphosis. J. Comp. Neurol. 472(4), 423-436.

Crowe, M.J., Brown, T.J., Bresnahan, J.C., Beattie, M.S., 1995. Distribution of NADPH-diaphorase reactivity in the spinal cord of metamorphosing and adult *Xenopus laevis*. Brain Res. Dev. Brain Res. 86, 155-166.

Delree, P., Martin, D., Sadzot-Delvaux, C., Rogister, B., Leprince, P., Robe, P., Rigo, J.M., Lefebvre, P.P., Malgrange, B., Schoenen, J., Moonen, G., 1992. In vitro and in vivo modulation of 5-hydroxytryptamine-, thyrotropin-releasing hormone- and calcitonin-gene related peptide-like immunoreactivities in adult rat sensory neurons. Neuroscience 51(2), 401-410.

Duelli, R., Kuschinsky, W., 2001. Brain glucose transporters: relationship to local energy demand. News Physiol. Sci. 16, 71-76.

Gleeson, T.T., 1991. Patterns of metabolic recovery from exercise in amphibians and reptiles. J. Exp. Biol. 160, 187-207.

Guedes, R.P., Marchi, M.I., Viola, G.G., Xavier, L.L., Achaval, M., Partata, W.A., 2004a. Somatostatin, calcitonin gene-related peptide, and Y-aminobutyric acid-like immunoreativitity in the frog lumbosacral spinal cord: distribution and effects of sciatic nerve transection. Comp. Biochem. Physiol. B 138, 19-28.

Guedes, R.P., Marchi, M.I., Achaval, M., Partata, W.A., 2004b. Complete sciatic nerve transection induces increase of neuropeptide Y-like immunoreactivity in primary sensory neurons and spinal cord of frogs. Comp. Biochem. Physiol. A 139, 461-467.

Guo, T., Mandai, K., Condie, B.G., Wickramasinghe, S.R., Capecchi, M.R., Ginty, D.D., 2011. An evolving NGF-Hoxd1 signaling pathway mediates development of divergent neural circuits in vertebrates. Nat. Neurosci. 14, 31-36.

Hanani, M., 2005. Satellite glial cells in sensory ganglia: from form to function. Brain Res Brain Res Rev. 48(3), 457-76.

Hanani, M., 2010. Satellite glial cells in sympathetic and parasympathetic ganglia: in search of function. Brain Res. Rev. 64(2), 304-327.

Hope, B.T., Michael, G.J., Knigge, K.M., Vincent, S.R., 1991. Neuronal NADPH-diaphorase is a nitric oxide synthase. Proc. Nat. Acad. Sci. USA 88, 2811-2814.

Hunt, C.C., Nelson, P.G., 1965. Structural and functional changes in the frog sympathetic ganglion following cutting of the presynaptic nerve fibres. J. Physiol. 177, 1-20.

Jhaveri, S., Frank, E., 1983. Central projections of the brachial nerve in bullfrogs: muscle and cutaneous afferents project to different regions of the spinal cord. J. Comp. Neurol. 221(3), 304-312.

Kaeser, G.F., Rabe, B.A., Saha, M.S., 2011. Cloning and characterization of GABAA α subunits and GABAB subunits in Xenopus laevis during development. Dev. Dyn. 40(4), 862-873.

Larrabee, M.G., 1987. Ontogeny of glucose and lipd metabolism in dorsal root ganglia of chickens. Similarities and contrasts with sympathetic ganglia. J. Neurochem. 49, 393-398.

Larrabee, M.G., 1996. Partitioning of CO_2 production between glucose and lactate in excised sympathetic ganglia, with implication for brain. J. Neurochem. 67, 1726-1734.

Li, J.Y., Xie, W., Strong, J.A., Guo, Q.L., Zhang, J.M., 2011. Mechanical hyperchanical sensitivity, sympathetic sprouting, and glial activation are attenuated by local injection of corticosteroid near the lumbar ganglion in a rat model of neuropathic pain. Reg. Anesth. Pain Med. 36(1), 56-62.

Maruhashi, J., Mizuguchi, K., Tasaki, I., 1952. Action currents in single afferents nerve fibres elicited by stimulation of the skin of the toad and the cat. J. Physiol. 117(2), 129-151.

Matsumoto, E., Rosenbluth, 1986. Structure of the satellite cell sheath around the cell body, axon hillock, and initial segment of frog dorsal root ganglion cells. Anat. Rec. 215(2), 182-191.

Nascimento, R.S., Santiago, M.F., Marques, S.A., Allodi, S., Martinez, A.M.B., 2008. Diversity among satellite glial cells in dorsal root ganglia of the rat. Braz. J. Med. Biol. Res. 41(11), 1011-1017.

Ohkita, M., Saito, S., Imagawa, T., Takahashi, K., Tominaga, M., Ohta, T., 2012. Molecular cloning and functional characterization of *Xenopus tropicalis* frog transient receptor potential vanilloid 1 reveal its functional evolution for heat, acid, and capsaicin sensitivities in terrestrial vertebrates. J. Biol. Chem. 287(4), 2388-2397.

Pannese, E., 1981. The satellite cells of the sensory ganglia. Adv. Anat. Embryol. Cell Biol. 65, 1-111.

Pannese, E., 2010. The structure of the perineuronal sheath of satellite glial cells (SGCs) in sensory ganglia. Neuron Glia Biol. 6(1), 3-10.

Partata, W.A., Cerveira, J.F., Xavier, L.L., Viola, G.G., Achaval, M., 2002. Sciatic nerve transection decrease P immunoreactivity in the lumbosacral spinal cord of the (*Rana catesbeiana*). Comp. Biochem. Physiol. B 131, 807-814.

Philippi, M., Vyklický, L., Kuffler, D.P., Orkand, R.K., 1995. Serotonin- and proton-induced and modified ionic currents in frog sensory neurons. J. Neurosci. Res. 40(3), 387-395.

Siemionow, K., Weinstein, J.N., McLain, R.F., 2006. Support and satellite cells within the rabbit dorsal root ganglion: ultrastructure of a perineuronal support cell. Spine 31(17), 1882-1887.

Stevens, C.W., 2004. Opioid research in amphibians: a unique perspective on mechanism of opioid analgesia and the evolution of opioid receptors. Brain Res. Rev. 46, 204-215.

Székely, G., Antal, M., 1984. Segretion of muscle and cutaneous afferent fiber terminals in the brachial spinal cord of the frog. J. Hirnforsch. 25(6), 671-675.

Ten Donkelaar, H.J., 1998. Anurans. In Nieuwenhuys, R., Ten Donkellar, H.J., Nicholson, C. (Ed.), *The Central Nervous system of vertebrates*. pp.1151-1314. Springer-Verlag, Berlin.

Thippeswamy, T., Morris, R., 2002. The roles of nitric oxide in dorsal root ganglion neurons. Ann. N Y Acad. Sci. 962, 103-110.

Xia, C.M., Colomb, D.G. Jr., Akbarali, H.I., Qiao, L.Y., 2011. Prolonged sympathtic innervation of sensory neurons in rat thoracolumbar dorsal root ganglia during chronic colitis. Neurogastroenterol Motil. 23(8), 801-e339.

Yamamoto, T., 1963. Some observations on the fine structure of the sympathetic ganglion of bullfrog. J. Cell. Biol. 16, 159-170.

Legends to Figures

Fig. 1. Cross section of *Rana catesbeiana*'s dorsal root ganglion. (A) Note the projections emerging from neuron (NEU) and the lamellar expansions of the satellite glial cell (SGC) (arrows). (B) From SGC cytoplasm, a lamellar expansion (Le) emerges and spreads through the interstitial space. (C) Two SGC (SGC1 and SGC2) with lamellar expansions (arrows) are visible. Scale bars: A = 1µm; B = 0.5 µm; C = 2 µm.

Fig. 2. (A) Cross section of *Rana catesbeiana*'s dorsal root ganglion showing satellite glial cell (SGC) nucleus with heterochromatin (large arrow) attached to the nuclear membrane. Note the nuclear pore (arrow). (B), (C), (D) and (E) Mitochondria (M) with mitochondrial cristae (MC) and dense granules (DG), Golgi complex (GC), vesicles (V), ribosomes (R), filaments (F), lysosomes (LY) and lipid droplets (LD) are seen in the SGC cytoplasm. Scale bars: A, E = 2µm; B, C, D = 0.5 µm.

Fig. 3. Cross section of *Rana catesbeiana*'s dorsal root ganglion showing Hotchkiss' periodic acid-Schiff (A) and NADPH-diaphorase (B) positive reactions in neuron (NEU) and satellite glial cell (SGC). Scale bars: A and B = 20 µm.

Fig. 4. Cross section of *Rana catesbeiana*'s dorsal root ganglion immunostained with serotonin (A), tyrosine hydroxylase (B), and glucose transporter (Glut) type 3 (C) and 1 (D). Note the presence of immunoreactivity in neuronal (NEU) cytoplasm (serotonin and Glut-3), satellite glial cell (SGC) (Glut-1) and around neurons (arrows) (tyrosine hydroxilase). Scale bars: A-E = 20 µm.

Figure 1

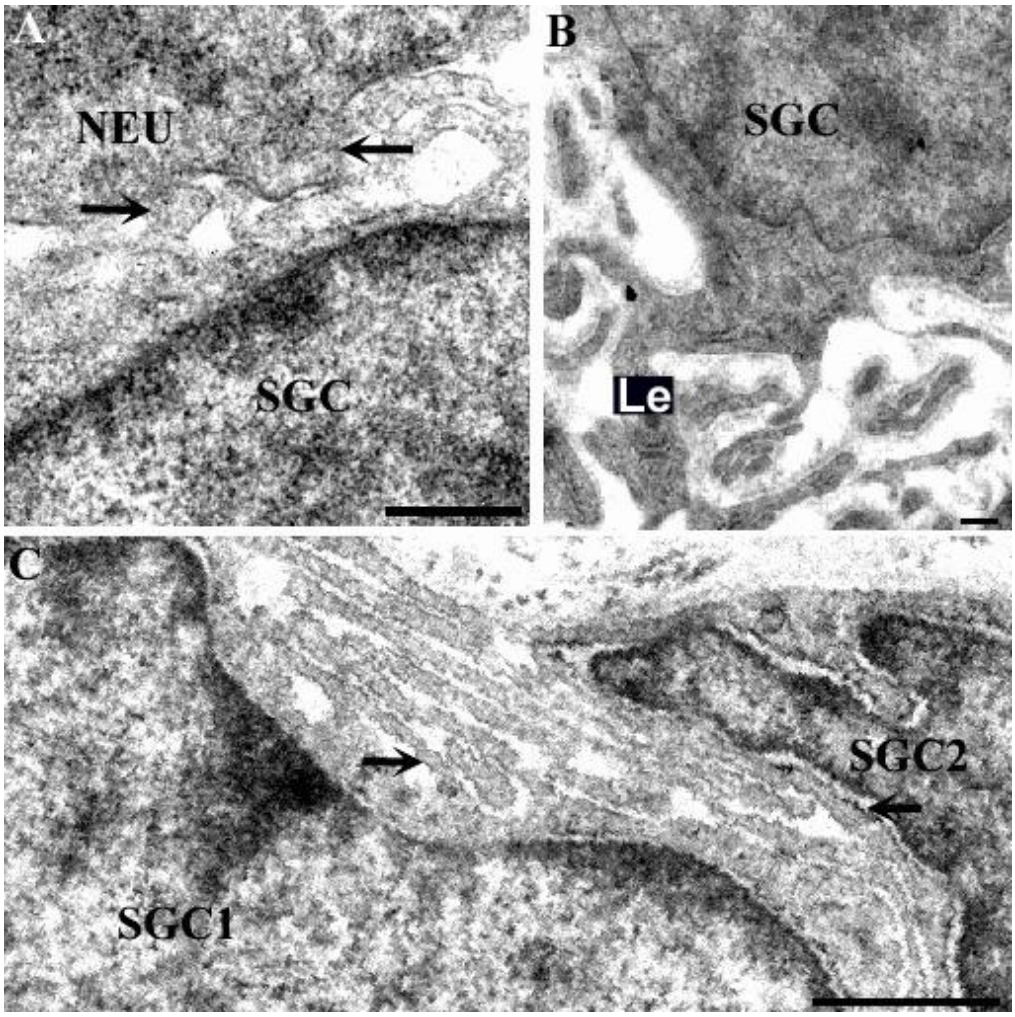

Figure 2

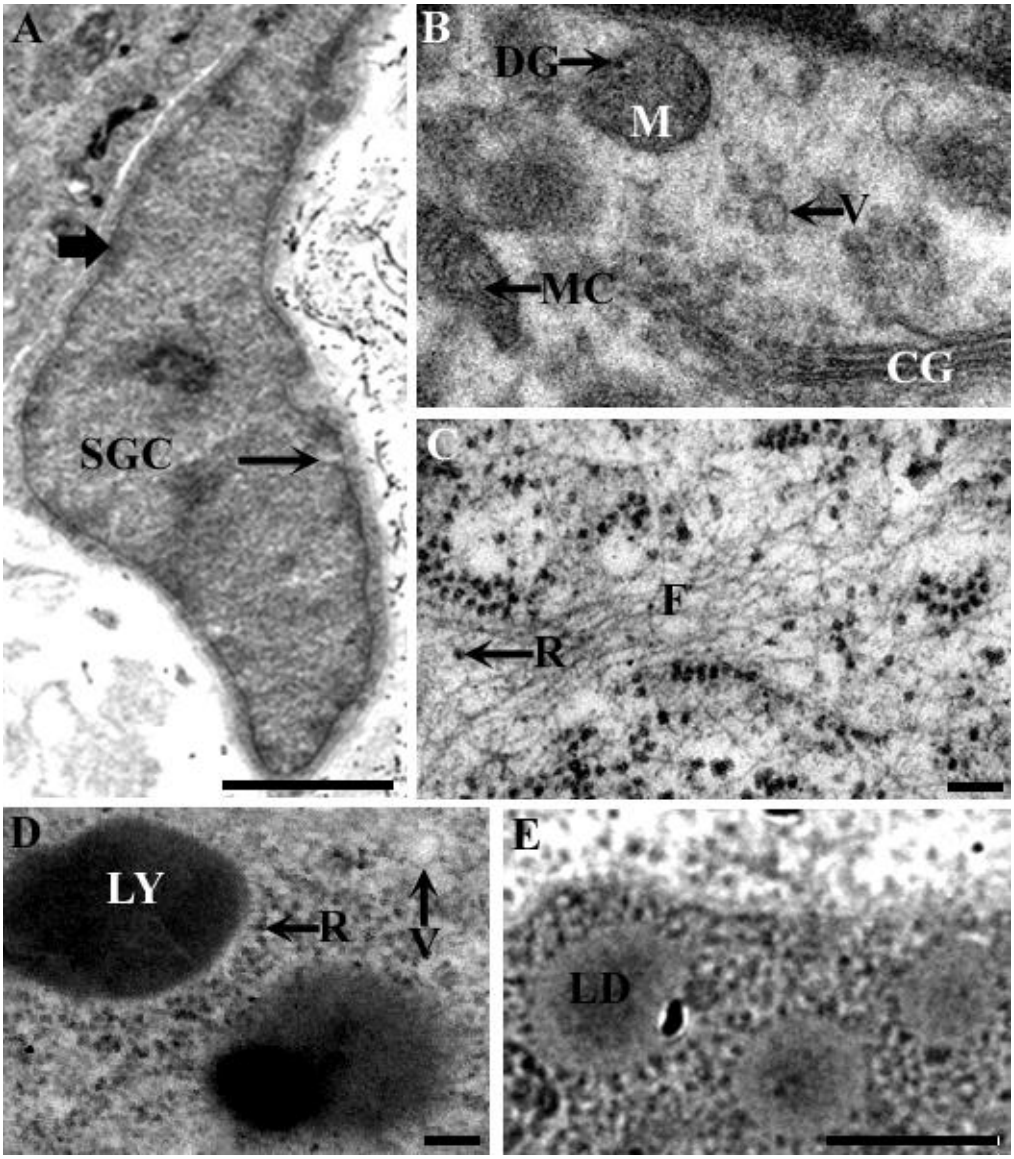

Figure 3

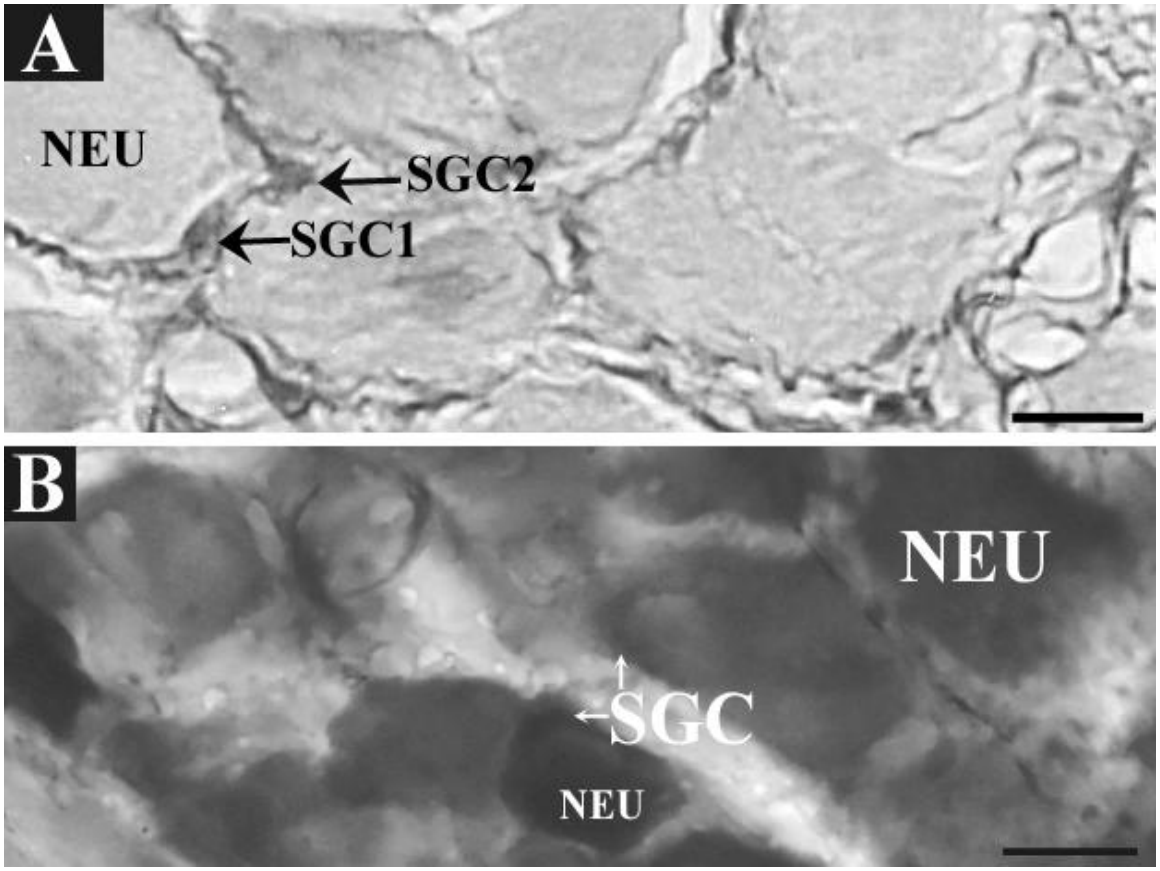

Figure 4

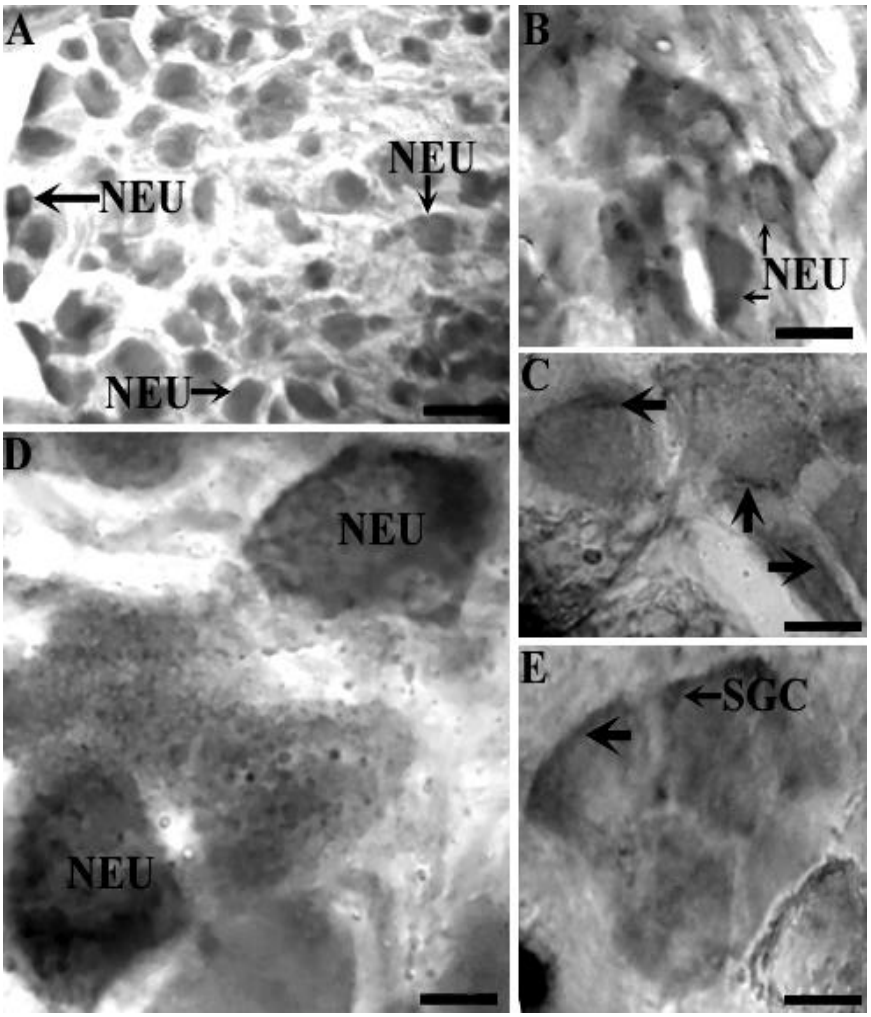

3.2. Artigo publicado na revista Brazilian Journal of Medical and Biological Research.

Brazilian Journal of Medical and Biological Research (2013) 00: 1-8, http://dx.doi.org/10.1590/1414-431X20132853
ISSN 1414-431X

Effects of sciatic nerve transection on ultrastructure, NADPH-diaphorase reaction and serotonin-, tyrosine hydroxylase-, c-Fos-, glucose transporter 1- and 3-like immunoreactivities in frog dorsal root ganglion

F. Rigon[1], D. Rossato[1], V.B. Auler[1], L. Dal Bosco[1], M.C. Faccioni-Heuser[2,3] and W.A. Partata[1]

[1]Departamento de Fisiologia, Instituto de Ciências Básicas da Saúde, Universidade Federal do Rio Grande do Sul, Porto Alegre, RS, Brasil
[2]Departamento de Ciências Morfológicas, Universidade Federal do Rio Grande do Sul, Porto Alegre, RS, Brasil
[3]Centro de Microscopia Eletrônica, Universidade Federal do Rio Grande do Sul, Porto Alegre, RS, Brasil

Abstract

Frogs have been used as an alternative model to study pain mechanisms. Since we did not find any reports on the effects of sciatic nerve transection (SNT) on the ultrastructure and pattern of metabolic substances in frog dorsal root ganglion (DRG) cells, in the present study, 18 adult male frogs (*Rana catesbeiana*) were divided into three experimental groups: naive (frogs not subjected to surgical manipulation), sham (frogs in which all surgical procedures to expose the sciatic nerve were used except transection of the nerve), and SNT (frogs in which the sciatic nerve was exposed and transected). After 3 days, the bilateral DRG of the sciatic nerve was collected and used for transmission electron microscopy. Immunohistochemistry was used to detect reactivity for glucose transporter (Glut) types 1 and 3, tyrosine hydroxylase, serotonin and c-Fos, as well as nicotinamide adenine dinucleotide phosphate diaphorase (NADPH-diaphorase). SNT induced more mitochondria with vacuolation in neurons, satellite glial cells (SGCs) with more cytoplasmic extensions emerging from cell bodies, as well as more ribosomes, rough endoplasmic reticulum, intermediate filaments and mitochondria. c-Fos immunoreactivity was found in neuronal nuclei. More neurons and SGCs surrounded by tyrosine hydroxylase-like immunoreactivity were found. No change occurred in serotonin- and Glut1- and Glut3-like immunoreactivity. NADPH-diaphorase occurred in more neurons and SGCs. No sign of SGC proliferation was observed. Since the changes of frog DRG in response to nerve injury are similar to those of mammals, frogs should be a valid experimental model for the study of the effects of SNT, a condition that still has many unanswered questions.

Key words: Axotomy; Immunoreactivity; Histochemistry

Introduction

In amphibians, as in mammals, the dorsal root ganglion (DRG) is composed of three classes of neurons classified according to morphology and function. In addition to neurons, myelinated and unmyelinated fibers, macrophages, fibroblasts, and satellite glial cells (SGCs) are also resident components (1,2). In this ganglion some neurons show reactivity to nicotinamide adenine dinucleotide phosphate diaphorase (NADPH-diaphorase) (3,4), which is considered to be equivalent to nitric oxide (NO) synthase, the enzyme responsible for NO synthesis (5). DRG cells also respond to application of serotonin (6,7) and catecholamine (8).

Amphibians have been used as a model for the study of pain mechanisms (9-15). The reasons for using amphibians in pain research are varied. According to Stevens (9), the use of these animals provides a phylogenetic perspective on the mechanisms of pain research. Other issues include the simplicity of the amphibian central nervous system, the economic advantage of using these animals, and ethical considerations about conducting pain research in non-mammalian vertebrate species. In this context, frog spinal cord and DRG have been used to demonstrate the changes in different neurotransmitters and neuropeptides after sciatic

Correspondence: W.A. Partata, Departamento de Fisiologia, Instituto de Ciências Básicas da Saúde, UFRGS, 90050-170 Porto Alegre, RS, Brasil. Fax: +55-51-3308-3166. E-mail: partataw@gmail.com

Received November 22, 2012. Accepted March 18, 2013. First published online.

nerve transection (SNT), one of the models that mimic the clinical conditions of neuropathic pain (16-18). These studies reported alterations that shared similarities with those observed in mammals, while others were unique to this animal species. Moreover, further studies are necessary to better understand the effects of SNT on frog nervous tissue to support the use of this model in this experimental condition.

In mammals, serotonin transporter deficiency attenuated the mechanical allodynia and heat hyperalgesia, symptoms frequently observed in neuropathic pain (19). Tyrosine hydroxylase, a rate-limiting enzyme responsible for catalyzing the conversion of L-tyrosine to the precursor of dopamine and then norepinephrine and epinephrine, shows changes in its immunoreactivity pattern in DRG cells after SNT (20). Glucose transport (Glut) also appears to be modulated by noxious stimuli and denervation (21). These experimental conditions upregulated c-Fos, a protein that is regarded as a marker of neural activation by noxious stimulation (22). SNT also increases NADPH-diaphorase staining in mammalian DRG cells (23,24). SGCs, cells that support DRG neurons both physically and metabolically (25), also change their ultrastructure after peripheral nerve lesion (26).

In order to elucidate the effects of SNT on the ultrastructure and pattern of metabolic substances in bullfrog DRG cells, we used transmission electron microscopy to reveal the effects on the ultrastructure of these cells, and light microscopy to demonstrate the distribution of NADPH-diaphorase reaction and the pattern of Glut1- and Glut3-, serotonin-, tyrosine hydroxylase-, and c-Fos-like immunoreactivity. The experiment was performed 3 days after SNT because previous studies demonstrated that the functional changes in frog nervous tissue are already present 3 days after axotomy (16-18). We think that these findings will determine if these responses are similar across amphibians and mammals, potentially increasing our knowledge of the effects of SNT on frog nervous tissue.

Material and Methods

Animals

Eighteen adult male frogs, *Rana catesbeiana*, weighing 100-200 g were obtained from Ranasul (Brazil). Upon arrival at the laboratory they were housed in cages with water and kept under natural conditions of temperature and photoperiod. The animals were fed specific food *ad libitum* and acclimated to laboratory conditions for at least 2 weeks before being used. They were divided into 3 experimental groups of 6 animals each: naive (animals did not undergo surgical manipulation), sham (animals in which all surgical procedures to expose the sciatic nerve were used except transection of this nerve), and SNT (animals in which the sciatic nerve was exposed and transected). For the surgical procedures, frogs were anesthetized intramuscularly with 3% prilocaine (Prilonest®, DFL Indústria e Comércio S.A., Brazil; 0.1 mL/100 g body weight). In the SNT group, the right sciatic nerve was exposed and transected approximately 5 mm distal to the sciatic notch. Flexion and ocular reflexes were used to monitor the anesthesic effect. After surgery, the muscle and skin layer were immediately sutured with thread and a topical antibiotic was applied. The animals were killed 3 days after the procedure. The experimental protocol followed the NIH Guide for the Care and Use of Laboratory Animals (NIH publication 85-23, revised 1985) and was approved by the Neuroscience Graduate Committee of Instituto de Ciências Básicas da Saúde, Universidade Federal do Rio Grande do Sul.

Transmission electron microscopy

The bilateral DRG of the sciatic nerve were dissected out within 3 min after frog decapitation. They were fixed immediately by immersion in 2% paraformaldehyde, 1.5% glutaraldehyde (Sigma, USA) and 0.1 M phosphate buffer (PB), pH 7.3, for 1 h. The material was washed in the same buffer and postfixed in 1% osmium tetroxide (Sigma) diluted in PB for 1 h at room temperature. Next, the sections were washed in PB and subsequently dehydrated with an ascending series of acetone, and then embedded in Araldite (Durcupan, Fluka, Switzerland). Semithin sections (1 µM) were obtained using an ultramicrotome (MT6000-XL, RMC, USA) with a diamond knife (Diatome, Switzerland) and stained with 1% toluidine blue for examination under a light microscope. Ultrathin sections (70 nm) were cut with the same ultramicrotome using a diamond knife (Drukker, The Netherlands). These sections were stained with 2% uranyl acetate (Merck, Germany) followed by 1% lead citrate and examined with a JEM 120 EX II electron microscope (Joel, Japan).

Histochemistry and immunohistochemistry

For the NADPH-diaphorase and immunohistochemical procedure, the frogs were decerebrated and after a brief saline flush they were perfused intracardially with 4% paraformaldehyde in 0.1 M PB, pH 7.4. The DRG were quickly dissected out, immersed in the same fixative solution for 4 h and then cryoprotected in 15 and 30% sucrose solutions in PB at 4°C. Serial coronal sections (50 µM) were obtained with a cryostat and collected in cold phosphate-buffered saline (PBS).

For the NADPH-diaphorase procedure, free-floating sections were pre-incubated in 10 mL PB containing 12 µL Triton X-100 for 10 min. The sections were then transferred to fresh NADPH-diaphorase medium containing 0.5 mg/mL β-NADPH, 0.2 mg/mL nitroblue tetrazolium, and 0.2 M PB containing 12 µL Triton X-100. After pre-incubation at room temperature for 5 min under continuous shaking, they were incubated at 37°C for 4 h. The reaction was stopped by the addition of excess

0.1 M PB. Control sections were incubated in a reaction medium without substrate.

For immunohistochemistry, the sections were treated with 3% hydrogen peroxide in 10% methanol for 30 min, washed with PBS for a further 30 min and incubated for 30 min in 3% normal goat serum in PBS containing 0.4% Triton X-100 (PBS-T). The sections were incubated overnight with gentle shaking at 4°C with a primary antibody [c-Fos, a polyclonal antibody against 4-17 amino acids, diluted 1:700 (Calbiochem, Germany); Glut1, a polyclonal antibody that recognizes ~42- to 45-kDa protein, diluted 1:1000 (Sigma); Glut3, a polyclonal antibody that recognizes the C-terminal sequence of the protein, diluted 1:1000 (Sigma); serotonin, a polyclonal antibody diluted 1:1200 (Sigma); tyrosine hydroxylase, a polyclonal antibody diluted 1:1000 (Calbiochem)]. The primary antibody was then removed and the sections washed in PBS-T for 30 min. The sections were then immersed in a secondary antibody (anti-IgG, Sigma), diluted 1:50 in PBS-T for 2 h at room temperature with gentle shaking. After washing with PBS-T for 30 min, a peroxidase anti-peroxidase soluble complex andibody (Sigma) diluted 1:500 was applied for 2 h at room temperature. The samples were then washed in PBS and incubated in a solution of 3,3′-diaminobenzidine tetrahydrochloride (60 mg/100 mL, Sigma) and 0.005% (v/v) hydrogen peroxide in PBS. Specific immunostaining was abolished when the primary antibody was omitted from the staining sequence.

After the histochemical and immunohistochemical procedures, the sections were mounted onto gelatinized slides, dehydrated, cleared, and covered with Entellan (Merck). The sections were examined and photographed with a Nikon Optiphot-2 microscope equipped with a Nikon FX-35DX camera (Japan).

Results

In naive animals, DRG neurons had a typical aspect. Ultrastructurally, some neurons exhibited electron-dense cytoplasm while others showed intermediate electron densities. Neuronal cell bodies (Figure 1A) were ensheathed by SGCs. Sometimes only a thin ring of SGC cytoplasm was observed around the soma of the sensory neuron (Figure 1B). In the SGC cytoplasm, there were well-developed rough endoplasmic reticulum (RER), ribosomes and mitochondria (Figures 1 and 2A-C). Polyribosomes with characteristic rosettes were also found. SGCs had a fusiform shape and were separated from adjacent neurons by a space of about 20 nm. Lamellar cytoplasmic expansions emerging from SGCs and projections from neurons were commonly observed in this space (Figure 1A,B).

Three days after SNT, several sensory neurons showed increased size, mitochondrial accumulation, and vacuolation in their cytoplasm (Figure 1C). Some mitochondria were so dilated and vacuolated that there were empty spaces (Figure 1D). The nuclei of these neurons began to take an irregular shape. SGCs did not show these changes. The nucleus of SGCs showed a characteristic chromatin condensation, with heterochromatin attached to the nuclear membrane. The nuclear envelope showed regular outlines and no changes were observed in its pores (Figure 2D). A 10-12-nm thick plasma membrane was observed in SGCs and no interruptions along this membrane were seen. Although no statistical analysis was performed, more ribosomes, RER, intermediate filaments, and mitochondria were observed in SGC cytoplasm (Figure 2D-F). Many free ribosomes, polysomes, RER and mitochondria were evenly distributed throughout the SGC cytoplasm, while intermediate filaments (8-10 nm in diameter) were more common in the perinuclear region, which seemed to form a very dense network. Mitochondria and RER generally appeared normal. Mitochondria showed intracristal spaces of normal aspect. While in most cells the RER showed the usual features, sometimes it appeared to be a little dilated. Many lamellar cytoplasmic expansions emerged from SGCs. These expansions had different diameters and lengths and assumed an irregular shape (Figure 3). Although no statistical analysis was performed, the number of SGCs did not seem to be altered after SNT. In the DRG of sham animals, no ultrastructural change was seen in ganglion cells (data not shown).

In naive animals, a strong NADPH-diaphorase reaction occurred in medium and small neurons and in SGCs. In neurons, the positive reaction was more common in medium-sized neurons. The positive SGCs surrounded either positive or non-positive large, medium or small neurons (Figure 4A). Immunoreactivity for c-Fos was found predominantly in the cytoplasm of large and medium neurons (Figure 4C), but no immunoreaction was found in SGCs. Tyrosine hydroxylase-like immunoreactivity was found surrounding neurons (Figure 4E) and SGCs. This glial cell did not show immunoreactivity to serotonin. Some serotonin-like immunoreactivity was found in a few neurons (Figure 5A). While Glut3-like immunoreactivity was found in neurons (Figure 5B), Glut1-like immunoreactivity was located in the capsule of the DRG, blood vessels and SGCs.

SNT also caused changes in histochemical and immunohistochemical patterns. The NADPH-diaphorase reaction was more common in neurons from ipsilateral ganglia. This reaction was strong and prevailed in medium and small neurons (Figure 4B). The number of positive SGCs was also higher after SNT, regardless of whether these cells surrounded positive large, medium or small neurons. Immunoreactivity for c-Fos was found in a larger number of nuclei of sensory neurons (Figure 4D), but it was observed in the cytoplasm of only few neurons. SGCs did not exhibit this immunoreactivity. The number of DRG neurons and SGCs surrounded by tyrosine hydroxylase-like immunoreactivity was also increased after SNT (Figure 4F). However, no change was found in the serotonin immuno-

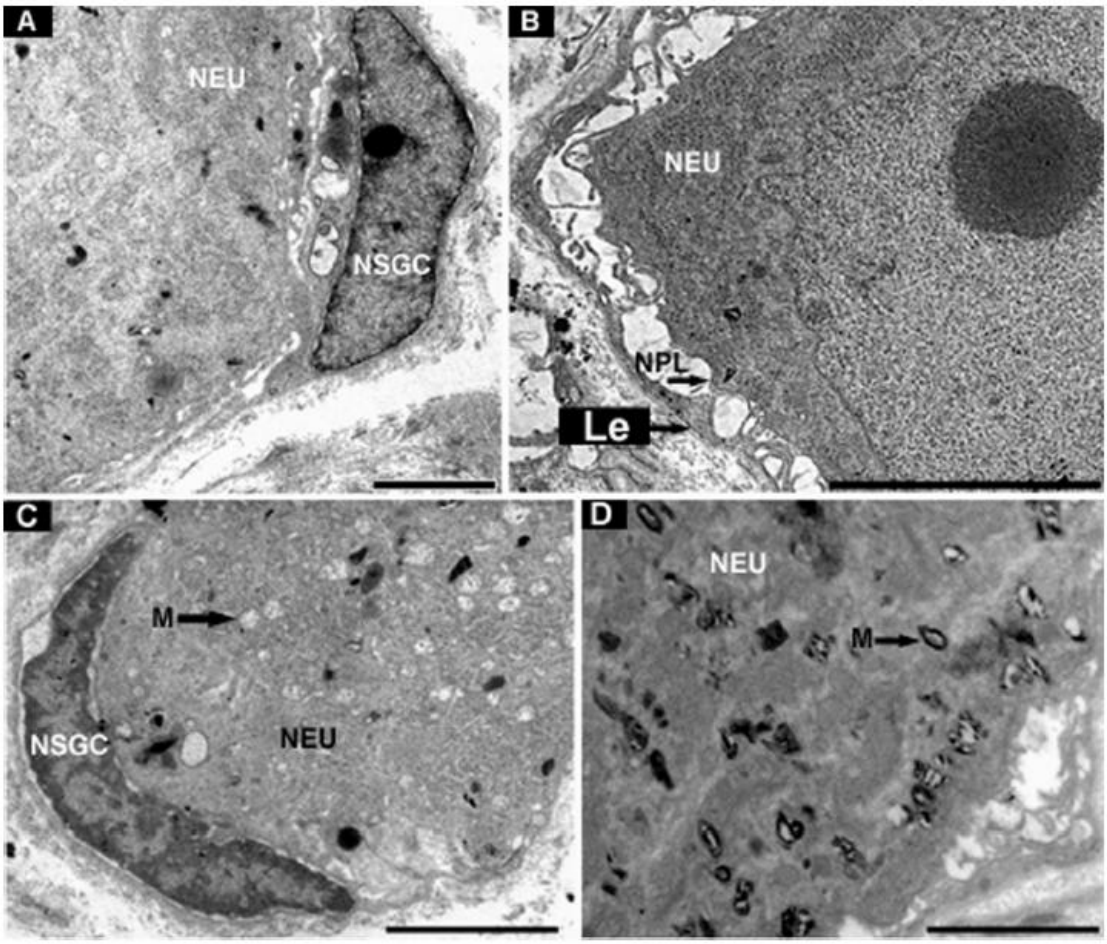

Figure 1. Cross-section of a naive (*A*, *B*) and transected (*C*, *D*) *Rana catesbeiana*'s dorsal root ganglion. *A*, Nuclear satellite glial cells (NSGC) close to a sensory neuron (NEU). *B*, Lamellar cytoplasmic expansions (Le) from a satellite glial cell near the neuronal projection (NPL). *C*, Sensory NEU in the chromatolysis process. Note the mitochondrial (M) accumulation in the neuronal cytoplasm and the characteristic chromatin condensation in the NSGC. *D*, Sensory NEU in the chromatolysis process and vacuolated M. Scale bars: *A* (0.2 µm); *B* (5 µm), *C* and *D* (2 µm).

reactivity pattern. Similarly, Glut1 and Glut3 immunoreactivity did not change after SNT (data not shown).

Discussion

In naive frogs, our results confirmed previous reports (1-4). SNT, in turn, induced prominent morphological changes in the ipsilateral ganglion from axotomized frogs. Most of these changes were similar to those described in mammals. Differently from mammals, however, SNT did not induce proliferation of SGCs 3 days after the surgical procedure in frogs. SGC proliferation appears to be part of the glial responses to nerve injury in mammalian sensory ganglia (26-29). According to Humbertson Jr. et al. (27), the SGC/neuron ratio begins to change on the first day after axotomy, with its value doubling at 6 days and returning to baseline values around day 18. A possible explanation for this difference may be the nervous system's slower metabolic rate in frogs than in mammals (30). If this is true, we can think that the proliferation of SGCs may be occurring in a slower fashion in frog DRG. Clarification of this issue depends on the demonstration of morphological changes in SGCs from axotomized frogs at later times. Research into this matter is underway in our

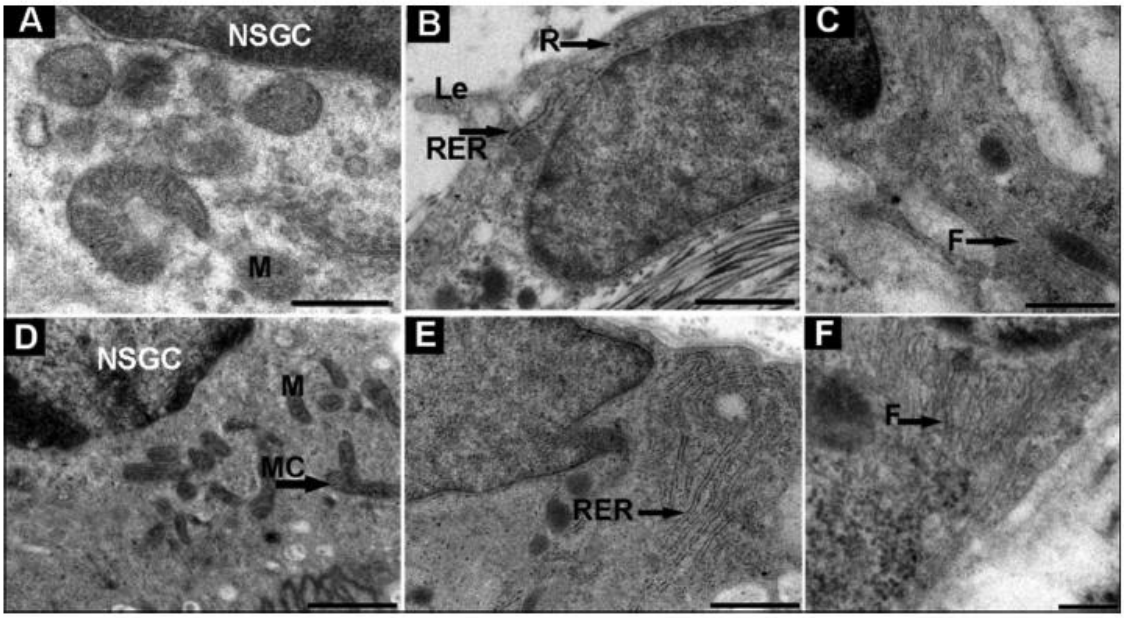

Figure 2. Cross-section of a naive (*A*, *B*, *C*) and transected (*D*, *E*, *F*) *Rana catesbeiana*'s dorsal root ganglion. *A*, Nuclear satellite glial cells (NSGC) with chromatin condensation and heterochromatin attached to the nuclear membrane. Note mitochondria (M) with an intracristal space of normal aspect. *B* and *C*, Ribosomes (R), rough endoplasmic reticulum (RER) and intermediate filaments (F) in the cytoplasm of satellite glial cell (SGC). Note the lamellar cytoplasmic expansion (Le) emerging from SGC. *D*, Nucleus of SGC of normal aspect 3 days after sciatic nerve transection. Note the greater number of M (*D*), RER (*E*) and F (*F*) in SGC cytoplasm. MC = tranverse mitochondrial cristae. Scale bars: *A*, *B*, *C* = 0.5 µm; *E* and *F* = 1 µm; *D* = 0.2 µm.

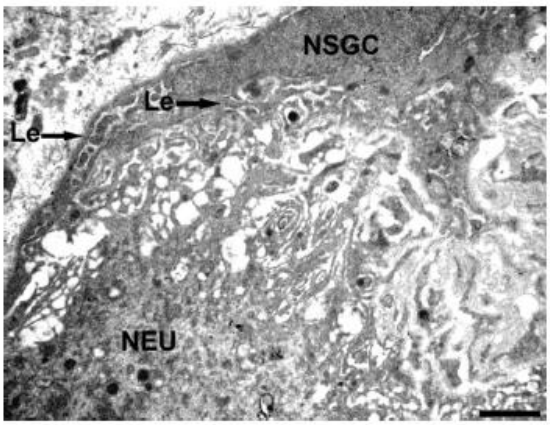

Figure 3. Cross-section of a *Rana catesbeiana*'s dorsal root ganglion 3 days after sciatic nerve transection. Lamellar cytoplasmic expansions (Le) from the cytoplasm of a satellite glial cell (SGC) can be seen, spreading through the interstitial space toward the projections that depart from the neuronal body (NEU). Note chromatin condensation of the nuclear SGC (NSGC). Scale bar = 2 µm.

laboratory. Supportive of the continuation of this research line is the report of increased numbers of SGCs 30 and 90 days after nerve transection in mammals (26).

Some differences between frog and rat responses appear to be common. While moderate neuropeptide Y immunoreactivity was found in normal frog DRG, no immunoreaction to this neuropeptide was observed in rat spinal ganglia. SNT increased neuropeptide Y immunoreaction in ipsilateral and contralateral ganglia of the frogs, while this increase was only seen ipsilaterally in rats (18). It is probable that the differences between frogs and rats represent peculiar responses of frogs. Nevertheless, they do not preclude the use of frogs to study the effects of SNT on nervous tissue. Similar to mammals (31,32), the axotomized frogs' DRG exhibited sensory neurons with enlarged perikarya, swelling in mitochondria and a nuclear membrane with enfolding and indentation. In SGCs there were more intermediate filaments, ribosomes, endoplasmic reticulum, and mitochondria. Histochemical and immunohistochemical changes were also similar to those described in mammals (2,22-24,33-37), with an increase in NADPH-diaphorase reaction and in immunoreactivity to c-Fos and tyrosine hydroxylase, but with no change in serotonin, Glut1 or Glut3 immunoreactivity. Thus, these changes may be playing the same

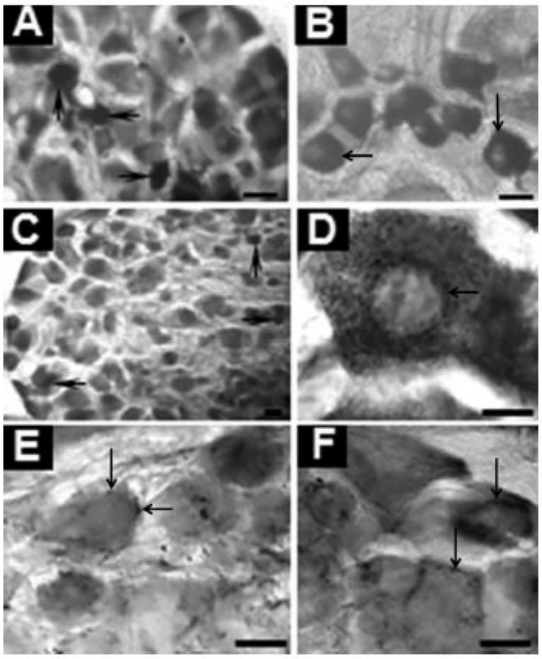

Figure 4. Cross-section of a naive (*A*, *C*, *E*) and transected (*B*, *D*, *F*) *Rana catesbeiana*'s dorsal root ganglion. Note the larger number of cells positive for the NADPH-diaphorase reaction (*B*), the c-Fos-like immunoreactivity in the nucleus of the neuron (*D*), and the more intense tyrosine hydroxylase-like immunoreactivity surrounding neurons (*F*) 3 days after sciatic nerve transection. Arrows point to neurons positive for NADPH-diaphorase (*A*) and c-FOS (*C*). Scale bars: A and B = 20 µm, C = 10 µm, D and F = 40 µm.

functional role in frogs. Because total mitochondrial mass and maximum rate of oxygen consumption appear to be directly linked in mammals (38), the increased number of mitochondria found in frog DRG may indicate a higher ability of SGCs to produce energy. This hypothesis was suggested to explain the enlargement of mitochondria in SGCs from mammalian DRG observed after peripheral nerve injury (29). The greater number of ribosomes and RER reinforces the higher activation of SGCs from frog DRG as early as 3 days after SNT. This higher activation of these cells also occurs in mammals (39). Another change that reinforces the activation of SGCs in frog DRG in response to SNT is the increased NADPH-diaphorase reaction in these cells and sensory neurons. In mammals, it was suggested that neuronal NO signals satellite glia in axotomized DRG to neutralize the cytotoxic effect of inducible NO synthase by inducing neurotrophic factors in the glial cell (40). A similar hypothesis may be raised for frogs to explain the increased NADPH-diaphorase reaction in parallel to the ultrastructural changes in SGCs.

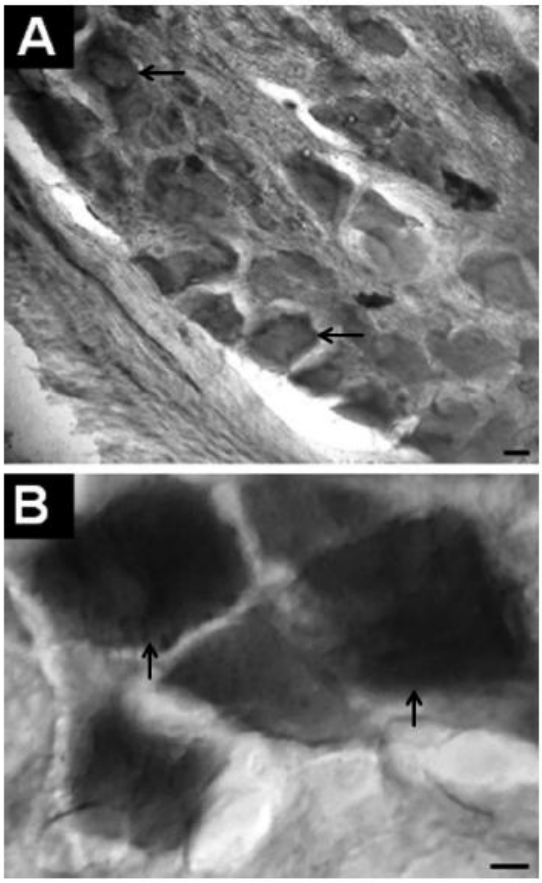

Figure 5. Serotonin- (*A*) and Glut3-like (*B*) immunoreactivity in a medium neuron of the dorsal root ganglion from a naive frog. Scale bars: *A* = 20 µm; *B* = 40 µm.

Overall, the present study provides evidence that SNT induces ultrastructural, histochemical and immunohistochemical changes in frog DRG that are very similar to those described in mammals. The difference appears to be the beginning of SGC proliferation. Thus, our results support the use of frogs to study the effects of SNT, a model of neuropathic pain, on nervous tissue. The use of frogs in these studies provides knowledge not only about this issue, which still has many unanswered questions, but also about the evolution of these responses in vertebrates.

Acknowledgments

Research supported by FAPERGS and CNPq.

References

1. Ten Donkelaar HJ. Anurans. In: Nieuwenhuys R, Ten Donkellar HJ, Nicholson C (Editors), *The central nervous system of vertebrates*. Berlin: Springer-Verlag; 1998. p 1151-1314.
2. Matsuda S, Kobayashi N, Terashita T, Shimokawa T, Shigemoto K, Mominoki K, et al. Phylogenetic investigation of Dogiel's pericellular nests and Cajal's initial glomeruli in the dorsal root ganglion. *J Comp Neurol* 2005; 491: 234-245, doi: 10.1002/cne.20713.
3. Crowe MJ, Brown TJ, Bresnahan JC, Beattie MS. Distribution of NADPH-diaphorase reactivity in the spinal cord of metamorphosing and adult *Xenopus laevis*. *Brain Res Dev Brain Res* 1995; 86: 155-166, doi: 10.1016/0165-3806(95)00021-5.
4. Cristino L, Florenzano F, Bentivoglio M, Guglielmotti V. Nitric oxide synthase expression and cell changes in dorsal root ganglia and spinal dorsal horn of developing and adult *Rana esculenta* indicate a role of nitric oxide in limb metamorphosis. *J Comp Neurol* 2004; 472: 423-436, doi: 10.1002/cne.20057.
5. Hope BT, Michael GJ, Knigge KM, Vincent SR. Neuronal NADPH diaphorase is a nitric oxide synthase. *Proc Natl Acad Sci U S A* 1991; 88: 2811-2814, doi: 10.1073/pnas.88.7.2811.
6. Holz GG, Anderson EG. The actions of serotonin on frog primary afferent terminals and cell bodies. *Comp Biochem Physiol C* 1984; 77: 13-21, doi: 10.1016/0742-8413(84)90124-5.
7. Philippi M, Vyklicky L, Kuffler DP, Orkand RK. Serotonin- and proton-induced and modified ionic currents in frog sensory neurons. *J Neurosci Res* 1995; 40: 387-395, doi: 10.1002/jnr.490400313.
8. Chen Y, Wang AJ, Ma YL. [Effects of morphine on sensitivities of alpha-adrenoceptors in toad spinal ganglion neurons]. *Zhongguo Yao Li Xue Bao* 1993; 14: 417-420.
9. Stevens CW. Opioid research in amphibians: an alternative pain model yielding insights on the evolution of opioid receptors. *Brain Res Brain Res Rev* 2004; 46: 204-215, doi: 10.1016/j.brainresrev.2004.07.003.
10. Stevens CW, Brasel CM, Mohan S. Cloning and bioinformatics of amphibian mu, delta, kappa, and nociceptin opioid receptors expressed in brain tissue: evidence for opioid receptor divergence in mammals. *Neurosci Lett* 2007; 419: 189-194, doi: 10.1016/j.neulet.2007.04.014.
11. Stevens CW, Martin KK, Stahlheber BW. Nociceptin produces antinociception after spinal administration in amphibians. *Pharmacol Biochem Behav* 2009; 91: 436-440, doi: 10.1016/j.pbb.2008.08.022.
12. Chen NC, Srinivasan RC, Shauver MJ, Chung KC. A systematic review of outcomes of fasciotomy, aponeurotomy, and collagenase treatments for Dupuytren's contracture. *Hand* 2011; 6: 250-255, doi: 10.1007/s11552-011-9326-8.
13. Coble DJ, Taylor DK, Mook DM. Analgesic effects of meloxicam, morphine sulfate, flunixin meglumine, and xylazine hydrochloride in African-clawed frogs (*Xenopus laevis*). *J Am Assoc Lab Anim Sci* 2011; 50: 355-360.
14. Ohkita M, Saito S, Imagawa T, Takahashi K, Tominaga M, Ohta T. Molecular cloning and functional characterization of *Xenopus tropicalis* frog transient receptor potential vanilloid 1 reveal its functional evolution for heat, acid, and capsaicin sensitivities in terrestrial vertebrates. *J Biol Chem* 2012; 287: 2388-2397, doi: 10.1074/jbc.M111.305698.
15. Saito S, Nakatsuka K, Takahashi K, Fukuta N, Imagawa T, Ohta T, et al. Analysis of transient receptor potential ankyrin 1 (TRPA1) in frogs and lizards illuminates both nociceptive heat and chemical sensitivities and coexpression with TRP vanilloid 1 (TRPV1) in ancestral vertebrates. *J Biol Chem* 2012; 287: 30743-30754, doi: 10.1074/jbc.M112.362194.
16. Partata WA, Cerveira JF, Xavier LL, Viola GG, Achaval M. Sciatic nerve transection decrease substance P immunoreactivity in the lumbosacral spinal cord of the frog (*Rana catesbeiana*). *Comp Biochem Physiol B Biochem Mol Biol* 2002; 131: 807-814, doi: 10.1016/S1096-4959(02)00041-6.
17. Guedes RP, Marchi MI, Viola GG, Xavier LL, Achaval M, Partata WA. Somatostatin-, calcitonin gene-related peptide, and gamma-aminobutyric acid-like immunoreactivitity in the frog lumbosacral spinal cord: distribution and effects of sciatic nerve transection. *Comp Biochem Physiol B Biochem Mol Biol* 2004; 138: 19-28, doi: 10.1016/j.cbpc.2004.01.004.
18. Guedes RP, Marchi MI, Achaval M, Partata WA. Complete sciatic nerve transection induces increase of neuropeptide Y-like immunoreactivity in primary sensory neurons and spinal cord of frogs. *Comp Biochem Physiol A Mol Integr Physiol* 2004; 139: 461-467, doi: 10.1016/j.cbpb.2004.10.006.
19. Hansen N, Uceyler N, Palm F, Zelenka M, Biko L, Lesch KP, et al. Serotonin transporter deficiency protects mice from mechanical allodynia and heat hyperalgesia in vincristine neuropathy. *Neurosci Lett* 2011; 495: 93-97, doi: 10.1016/j.neulet.2011.03.035.
20. Joseph L, Butera RJ. High-frequency stimulation selectively blocks different types of fibers in frog sciatic nerve. *IEEE Trans Neural Syst Rehabil Eng* 2011; 19: 550-557, doi: 10.1109/TNSRE.2011.2163082.
21. Stark B, Carlstedt T, Cullheim S, Risling M. Developmental and lesion-induced changes in the distribution of the glucose transporter Glut-1 in the central and peripheral nervous system. *Exp Brain Res* 2000; 131: 74-84, doi: 10.1007/s002219900300.
22. Soares HD, Chen SC, Morgan JI. Differential and prolonged expression of Fos-lacZ and Jun-lacZ in neurons, glia, and muscle following sciatic nerve damage. *Exp Neurol* 2001; 167: 1-14, doi: 10.1006/exnr.2000.7558.
23. Keilhoff G, Fansa H, Wolf G. Nitric oxide synthase, an essential factor in peripheral nerve regeneration. *Cell Mol Biol* 2003; 49: 885-897.
24. Lukacova N, Cizkova D, Krizanova O, Pavel J, Marsala M, Marsala J. Peripheral axotomy affects nicotinamide adenine dinucleotide phosphate diaphorase and nitric oxide synthases in the spinal cord of the rabbit. *J Neurosci Res* 2003; 71: 300-313, doi: 10.1002/jnr.10470.
25. Hanani M. Satellite glial cells in sensory ganglia: from form to function. *Brain Res Rev* 2005; 48: 457-476, doi: 10.1016/j.brainresrev.2004.09.001.
26. Arkhipova SS, Raginov IS, Mukhitov AR, Chelyshev YA. Satellite cells of sensory neurons after various types of sciatic nerve trauma in the rat. *Neurosci Behav Physiol* 2010; 40: 609-614, doi: 10.1007/s11055-010-9303-7.
27. Humbertson A Jr, Zimmermann E, Leedy M. A chronological study of mitotic activity in satellite cell hyperplasia associated

with chromatolytic neurons. *Z Zellforsch Mikrosk Anat* 1969; 100: 507-515, doi: 10.1007/BF00344371.

28. Pannese E. The structure of the perineuronal sheath of satellite glial cells (SGCs) in sensory ganglia. *Neuron Glia Biol* 2010; 6: 3-10, doi: 10.1017/S1740925X10000037.
29. Hanani M. Satellite glial cells in sympathetic and parasympathetic ganglia: in search of function. *Brain Res Rev* 2010; 64: 304-327, doi: 10.1016/j.brainresrev.2010.04.009.
30. McDougal DB Jr, Holowach J, Howe MC, Jones EM, Thomas CA. The effects of anoxia upon energy sources and selected metabolic intermediates in the brains of fish, frog and turtle. *J Neurochem* 1968; 15: 577-588, doi: 10.1111/j.1471-4159.1968.tb08956.x.
31. Oliveira AL. Apoptosis of sensory neurons and satellite cells after sciatic nerve transection in C57BL/6J mice. *Braz J Med Biol Res* 2001; 34: 375-380, doi: 10.1590/S0100-879X2001000300012.
32. Atlasi MA, Mehdizadeh M, Bahadori MH, Joghataei MT. Morphological identification of cell death in dorsal root ganglion neurons following peripheral nerve injury and repair in adult rat. *Iran Biomed J* 2009; 13: 65-72.
33. Lukacova N, Davidova A, Kolesar D, Kolesarova M, Schreiberova A, Lackova M, et al. The effect of N-nitro-L-arginine and aminoguanidine treatment on changes in constitutive and inducible nitric oxide synthases in the spinal cord after sciatic nerve transection. *Int J Mol Med* 2008; 21: 413-421.
34. Lin CT, Tsai YJ, Chen SH, Wang HY, Lin LH, Lue JH. Early expression of injury-induced neuropeptide Y in primary sensory neurons and the cuneate nucleus in diabetic rats with median nerve transection. *J Chem Neuroanat* 2010; 40: 102-111, doi: 10.1016/j.jchemneu.2010.05.006.
35. Wang D, Gao Y, Ji H, Hong Y. Topical and systemic administrations of ketanserin attenuate hypersensitivity and expression of CGRP in rats with spinal nerve ligation. *Eur J Pharmacol* 2010; 627: 124-130, doi: 10.1016/j.ejphar.2009.11.011.
36. Brumovsky PR, Seroogy KB, Lundgren KH, Watanabe M, Hokfelt T, Gebhart GF. Some lumbar sympathetic neurons develop a glutamatergic phenotype after peripheral axotomy with a note on VGLUT(2)-positive perineuronal baskets. *Exp Neurol* 2011; 230: 258-272, doi: 10.1016/j.expneurol.2011.05.004.
37. Xia CM, Colomb DG Jr, Akbarali HI, Qiao LY. Prolonged sympathetic innervation of sensory neurons in rat thoracolumbar dorsal root ganglia during chronic colitis. *Neurogastroenterol Motil* 2011; 23: 801-e339, doi: 10.1111/j.1365-2982.2011.01728.x.
38. Hoppeler H, Hudlicka O, Uhlmann E. Relationship between mitochondria and oxygen consumption in isolated cat muscles. *J Physiol* 1987; 385: 661-675.
39. Liu FY, Sun YN, Wang FT, Li Q, Su L, Zhao ZF, et al. Activation of satellite glial cells in lumbar dorsal root ganglia contributes to neuropathic pain after spinal nerve ligation. *Brain Res* 2012; 1427: 65-77, doi: 10.1016/j.brainres.2011.10.016.
40. Bradman MJ, Arora DK, Morris R, Thippeswamy T. How do the satellite glia cells of the dorsal root ganglia respond to stressed neurons? Nitric oxide saga from embryonic development to axonal injury in adulthood. *Neuron Glia Biol* 2010; 6: 11-17, doi: 10.1017/S1740925X09990494.

3.3. Artigo aceito para publicação na revista Brazilian Journal of Biology

Effects of Sciatic Nerve Transection on Glucose Uptake and Lactate Oxidation in Frog Dorsal Root Ganglia and Spinal Cord

Rigon, F.[a], *Horst, A.*[b], *Kucharski, LC.*[b], *Silva, RSM*[b], *Faccioni-Heuser, MC.*[c] *and Partata, WA.*[b*]

[a]Departamento de Fisioterapia, Universidade Luterana do Brasil – ULBRA, CEP 95560000, Torres, RS, Brazil

[b]Departamento de Fisiologia, Instituto de Ciências Básicas da Saúde, Universidade Federal do Rio Grande do Sul, CEP: 90040060, Porto Alegre, RS, Brazil

[c]Departamento de Ciências Morfológicas, ICBS, Universidade Federal do Rio Grande do Sul, CEP: 90040060, Porto Alegre, RS, Brazil

*e-mail: partataw@gmail.com

Number of figures: 03

Number of Table: 01

Running Title: Glucose uptake and lactate oxidation in frog nervous tissue

Abstract

Frogs have been used as an alternative model to study pain mechanisms because the simplicity of its nervous tissue and the phylogenetic approach on this question. One of these models is the sciatic nerve transection (SNT), which mimics the clinical symptoms of "phantom limb", a condition that arises in humans after amputation or transversal spinal lesions. In mammals, the SNT increase glucose metabolism and the lactate appears to serve as an energetic source to nerve cells. These questions are unknown to amphibians which have glucose as the major energy substrate and accumulate lactic acid in some conditions. Thus, our study demonstrated the effect of SNT on frog dorsal root ganglia (DRG) and spinal cord 1-[^{14}C] 2-deoxy-D-glucose (^{14}C-2-DG) uptake in the presence and absence of lactate. We also investigated the effect of this condition on the formation of $^{14}CO_2$ from ^{14}C-glucose and ^{14}C-L-lactate, and plasmatic glucose and lactate levels. The 3-O-[^{14}C] methyl-D-glucose (^{14}C-3-OMG) uptake was used to demonstrate the steady state tissue/medium glucose distribution ratio in these conditions. Three days after SNT there was increase in ^{14}C-2-DG uptake but no change in ^{14}C-3-OMG uptake. The increment in ^{14}C-2-DG uptake was reduced when lactate was added in the incubation medium. No change was found in glucose and lactate oxidation after SNT, but it reduced lactate and glucose blood levels. As in mammals, SNT increased the glucose metabolism in frog DRG. Considering the lactate effect on this uptake, it may be suggested the use of glucose in glycolitic pathways after SNT in frogs. Thus, our results strengthen frogs as experimental model to study the effects of SNT on nervous tissue, condition that still has many unanswered questions.

Keywords: Peripheral Nerve Lesion, 1-[^{14}C] 2-deoxy-D-glucose, 3-O-[^{14}C] methyl-D-glucose.

Efeito da secção do nervo isquiático sobre a captação de glicose e a oxidação de lactato em gânglio da raiz dorsal e medula espinhal de rãs

Resumo

As rãs vem sendo usadas como modelos experimentais alternativos no estudo da nocicepção, tanto pela simplicidade do seu tecido nervoso como por permitirem uma abordagem filogenética sobre o tema. Um desses modelos é a secção no nervo isquiático (SNI), o qual simula os sintomas clínicos do "membro fantasma", uma condição que ocorre nos humanos após amputação ou secção transversal da medula espinal. Em mamíferos, a SNI aumenta o metabolismo da glicose, e o lactato é uma fonte energética para as células nervosas. Todavia, essas questões são desconhecidas nos anfíbios, animais onde a glicose constitui o principal substrato energético do tecido nervoso e a concentração plasmática de lactato está aumentada em distintas situações. Assim, nós demonstramos os efeitos da SNI sobre a captação de 1-[^{14}C] 2-deoxi-D-glicose (^{14}C-2-DG), na presença e ausência de lactato no meio de incubação, em gânglio da raiz dorsal (GRD) e medula espinal de rã. Foram demonstrados ainda os efeitos dessa condição experimental sobre a formação de $^{14}CO_2$ a partir de ^{14}C-glicose e ^{14}C-L-lactato, e a concentração plasmática de glicose e lactato. A captação de 3-O-[^{14}C] metil-D-glicose (^{14}C-3-OMG) foi usada para demonstrar a relação tecido/meio estável da glicose nessas condições. A captação de ^{14}C-2-DG aumentou três dias após a SNI, sem qualquer alteração na captação de ^{14}C-3-OMG. O aumento foi reduzido quando o lactato foi acrescentado ao meio de incubação. A taxa de oxidação da glicose e do lactato não modificou após SNI, mas houve redução na concentração plasmática de glicose e de lactato. Esses resultados mostram que a SNI aumenta o metabolismo da glicose no DRG

de rãs, assim como ocorre nos mamíferos. Os efeitos do lactato sobre essa captação sugerem o uso da glicose na via glicolítica após a SNT em rãs. Assim, nossos resultados reforçam o uso das rãs como modelo experimental em estudos que visam demonstrar os efeitos da SNI sobre o tecido nervoso, já que ainda há muitas questões não respondidas sobre esse tema.

Palavras-chave: Lesão nervosa periférica, 1-[^{14}C] 2-deoxi-D-glicose, 3-O-[^{14}C] metil-D-glicose.

1. Introduction

The sciatic nerve transection (SNT) model mimics the clinical symptoms of "phantom limb", a condition that arises in humans after amputation or transversal spinal lesions (Klusáková and Dubový, 2009). Studies have been demonstrated that this condition causes structural, electrophysiological, molecular and metabolic changes in mammalian dorsal root ganglia (DRG) cells and spinal cord. These changes include progressive cellular loss (Oliveira, 2001; Yun and Jakobsen, 2010), proliferation and activation of satellite glial cells (Hanani, 2005) and reorganization of the metabolic priorities of neural cells (Enes et al., 2010). There is evidence that the transection of facial and hypoglossal nerves produced significant increase in glucose utilization in motor nuclei of these nerves in rats (Kreutzberg and Emmerst, 1980). Changes in the glucose uptake also occurred in rat auditory pathways after bilateral ablation of the cochlea (Ahn et al., 2004). In addition, after SNT there was a remarkable increase in vesicular glutamate transporter-2 ($VGLUT_2$) in the dorsal root fibers of these animals (Brumovsky et al., 2007). Studies have demonstrated that conditions where release of

glutamate is increased there is also a rise in lactate, which may be serving as an energetic source to nerve cells (Schurr et al., 1999; Schurr and Payne, 2007; Barros and Deitmer, 2010; Schurr and Gozal, 2012).

Amphibians have been used as an alternative model to study pain mechanisms (Stevens, 2004; Stevens et al., 2007; Stevens et al., 2009; Coble et al., 2011; Ohkita et al., 2012; Saito et al., 2012). The reasons for using amphibians in pain research are varied. According Stevens (2004) the use of these animals provides a phylogenetic perspective on the mechanisms of pain research. Other issues include the simplicity of the amphibian central nervous system and the economic advantage of using these animals. In addition, the metabolic changes are much slower in frog brain than those found in mammalian one (McDougal et al., 1968). Thus, frog nervous tissue offers a unique model to examine the relationship between SNT and glucose metabolism.

The bullfrog *Lithobates catesbianus* is an aquatic amphibian native from Unites States which was imported during the early 1930s and have been raised in Brazil ever since (Rocha and Branco, 1998). As this frog adapted to the climatic conditions of the Brazil, it is the specimen found in the breeding grounds. The ease of acquiring *Lithobates catesbianus* specimens has allowed the use of this animal as experimental model in our studies. One of the experimental situations is the SNT. In this condition, our results demonstrated changes in different neurotransmitters and neuropeptides after SNT. Some of alterations share similarities with those observed in mammals, but others are peculiar to this animal species (Partata et al., 2002; Guedes et al., 2004a, b). Moreover, further studies are necessary to better understand the effects of SNT on frog nervous tissue to support the use of this model in this experimental condition. Since there is a clear linkage between glucose uptake, lactate utilization and SNT in mammals, we hypothesized a similar relation in frogs because glucose has been

considered the major energy substrate to frog brain (McDougal et al., 1968), glucose transporters (Glut) types 1 and 3 are found in nervous tissue of these animals (Rigon et al., *in press*) and they accumulate lactic acid in some conditions (Warren and Jackson, 2005). Thus, the purpose of the present study was to demonstrate the effect of SNT on frog DRG 1-[^{14}C] 2-deoxy-D-glucose (^{14}C-2-DG) uptake in the presence and absence of lactate. In addition, it was demonstrated the formation of $^{14}CO_2$ from ^{14}C-glucose and ^{14}C- L-lactate, and glucose and lactate plasma levels after SNT. The 3-O-[^{14}C] methyl-D-glucose (^{14}C-3-OMG) uptake was used to demonstrate the steady state tissue/medium glucose distribution ratio in these conditions. All these parameters were also analyzed in lumbosacral spinal cord where the most sciatic nerve afferent fibers enter and motor neurons of this nerve are located (Penicnak and Dunlap, 1962; Sutherland and Nunnemacher, 1974). We used ^{14}C-2-DG because this molecule is a glucose analogue that is incorporated in neural tissue by the same pathways, and the same rate, as glucose, but it is not completely metabolized and therefore becomes trapped in the cell as deoxyglucose-6-phosphate and not further metabolized by the glycolytic pathway. All experiments were performed 3 days after SNT because previous works demonstrated that functional changes in frog nervous tissue are already present 3 days following axotomy (Partata et al., 2002; Guedes et al., 2004a, b).

2. Material and Methods

2.1. Experimental Animals

Specimens of adult male frogs *Rana catesbeiana* weighing 100-200g were obtained from RANASUL (Imbé, RS). Upon arrival at the laboratory they were housed

in cages with water and kept at 15-25^{o} C temperature (the average laboratory temperature) and photophase. The animals were fed *ad libitum* with specific food which was offered on the vibration plate where the pellets moved. The animals stayed in these laboratory conditions for at least 2 weeks being used. They were divided in three experimental groups (six animals/group): naive (animals did not undergo surgical manipulation), Sham (animals in which all surgical procedures to expose the sciatic nerve were used except transection of this nerve) and SNT (animals in which the sciatic nerve was exposed and transected). For surgical procedures, frogs were anesthetized with prilocaine (0.1 mL/100 g body weight). In SNT group, the right sciatic nerve was exposed and transected approximately 5 mm distal to the sciatic notch. In all animals the wound was closed and the animals were killed 3 days after the procedure. The results reported here were obtained between April and September. The experimental protocol followed the NIH *Guide for the Care and Use of Laboratory Animals* (NIH publication 85-23 revised 1985). All efforts were made to minimize the number of animals used and their suffering. The experimental protocol was approved by the graduate committee of the Institute of Basic Health Sciences, Federal University of Rio Grande do Sul.

2.2. Glucose uptake

Ganglia were excised from naive and transected frogs over a period of 3 min and rapidly transferred to sterile chilled Ringer's solution. The Ringer's solution was composed of NaCl 110 mM, KCl 1 mM, $CaCl_2$ 2 mM and $NaHCO_3$ 2 mM. The pH was adjusted to 7.4. Glucose was not added to guarantee availability of glucose transporter as done in other studies (Machado et al., 1991; Kaloyianni and Doukakis, 2003; De

Fraga et al., 2010). Each ganglion was placed in chilled Eppendorf tubes with known weight and weighed again. The difference was taken as ganglion weight and the value used to calculate the uptake. The tissues were then incubated at 25°C with constant shaking in 250 μL of frog Ringer`s solution in the presence of 0.15 μCi of ^{14}C-2-DG (39 mCi/mmol, Amersham). Incubation in the presence 0.15 μCi of 3-O-[^{14}C] methyl-D-glucose (^{14}C-3-OMG) (53 mCi/mmol, Amersham) was used in the same conditions to demonstrate the steady state tissue/medium glucose distribution ratio (Dienel et al., 1997). Incubations were performed in a Dubnoff incubator with an atmosphere of O_2:CO_2 (95:5, v/v). Following the incubations, the tissues were removed from the medium, rinsed twice in cold frog Ringer`s solution (without radiolabeled products), blotted on filter paper and immediately transferred to screw-cap tubes containing 1 Ml of distilled water, and alternately frozen and boiled three times. Aliquots (100 μl) of this solution and of the incubation medium were used for radioactive counting in toluene-TritonX-100 (2:1, v/v) -PPO 0.4%-POPO 0.01%. Radioactivity was measured in a liquid scintillation spectrometer (LKB Wallac scintillation counter). Results were expressed as tissue/medium (T/M) rate, i.e., dpm/mL of tissue fluid divided by dpm/mL of incubation medium.

For better visualization of the sequence of experiments, they are described below in separate experiments and in the sequence of their performance.

Experiment 1: Time curve. DRG and spinal cord from naive frogs were incubated under the above conditions with 0.15 μCi of ^{14}C-2-DG or ^{14}C-3-OMG for 5, 15, 60 and 120 minutes.

Experiment 2: Effects of SNT on ^{14}C-2-DG uptake. Three days after peripheral injury the DRG and lumbosacral spinal cord were quickly dissected out and incubated, separately, under the above conditions. The ganglia obtained from the same spinal cord

segment were separated ipsilaterally and contralaterally to the nerve lesion. The tissues were incubated with 0.15 μCi ^{14}C-2-DG or ^{14}C-3-OMG for 60 minutes under the same conditions initially described.

Experiment 3: Effects of lactate on ^{14}C-2-DG uptake. The tissues were incubated with 0.15 μCi of ^{14}C-2-DG plus 10 mM lactate for 60 minutes under the same conditions initially described. This value was chosen for lactate because it was used in other studies with ganglion (Larrabee, 1980; 1996).

2.3. Formation of $^{14}CO_2$

DRG obtained from the same spinal cord segment (separately ipsilaterally and contralaterally to the nerve lesion) and lumbosacral spinal cord were incubated in flasks sealed with rubber caps at 25°C with constant shaking in 1 mL of frog Ringer`s solution pH 7.4. In this incubation medium it was added 0.15 μCi [U-^{14}C] L-lactate (108.30 mCi/mmol, Amersham) plus 10 mM of unlabeled lactate or 0.15 μci [U-^{14}C] glucose (115.00 mCi/mmoL, Amersham) plus 10 mM glucose (Torres et al., 2001). The incubation occurred in atmosphere of O_2:CO_2 (95:5, v/v) for 60 min. After addition of the unlabeled lactate or glucose the incubation medium pH was determined. Saturating lactate or glucose concentration was used for CO_2 production. 3MM Whatman papers were placed into glass wells inserted in the rubber stoppers of the flasks. Incubation was stopped by adding 0.2 ml of 50% TCA through the rubber cap. Then 0.2 mL of 2 M sodium hydroxide was injected into the central wells to trap $^{14}CO_2$. These were small glass wells placed inside the flasks and above the level of the incubation medium. The flasks were shaken for a further 60 min at 25°C to trap $^{14}CO_2$ after which the contents of the center well were transferred to vials containing toluene-TritonX-100 (2:1, v/v) -

PPO 0.4%-POPO 0.01% and assayed for CO_2 radioactivity in a liquid scintillation counter. The values of $^{14}CO_2$ production were expressed as µmol of ^{14}C-L-lactate or ^{14}C-glucose converted to $^{14}CO_2$. mg of tissue^{-1} . h^{-1} of incubation.

2.4. Determination of plasma lactate and glucose

Samples of plasma were obtained from naive, sham and transected frogs. Glucose blood concentration was determined by the glucose oxidase method with a Labtest kit (Brazil), while blood lactate was determined by Bioclin kit (Quibasa, Brazil). Values of glucose and lactate were expressed in mmol/L.

2.5. Statistical Analysis

The results obtained from frog ganglia with peripheral lesion were compared between ipsilateral and contralateral ganglia and with naïve and sham ganglia. For spinal cord the results were compared only between naïve, sham and injured frogs. Data were analyzed by one-way ANOVA followed by Tukey`s *post hoc* test. The significance level was $P<0.05$. All tests were performed with the Statistical Package for the Social Sciences, version 13.0 (SPSS).

3. Results

3.1. Glucose uptake and $^{14}CO_2$ formation

In DRG and spinal cord, the ^{14}C-2-DG uptake was not affected by incubation time. The ^{14}C-3-OMG uptake did not show any change in DRG and spinal cord (Table 1).

In spinal cord from naive animals, the ^{14}C- 2-DG uptake was 3.5 times higher than in DRG (Figure 1). This uptake changed in DRG when lactate was added in the incubation medium. Although ^{14}C- 2-DG uptake decreased around 36% in DRG of naive animals, it remained the same in spinal cord (Figures 1A, B, C).

The ^{14}C-2-DG uptake was increased in DRG three days after SNT. The increase of ^{14}C-2-DG uptake was 223% and 141% in the ipsilateral and contralateral DRG, respectively (Figure 1A) as compared to DRG from the naive group. No significant change occurred in the sham group, showing that the effect is specific to SNT. Likewise, the ^{14}C-2-DG uptake was not significantly changed in the spinal cord of the sham group. Moreover, the uptake increased in the spinal cord of transected animals. The increase was approximately 41% after axotomy (Figure 1B). No change was found in this uptake in DRG and spinal cord from naive frogs, showing that this effect is specific to SNT.

In the DRG, the increase in ^{14}C-2-DG uptake caused by SNT was smaller in the presence of lactate in the incubation medium. This increase was approximately 58% in ipsilateral and contralateral ganglia as compared to those of the naive group (Figure 1C). The values of ^{14}C-2-DG uptake in presence of lactate were reduced around 57% and 46% in ipsilateral and contralateral ganglia, respectively, as compared to ganglia from SNT frogs (Figures 1A and C). Similarly, ^{14}C-2-DG uptake in the spinal cord was also reduced in the presence of lactate by about 50% as compared to the naive group (Figure 1C), but 59% when compared to spinal cord from SNT frogs (Figures 1B and C).

Both DRG and spinal cord use lactate, but the DRG rate was about 100 times higher than the spinal cord one (Figure 2A). Sciatic nerve transection failed to induce any significant changes in the formation of $^{14}CO_2$ from ^{14}C-L-lactate in these tissues (Figure 2A). The rate of ^{14}C-glucose oxidation did not show change after SNT (Figure 2B).

3.2. Lactate and glucose plasma levels

SNT significantly decreased lactate and glucose plasma levels, but the reduction was greater in lactate than in glucose. Lactate levels decreased about 65% (Figure 3A), while glucose levels about 39% (Figure 3B).

4. Discussion

Our results demonstrate that SNT induce increase in ^{14}C-2-DG uptake, but no change in ^{14}C-3-OMG uptake in frog DRG and spinal cord. The increment in ^{14}C-2-DG uptake was reduced when lactate was added in the incubation medium. No change was found in glucose and lactate oxidation after SNT, but this experimental condition reduced lactate and glucose blood levels. Thus, the frog DRG and spinal cord were able to transport ^{14}C-2-DG efficiently. The absence of changes in 3-OMG uptake in our experimental conditions demonstrates the steady state tissue/medium glucose distribution ratio during the incubations. In turn, the lack of changes in ^{14}C-2-DG uptake throughout the time may be due the animal species studied. The uptake of ^{14}C-2-DG by the turtle thyroid incubated at 25^{o} markedly increased at 240 minutes (Machado et al., 1991).

Interestingly, there was a reduction in ^{14}C-2-DG transport when lactate was added in the incubation medium. It has been demonstrated that the perineurium around frog DRG presents a reduced number of cell layers and greater frequency interruptions in these layers than the mammalian one (Matsumoto and Rosenbluth, 1988). According to these authors these characteristics increase the susceptibility of DRG to circulating molecules and permit trophic factors, hormones and nutrients to reach the ganglion cells more readily. This characteristic would be contributing to higher utilization of lactate by DRG compared to the spinal cord. In this tissue the blood-brain-barrier has many of the properties of a tight epithelium, including the presence of tight junctions and specific transport mechanisms (Abbott, 2005). The more developed barrier in the spinal cord may be limited the use of lactate by this tissue. By using less lactate, this tissue appears to depend principally of the glucose, which explains the elevated ^{14}C-2-DG uptake and the absence of change in the uptake when lactate was added in the incubation medium. The use of lactate as energy substrate by frog DRG is a result that is in agreement with mammalian and non-mammalian studies. Previous studies showed a preferential use for lactate in avian, mammalian and human neuronal oxidative metabolism (Larrabee, 1980; 1996; Bouzie-Sore et al., 2003; 2006; Pellerin and Magistretti, 2011).

After SNT, we found an increase in ^{14}C-2-DG uptake in frog DRG and lumbosacral spinal cord. A similar result was observed in mammalian cephalic nerves after peripheral lesion (Kreutzberg and Emmert, 1980; Singer and Mehler, 1980; Mao et al., 1993; Moreno-Flores et al., 1997; Moran and Graeber, 2004; Gómez et al., 2011). Since ^{14}C-2-DG is a glucose analogue that is incorporated in neural tissue by the same pathways, and the same rate, as glucose, the increase in ^{14}C-2-DG uptake possibly reflects the increased energy demand to attend the metabolic necessities of the frog nervous tissue after SNT. In mammals, glucose incorporation into neurons or

phosphorylation of glucose appear to be one of the earliest change in metabolism affected by the signal for regeneration (Kreutzberg and Emmert, 1980; Singer and Mehler, 1980; Mao et al., 1993; Moreno-Flores et al., 1997).

After SNT, the DRG ^{14}C-2-DG uptake was decreased when lactate was added in the incubation medium. Similar answer also occurred in spinal cord. Moreover, it is interesting that the conversion of ^{14}C-L-lactate and ^{14}C-glucose to $^{14}CO_2$ did not change after SNT in these tissues. This lack of change may be due to glycolysis. The rise in ^{14}C-2-DG uptake with SNT, but not CO_2 production, suggests that the cells may be producing lactate from the glucose metabolized, which explain, in part, the low oxidation rate of glucose. The higher lactate oxidation may be due the lactate efflux into much larger volume driven by glycolysis. It has been demonstrated that neurons produce lactate from glucose despite the presence of lactate in the extracellular space and its simultaneous utilization as an oxidative substrate (Bouzie-Sore et al., 2003; 2006; Pellerin and Magistretti, 2011).

Interestingly, the reduction in ^{14}C-2-DG uptake in the presence of lactate was around 50% in both DRG and spinal cord. As cited above, the morphologic characteristic of the perineurium around frog DRG may be contributing to use of lactate present in the incubation medium. The use of lactate by frog spinal cord may be due changes that occurred in blood-spinal cord-barrier. In mammals the permeability of this barrier increased after injury (Beggs et al., 2010). According to these authors, the increased blood-spinal cord barrier permeability could allow entry of soluble factors that are normally excluded but that could contribute to pain hypersensitivity in the dorsal horn. It can be the situation in frog spinal cord after SNT, which explain our results. In this context it is interesting to demonstrate the lactate uptake rate by frog

DRG and spinal cord, principally after SNT. These studies will contribute to better understanding the role of lactate in these tissues.

The low barrier of the frog DRG should be contributed for the bilateral increase in ^{14}C-2-DG uptake in this tissue. The released factors by regenerating nerve likely had access to both ganglia by the blood circulation. It was demonstrated that regenerating peripheral nerves stimulate a marked increase in vascular permeability in the portion of the nerve distal to the lesion (Sparrow and Kiernan, 1981).

Interestingly, while the glucose/lactate ratio (mmol/mmol) was 1.2 in the plasma of naive frogs, it increased to 2.9 after SNT. This reduction in blood lactate levels may be related to muscle denervation. However, it has been demonstrated that denervation decreases succinate and lactate dehydrogenase activities in mammalian muscles and down-regulates the expression of monocarboxylate transporters (Wilson et al., 1998; Juel and Halestap, 1999). Other possibility may be the role of mineralized tissues of the frog to buffering lactic acidosis. It has been demonstrated that the skeleton and endolymphatic lime deposits function as buffers during anoxia and exercise induced lactic acidosis in amphibians (Warren and Jackson, 2005). Additional work should examine the relative contributions of these hypotheses to reduce plasmatic lactate after SNT.

It could be assumed that utilization of plasma lactate is related to the anaesthesia performed in the present study. However, it has been demonstrated that anaesthesia changes haematological and cardiorespiratory parameters in toad, but they are recovered in 24 hours and the blood lactate concentration does not change in this condition (Andersen and Wang, 2002). Thus, the results of the present study are probably due to SNT and not to the anaesthesia by itself.

In conclusion, our results showed that SNT increases ^{14}C-2-DG uptake, showing similarities with mammal studies. The increase in ^{14}C-2-DG uptake suggests high levels of functional activity of frog DRG and spinal cord after SNT. Nevertheless, this increment is low in the presence of lactate. No change occurs in glucose and lactate oxidation after SNT, but it reduced glucose and lactate blood levels. Considering the effect of lactate on ^{14}C-2-DG uptake, it can be speculated that the glucose may be serving to glycolytic pathway. However, more detailed analyses are necessary to provide additional insights into the relationship of the changes found here and glycolysis after SNT in frogs. If this relation occurs in frogs, this result is also similar to mammals. Thus, our results strengthen the use of frogs to study the effects of SNT on nervous tissue, condition that still has many unanswered questions.

Acknowledgments

This study was supported by grants from Fundação de Amparo à Pesquisa do Estado do Rio Grande do Sul (FAPERGS) and Conselho Nacional de Desenvolvimento Científico e Tecnológico (CNPq).

References

ABBOTT, NJ., 2005. Dynamics of CNS barriers: Evolution, differentiation, and modulation. *Cellular and Molecular Neurbiology, vol.* 25, p. 5-23.

AHN, SH., OH, SH., LEE, JS., JEONG, JM., LIM, D., LEE, DS., KIM, CS., 2004. Changes of 2-deoxyglucose uptake in the rat auditory pathway after bilateral ablation of the cochea. *Hearing Research*, vol. 196, no. 1-2, p. 33-38.

ANDERSEN, JB., WANG, AT., 2002. Effects of anaesthesia on blood gases, acid-base status and ions in the toad *Bufo marinus*. *Comparative Biochemistry Physiology part A*, vol. 131, no. 3, p. 639-646.

BARROS, LF., DEITMER, JW., 2010. Glucose and lactate supply to the synapse. *Brain Research Reviews,* vol. 63, no. 1-2, p.149-159.

BEGGS, S., LIU, XJ., KWAN, C., SALTER, MW., 2010. Peripheral nerve injury and TRPV1-expressing primary afferent C-fibers cause opening of the blood-brain barrier. *Molecular Pain*, vol. 6, p. 3-12.

BOUZIER-SARE, AK., VOISIN, P., CANIONI, P., MAGISTRETTI, PJ., PELLERIN, L., 2003b. Lactate is a preferential oxidative energy substrate over glucose for neurons in culture. *Journal Cerebral Blood Flow Metabolism*, vol. 23, no. 11, p. 1298-1306.

BOUZIER-SARE, AK., VOISIN, NP., BOUCHAUD, V., BEZANCON, E., FRANCONI, JM. PELLERIN, L., 2006. Competition between glucose and lactate as oxidative energy substrates in both neurons and astrocytes: a comparative NMR study. *European Journal Neuroscience*, vol. 24, no. 6, p. 687-694.

BRUMOVSKY, P., WATANABE, M., HÖKFELT, T., 2007. Expression of the vesicular glutamate transporters-1 and -2 in adult mouse dorsal root ganglia and spinal cord and their regulation by nerve injury. *Neuroscience*, vol. 147, no. 2, p. 469-490.

COBLE DJ, TAYLOR DK, MOOK DM., 2011. Analgesic effects of meloxicam, morphine sulfate, flunixin meglumine, and xylazine hydrochloride in African-clawed frogs (*Xenopus laevis*). *Journal of the American Association for Laboratory Animal Science*, vol. 50, p. 355-360.

DE FRAGA, LS., DA SILVA, RS., ZANCAN, DM., 2010. Control of carbohydrate metabolism in anoxia-tolerant nervous system. *Journal Experimental Zoology part A Ecological Genetics and Physiology*, vol. 313, no. 9, p. 539-547.

DIENEL, GA., CRUZ, NF., ADACHI, K., SOKOLOFF, L., HOLDEN, JE., 1997. Determination of local brain glucose level with [14C]methylglucose: effects of glucose supply and demand. *American Journal of Physiology*, vol. 273, no. 5, p. E839-849.

ENES, J., LANGWIESER, N., RUSCHEL, J., CARBALLOSA-GONZALEZ, MM., KLUG, A., TRAUT, MH., YLERA, B., TAHIROVIC, S., HOFMANN, F., STEIN, V., MOOSMANG, S., HENTALL, ID., BRADKE, F., 2010. Electrical activity suppresses

axon growth through Ca(v) 1.2 channels in adult primary sensory neurons. *Current Biology*, vol. 20, no. 13, p. 1154-1164.

GÓMEZ, O., BALLESTER-LURBE, B., MESOERO, JE., TERRADO, J., 2011. Glucose transporters GLUT4 and GLUT8 are upregulated after facial nerve axotomy in adult mice. *Journal Anatomy*, vol. 219, no. 4, p. 525-530.

GUEDES, RP., MARCHI, MI., VIOLA, GG., XAVIER, LL., ACHAVAL, M., PARTATA, WA., 2004a. Somatostatin, calcitonin gene-related peptide, and Y-aminobutyric acid-like immunoreativitity in the frog lumbosacral spinal cord:distribution and effects of sciatic nerve transection. *Comparative Biochemistry Physiology part B*, vol. 138, no. 1, p. 19-28.

GUEDES, RP., MARCHI, MI., ACHAVAL, M., PARTATA, WA., 2004b. Complete sciatic nerve transection induces increase of neuropeptide Y-like immunoreactivity in primary sensory neurons and spinal cord of frogs. *Comparative Biochemistry Physiological part A*, vol. 139, no. 4, p. 461-467.

HANANI, M., 2005. Satellite glial cells in sensory ganglia: from form to function. *Brain Research Reviews*, vol. 48, no. 3, p. 457-76.

JUEL, C., HALESTRAP, AP., 1999. Lactate transport in skeketal muscle – role and regulation of the monocarboxylate transporter. *Journal Physiology*, vol. 517, no. 3, p. 633-642.

KALOYIANNI, M., DOUKAKIS, I., 2003. Effect of adrenaline on glucose transport in red cells of *Rana balcanica*. *General Physiology Biophysical*, vol. 22, no. 1, p. 69-80.

KLUSÁLOVÁ, I., DUBOVÝ, P., 2009. Experimental models of peripheral neurophatic pain based on traumatic nerve injuries – An anatomical perspective. *Annals of Anatomy*, vol. 191, p. 248-259.

KREUTZBERG, GW., EMMERT, H., 1980. Glucose utilization of motor nuclei during regeneration: A [^{14}C] 2-Deoxyglucose Study. *Experimental Neurology*, vol. 70, no. 3, p. 712-716.

LARRABEE, MG., 1980. Metabolic disposition of glucose carbon by sensory ganglia of 15-day-old chicken embryos, with new dynamic models of carbohydrate metabolism. *Journal of Neurochemistry*, vol. 35, no. 1, p. 210-231.

LARRABEE, MG., 1996. Partitioning of CO_2 production between glucose and lactate in excised sympathetic ganglia, with implication for brain. *Journal Neuroch*emistry, vol. 67, no. 4, p. 1726-1734.

MACHADO, VLA., WASSERMANN, GF., MARQUES, M., 1991. In vitro effect of insulin on the uptake of glucose and α-Aminoisobutyric acid in the thyroid gland of the turtle (*Chrysemys dorbigni*). *General and Comparative Endocrinology*, vol. 82, no. 1, p. 8-13.

MAO, J., MAYER, DJ., HAYES, RL., PRICE, DD., 1993. Spatial patterns of increased spinal cord membrane-bound protein kinase C and their relation to increases in ^{14}C-2-deoxyglucose metabolic activity in rats with painful peripheral mononeuropathy. *Journal Neurophysiology*, vol. 70, no. 2, p. 470-481.

MATSUMOTO, E., ROSENBLUTH, J., 1988. Freeze-fracture study of the perineurium around frog dorsal root ganglia. *Journal Neurocytolocy*, vol. 17, no. 4, p. 425-432.

McDOUGAL DB., HOLOWACH J., HOWE MC., JONES EM., THOMAS CA., 1968. The effects of anoxia upon energy sources and selected metabolic intermediates in the brains of fish, frog and turtle. *Journal of Neurochemistry*, vol. 15, p. 577-588.

MORAN, LB., GRAEBER, MB., 2004. The facial nerve axotomy model. *Brain Research Reviews*, vol. 44, no. 2-3, p. 154-178.

MORENO-FLORES, MT., OLAZÁBAL, UE., KREUTZBERG, GW., 1997. Axotomy increases the expression of glucose-regulated protein 78 kDa in rat facial nucleus. *Experimental Neurology*, vol. 146, no. 1, p. 10-16.

OHKITA M., SAITO S., IMAGAWA T., TAKAHASHI K., TOMINAGA M., OHTA T., 2012. Molecular cloning and functional characterization of *Xenopus tropicalis* frog transient receptor potential vanilloid 1 reveal its functional evolution for heat, acid, and capsaicin sensitivities in terrestrial vertebrates. *The Journal of Biological Chemistry*, vol. 287, p. 2388-2397.

OLIVEIRA, ALR., 2001. Apoptosis of sensory neurons and satellite cells after sciatic nerve transection in C57BL/6J mice. *Braziliam Journal of Medical and Biological Research*, vol. 34, no. 3, p. 375-380.

PARTATA, WA., CERVEIRA, JF., XAVIER, LL., VIOLA, GG., ACHAVAL, M., 2002. Sciatic nerve transection decrease P immunoreactivity in the lumbosacral spinal cord of the (*Rana catesbeiana*). *Comparative Biochemistry Physiology part B*, vol. 131, no. 4, p. 807-814.

PELLERIN, L., MAGISTRETTI, PJ., 2011. Sweet sixteen for ANLS. *Journal of Cerebral Blood Flow & Metabolism*, vol. 32, no. 7, p. 1152-1166.

PENICNAK, AJ., DUNLAP, DG., 1962. Localization and distribution of motor neurons in the lumbar enlargement of the spinal cord in *Rana pipiens*. *Proceedings of the South Dakota Academy of Sciences*, vol. 41, p. 113-118.

RIGON, F., Rossato, D., Auler, VB., Dal Bosco, L., Faccioni-Heuser, MC., PartatA, W A. Effects of sciatic nerve transection on ultrastructure, NADPH-diaphorase reaction and serotonin-, tyrosine hydroxylase-, c-Fos-, glucose transporter 1 and 3-like immunoreacivities in frog dorsal root ganglion. *Brazilian Journal of Medical and Biological Research*. *In press*

ROCHA, PL., BRANCO, LGS., 1998. Seasonal changes in the cardiovascular respiratory and metabolic responses to temperature and hypoxia in the bullfrog *Rana catesbeiana*. *The Journal of Experimental Biology*, vol. 201, p. 761-768.

STEVENS CW., 2004. Opioid research in amphibians: a unique perspective on mechanism of opioid analgesia and the evolution of opioid receptors. *Brain Research Reviews,* vol. 46, p. 204-215.

STEVENS CW., BRASEL CM., MOHAN S., 2007. Cloning and bioinformatics of amphibian mu, delta, kappa, and nociceptin opioid receptors expressed in brain tissue: evidence for opioid receptor divergence in mammals. *Neuroscience Letters,* vol. 419, p. 189-194.

STEVENS CW., MARTIN KK., STAHLHEBER BW., 2009. Nociceptin produces antinociception after spinal administration in amphibians. *Pharmacology Biochemistry and Behavior,* vol. 91, p. 436-440.

SAITO S., NAKATSUKA K., TAKAHASHI K., FUKUTA N., IMAGAWA T., OHTA T., TOMINAGA M., 2012. Analysis of transient receptor potential ankyrin 1 (TRPA1) in frogs and lizards illuminates both nociceptive heat and chemical sensitivities and coexpression with TRP vanilloid 1 (TRPV1) in ancestral vertebrats. *Journal of Biological Chemistry,* vol. 287, p. 30743-30754.

SCHURR, A., PAYNE, RS., MILLER, JJ., 1999. Study of Cerebral Energy Metabolism Using the Rat Hippocampal Slice Preparation. *Methods,* vol. 18, no. 2, p. 117-126.

SCHURR, A., PAYNE, RS., 2007. Lactate, not pyruvate, is neuronal aerobic glycolysis end product: an in vitro electrophysiological study. *Neuroscience,* vol. 147, no. 3, p. 613-619.

SCHURR, A., GOZAL, E., 2012. Aerobic production and utilization of lactate satisfy increased energy demand and support neuronal activation in hippocampal slices and provide neuroprotection against oxidative stress. *Frontiers in Pharmacology,* vol. 2, no. 96, p. 1-15.

SINGER, P., MEHLER, S., 1980. 2-Deoxy [^{14}C]glucose uptake in the rat hypoglossal nucleus after nerve transaction. *Experimental Neurology,* vol. 69, no. 3, p. 617-626.

SPARROW, JR., KIERNAN, JA., 1981. Endoneurial vascular permeability in degenerating and regenerating and regenerating peripheral nerves. *Acta Neuropathology,* vol. 53, no. 3, p. 181-188.

SUTHERLAND, RM., NUNNEMACHER, RF., 1974. Fibers in the ventral spinal nerves of the frog. *Journal of Comparative Neurology*, vol. 156, p. 39-47.

TORRES, ILS., CAMARO, CD., SILVEIRA-CUCCO, N., 2001. Effect of acute and repeated restraint stress on glucose oxidation to CO2 in hipocampal and cerebral cortex slices. *Braziliam Journal of Medical and Biological Research,* vol. 34, no. 1, p. 111-116.

WARREN, DE., JACKSON, DC., 2005. The role of mineralized tissue in the buffering of lactic acid during anoxia and exercise in the leopard frog *Rana pipiens*. *Journal Experimental Biology*, vol. 208, no. 8, p. 1117-1124.

WILSON, MC., JACKSON, VN., HEDDLE, C., PRICE, NT., PILEGAARD, H., JUEL, C., BONEN, A., MONTGOMERY, I., HUTTER, OF., HALESTRAP, AP.,

1998. Lactic acid efflux from white skeletal muscle is catalyzed by the monocarboxylate transporter isoform MCT3. *Journal Biological Chemistry*, vol. 273, no. 26, p. 15920-15926.

YUN, J., JAKOBSEN, J., 2010. Different apoptotic reactions of dorsal root ganglia A- and B-cells after sciatic nerve axotomy: effect of p75 neurotrophin receptor. *Chinese Medical Journal*, vol. 123, no. 1, p. 2695-2700.

Legends to Figures

Figure 1. Uptake of 1-[^{14}C] 2-deoxy-D-glucose (A and B) and 1-[^{14}C] 2-deoxy-D-glucose plus lactate (C) by dorsal root ganglia (A) and spinal cord (B) from naive, sham and transected frogs. The tissues were incubated at 25°C and processed as indicated under Materials and Methods. Data are given as means $\pm$ SEM. (n= 6/group). Results were expressed as tissue/medium (T/M) rate, i.e., dpm/ml of tissue fluid divided by dpm/ml of incubation medium. * indicates significant difference when compared with naive and sham groups; # indicates significant difference when compared to naive group ($P<0.05$, one-way ANOVA followed by Tukey`s post hoc test). IPSI, ipsilateral; CL, contralateral; SNT, sciatic nerve transection.

Figure 2. Formation of $^{14}CO_2$ from [U-^{14}C] L-lactate (A) and ^{14}C-glucose (B) by dorsal root ganglia (DRG) and spinal cord from naive and transected frogs. These tissues were incubated at 25°C and processed as indicated under Materials and Methods. Data are given as means $\pm$ SEM. (n= 6/group). Results are expressed as (A) µmol ^{14}C-L-lactate converted to $^{14}CO_2$ **.** mg of tissue^{-1}**.** h^{-1} of incubation and (B) $^{14}CO_2$ **.** mg of tissue^{-1}**.** h^{-1} of incubation. No significant difference was found (one way ANOVA). IPSI, ipsilateral; CL, contralateral; SNT, sciatic nerve transection.

Figure 3. Blood lactate (A) and glucose (B) in naive and transected frogs. Lactate and glucose levels were determined as indicated under Materials and Methods. Results were expressed in mmol/L. * indicates significant difference when compared with naive group ($P<0.05$, one-way ANOVA followed by Tukey`s post hoc test). SNT, sciatic nerve transection.

Table 1 Uptake of 1-[^{14}C] 2-deoxy-D-glucose and 3-O-[^{14}C] methyl-D-glucose by dorsal root ganglia (DRG) and spinal cord (SC) from naive frogs.

	1-[^{14}C] 2-deoxy-D-glucose		**3-O-[^{14}C] methyl-D-glucose**	
Time (min)	DRG	SC	DRG	SC
5	0.22 ± 0.06	0.22 ± 0.02	0.23 ± 0.06	0.26 ± 0.06
15	0.22 ± 0.02	0.26 ± 0.03	0.29 ± 0.07	0.27 ± 0.07
60	0.22 ± 0.04	0.47 ± 0.02	0.39 ± 0.06	0.31 ± 0.09
120	0.25 ± 0.05	0.74 ± 0.08	0.38 ± 0.06	0.33 ± 0.07

These tissues were incubated at 25°C for different times and were processed as indicated under Materials and Methods. Data are given as means ± SEM. Results are expressed as tissue/medium (T/M) rate, i.e., dpm/ml of tissue fluid divided by dpm/ml of incubation medium. No significant difference was found (one way ANOVA).

Figure 1

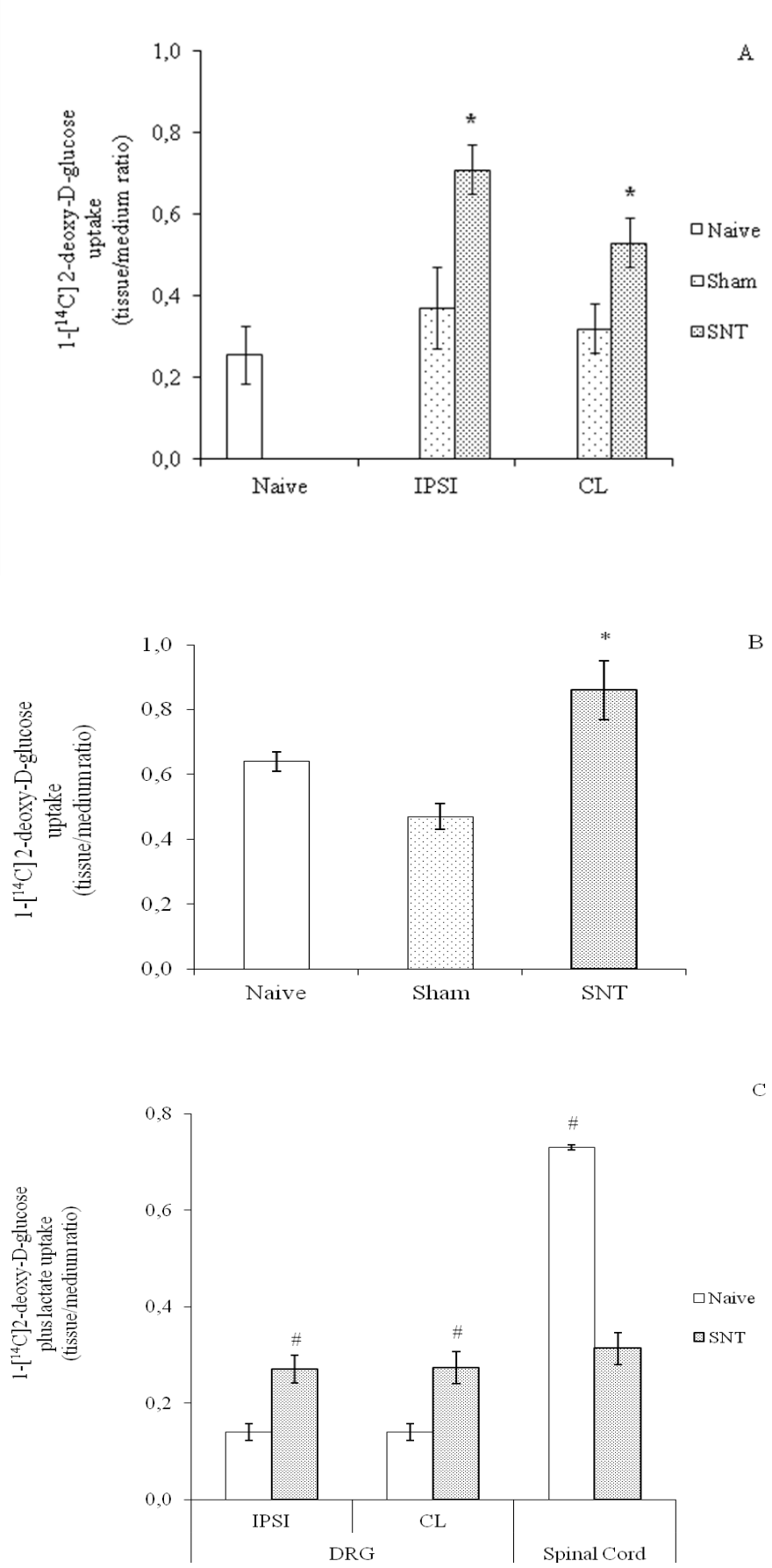
A
1-[14C] 2-deoxy-D-glucose uptake (tissue/medium ratio)
1,0
0,8
0,6
0,4
0,2
0,0
*
*
Naive
IPSI
CL
Naive
Sham
SNT
B
1-[14C] 2-deoxy-D-glucose uptake (tissue/medium ratio)
1,0
0,8
0,6
0,4
0,2
0,0
*
Naive
Sham
SNT
C
1-[14C]2-deoxy-D-glucose plus lactate uptake (tissue/medium ratio)
0,8
0,6
0,4
0,2
0,0
#
#
#
Naive
SNT
IPSI
CL
DRG
Spinal Cord

Figure 2

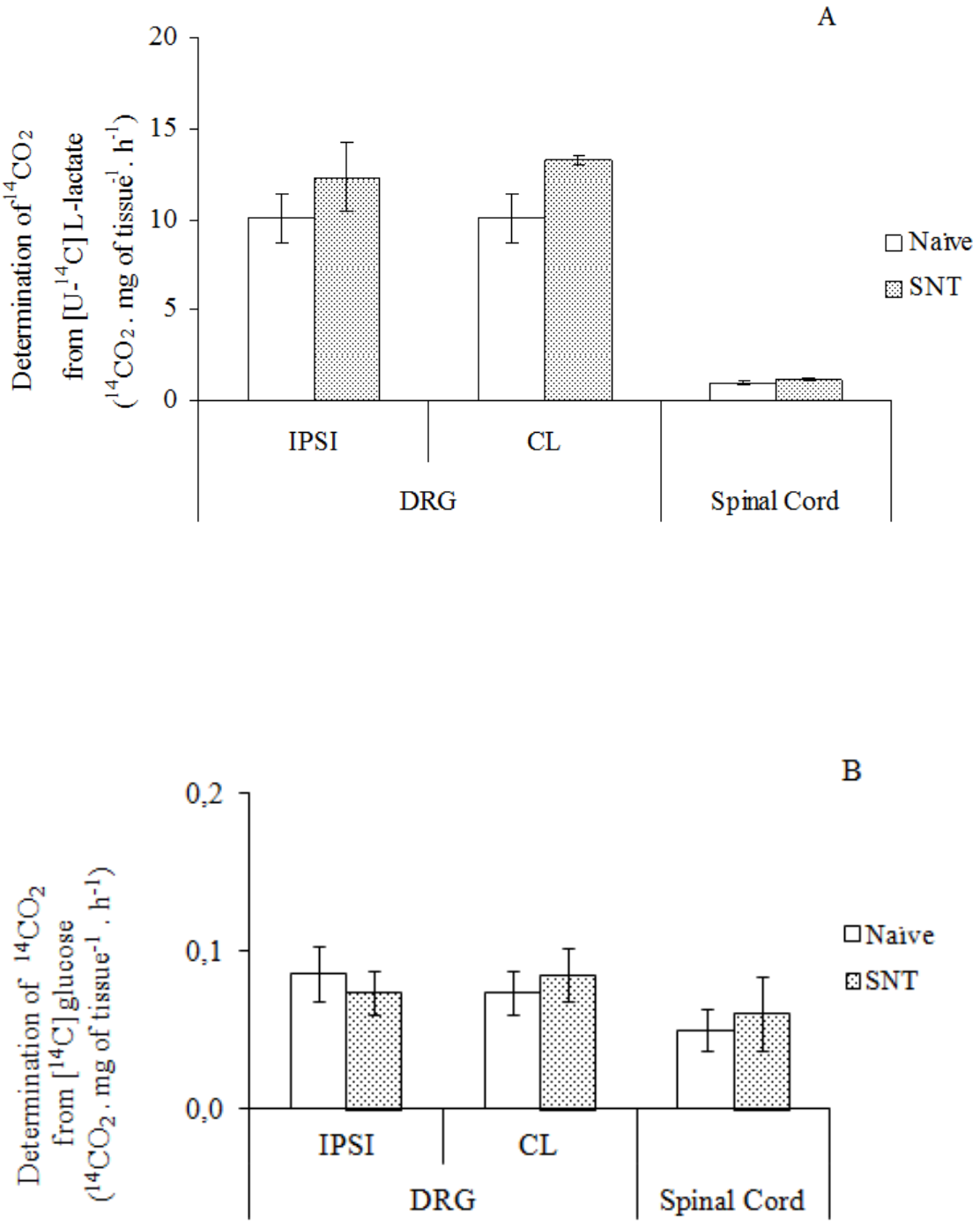
A
Determination of $^{14}CO_2$ from [U-^{14}C] L-lactate ($^{14}CO_2$. mg of tissue^{-1} . h^{-1})
20
15
10
5
0
IPSI
CL
DRG
Spinal Cord
Naive
SNT
B
Determination of $^{14}CO_2$ from [^{14}C] glucose ($^{14}CO_2$. mg of tissue^{-1} . h^{-1})
0,2
0,1
0,0
IPSI
CL
DRG
Spinal Cord
Naive
SNT

Figure 3

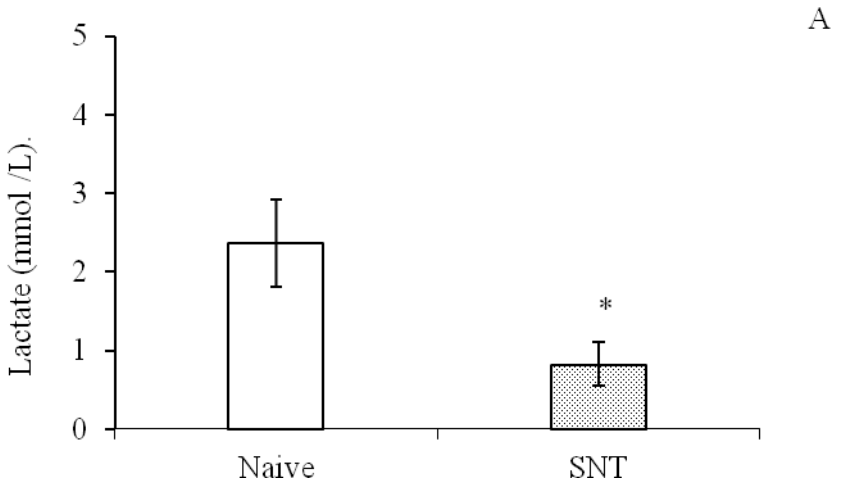
A
Lactate (mmol /L).
5
4
3
2
1
0
*
Naive
SNT

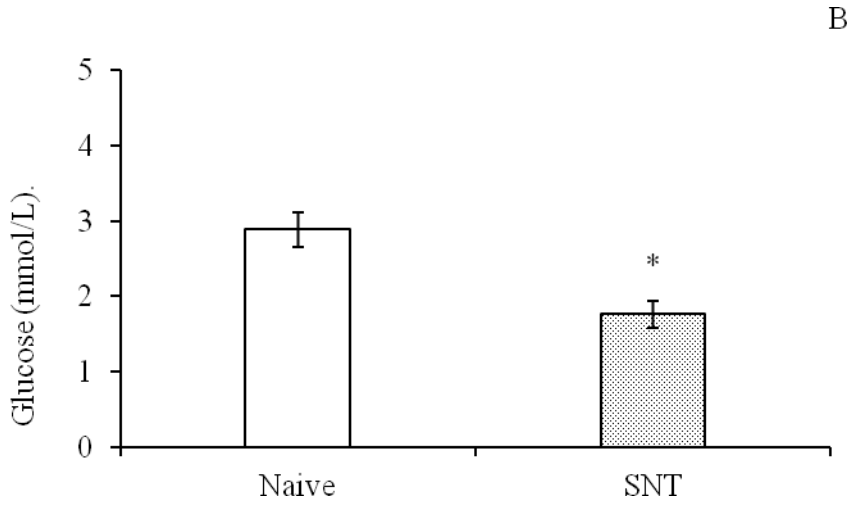
B
Glucose (mmol/L).
5
4
3
2
1
0
*
Naive
SNT

4. Discussão

O presente estudo teve como objetivo analisar a ultraestrutura de neurônios e CGSs do DRG de rãs *Lithobates catesbianus* sem e com secção no nervo isquiático, realizando as análises 3 dias após a lesão nervosa periférica. Objetivou ainda determinar, nessas mesmas condições, o padrão de atividade às reações NADPH-diaphorase e PAS, além do padrão de imunoreatividade à 5-HT, TH, c-Fos-, e GLUT 1 e 3. Demonstrou também o efeito da SNI sobre: 1) a captação de ^{14}C-2-DG, na presença e ausência de lactato, e 2) a concentração plasmática de glicose e lactato.

No primeiro e segundo artigos foi observado que no GRD de *Lithobates catesbianus* que não sofreu qualquer manipulação cirúrgica no nervo isquiático, os neurônios sensoriais tiveram distribuição, diâmetro e morfologia que foi similar àquela descrita para essas células em gânglio simpático de rãs (Yamamoto, 1962; 1963; Baluk, 1986) e no GRD de ratos e coelhos (Pannese, 1981; Feliciano et al., 2007). Assim como nessas espécies, os neurônios sensoriais do GRD de *Lithobates* também puderam ser classificados em neurônios grandes e pequenos (Maruhashi et al., 1952; Yamamoto, 1963). Provavelmente a fixação do GRD impediu a visualização dos seis diferentes subtipos funcionais de neurônios sensoriais descritos nesse gânglio (Berrios et al., 2008).

As CGSs do GRD de *Lithobates catesbianus* apresentaram morfologia similar àquela descrita para essas células em gânglios de outras espécies de vertebrados (Pannese, 1981; Hanani, 2005; Ohara et al., 2009). As CGSs dos tipos II e III, observadas no GRD de coelho (Siemionow et al., 2006), não foram observadas no DRG de *Lithobates catesbianus*. Nessa espécie de rã, as CGSs do GRD sempre se apresentaram com características morfológicas similares ao do tipo descrito por Pannese (1981), o que também foi observado por outros autores quando analisaram a ultraestrutura do gânglio simpático de outras espécies de rãs (Yamamoto, 1962; 1963;

Baluk, 1986) e gânglios de outros mamíferos (Pannese, 1981; 2010; Arkhipova et al., 2010; Hanani, 2005; 2010b).

O padrão de atividade à NADPH-diaforase e a distribuição da imunorreatividade à serotonina, tirosina hidroxilase e Glut 1 e 3 foram similares ao descrito em mamíferos (Delree et al., 1992; Stark el al., 2000; Brumovsky et al., 2007; Nascimento et al., 2008; Li et al., 2011; Xia et al, 2011). Ainda, assim como nos mamíferos (Nascimento et al., 2008), as CGSs do GRD de *Lithobates catesbianus* foram positivas à reação NADPH-diaforase. Essa foi a primeira descrição de reatividade a essa enzima em CGSs de anfíbios. Esse resultado salienta não apenas a similaridade funcional entre rãs e mamíferos, mas mostra que o uso de óxido nítrico na comunicação entre neurônios sensoriais ganglionares e CGSs apareceu precocemente na evolução dos vertebrados. Esse resultado deixa também evidente que o GRD de rãs pode ser usado como modelo em estudos que objetivam demonstrar o significado funcional do óxido nítrico na comunicação neurônio-célula glial.

Um resultado intrigante descrito no segundo artigo foi a moderada reação ao PAS no GRD da espécie de rã em estudo. Como a reação positiva ao PAS indica a presença de mucopolissacarídeos, e sabendo que a reserva de glicogênio do tecido nervoso de rãs varia nas diferentes estações do ano (Boutilier et al., 1997), é possível que esse resultado esteja indicando uma baixa concentração desse carboidrato nesse tecido. Boutilier et al. (1997) mostraram ainda que, nos anfíbios, há uma deposição sequencial nas reservas de lipídeos e carboidratos ao longo do verão e outono, sendo que a deposição de lipídeos começa antes da de carboidratos, o que explica a moderada reação ao PAS e a presença de lipídeos no citoplasma da CGS. Como os estudos atuais com GRD de mamíferos sugerem um importante papel metabólico para as CGSs (Pannese, 1981; Hanani, 2005; 2010a, b), é possível que a presença de lipídeos no citoplasma

dessas células no GRD de rã esteja indicando esse mesmo papel nesses animais. Estudos futuros abordando essa questão são necessários para esclarecer a hipótese aqui apresentada. Porém, caso seja essa a situação, o GRD de rãs poderá ser usado como modelo nos estudos que visam esclarecer a interação metabólica entre neurônios e células gliais.

Como ainda mostrado no primeiro artigo da tese, a SNI provocou alterações tanto na ultraestrutura como nos parâmetros histoquímicos e de imunoistoquímica avaliados nesse estudo. A maior parte das alterações foi similar àquelas descritas em mamíferos. Após a SNI, se observou somas neuronais com mitocôndrias dilatadas e membrana nuclear com invaginações. As CGSs mostraram mais filamentos intermediários, ribossomos, retículo endoplasmático e mitocôndrias em seu citoplasma, alterações essas que também ocorreram no GRD de mamíferos após lesão em nervo periférico (Hanani, 2010; Liu et al., 2012). Em mamíferos, a quantidade de mitocôndrias parece diretamente relacionada com a taxa máxima de consumo de oxigênio (Hoppler et al., 1987). Essa pode ser a situação nas rãs. Assim, pode-se pensar que o aumento no número de mitocôndrias que ocorreu nas CGSs do GRD de rãs indica maior capacidade de produção energética dessas células após a SNT, hipótese que também foi sugerida para as mudanças no número de mitocôndrias no GRD de mamíferos (Hanani, 2010b).

Outro indicador de maior interação entre neurônio sensorial e CGSs foi o aumento na reatividade à NADPH-diaforase em somas neuronais e CGSs do GRD de rãs após a SNI. Em mamíferos, foi sugerido que o óxido nítrico produzido pelo neurônio do GRD, após lesão em nervo periférico, atuaria como sinalizador para a CGSs, o qual induziria nessa célula glial a produção de fatores neurotróficos que controlariam, por sua vez, a ativação da isoforma induzível da enzima óxido nítrico sintase no neurônio (Bradman et al., 2010). Essa pode ser também a situação no GRD de rãs. Caso seja essa hipótese

verdadeira, o óxido nítrico está desempenhando um importante papel de sinalização no GRD de anfíbios e mamíferos.

Da mesma forma, as modificações observadas no padrão de imunorreatividade à serotonina, tirosina hidroxilase, c-Fos e Glut 1 e 3 após a SNI foram similares àquelas descritas em mamíferos (Stark et al., 2000; Soares et al., 2001; Keilhoff et al., 2003; Brumovsky et al., 2011; Hansen et al., 2011; Xia et al., 2011). Essa similaridade sugere os mesmos papéis funcionais para essas moléculas no GRD de rãs e mamíferos submetidos à lesão em nervo periférico, o que indica o aparecimento precoce dessas mudanças durante a evolução dos vertebrados.

Porém, nem todas as alterações provocadas pela SNI no GRD de rãs foram similares àquelas descritas em mamíferos. Essa condição experimental induziu, no GRD, mudanças que foram peculiares às rãs. No tecido desses animais, a SNI não provocou aumento no número de CGSs. O aumento dessas células após lesão em nervos periféricos de mamíferos está bem documentado na literatura (Humbertson, 1969; Arkhipova et al., 2010; Hanani, 2010a, b; Pannese, 2010). Segundo Humbertson et al. (1969), a razão CGS/neurônio muda no primeiro dia após a lesão nervosa periférica, estando esse valor duplicado aos 6 dias e igual ao valor pré-lesão no 18º dias após a cirurgia. É possível que a inexistência de alteração no número de CGSs no GRD de rãs submetidas à SNI seja consequência da menor taxa metabólica do tecido nervoso de anfíbios quando comparada à de mamíferos. De acordo com McDougal et al. (1968), as mudanças provocadas pela anoxia foram semelhantes em anfíbios e mamíferos. Porém, a razão na utilização de fosfatos energéticos foi de 1:20 quando comparados anfíbios/mamíferos. Outro apoio à hipótese de menor taxa metabólica no tecido nervoso de rãs foi a observação, no terceiro artigo, de que não há mudança na taxa de captação de ^{14}C-2-DG ao longo dos períodos de incubação. Esse resultado foi similar àquele

obtido em tartarugas (Machado et al., 1991). Segundo McDougal et al. (1968), enquanto a taxa de utilização de fosfatos energéticos foi 1:20 nas rãs, ela foi de 1:50 nas tartarugas, quando comparados às taxas obtidas em mamíferos. A menor taxa metabólica no tecido nervoso de rãs permite especular que o aumento no número de CGSs ocorre mais tardiamente no GRD de rãs submetidas à SNI. Para demonstrar essa hipótese, pretendemos avaliar as alterações provocadas pela lesão nervosa periférica no GRD de rãs 10 dias após a intervenção cirúrgica, experimentos que já foram iniciados em nosso laboratório. A motivação para a realização desses experimentos foi a demonstração, em mamíferos, de que o número de CGSs estava ainda aumentado 30 e 90 dias após a SNI (Arkhipova et al., 2010).

Interessantemente, a SNI ocasionou acréscimo na captação de ^{14}C-2-DG no GRD e na medula espinal de *Lithobates catesbianus*, o que foi similar à resposta observada em mamíferos com lesão nervosa periférica (Kreutzberg e Emmert, 1980; Singer e Mehler, 1980; Mao et al., 1993; Moreno-Flores et al., 1997; Moran e Graeber, 2004; Gómez et al., 2011). Como esse substrato é transportado para o interior das células pela mesma rota e na mesma taxa que a glicose, esse aumento sugere acréscimo no uso da glicose no GRD e medula espinal de rãs com nervo isquiático seccionado. Essa maior utilização da glicose provavelmente se relaciona com os mecanismos de regeneração do nervo lesionado, tal como sugerido para os mamíferos (Kreutzberg e Emmert, 1980; Singer e Mehler, 1980; Mao et al., 1993; Moreno-Flores et al., 1997). Essa hipótese parece plausível já que o processo de regeneração nervosa não estava impedido em nossas condições experimentais. Cabe ser relembrado que os cotos nervosos foram deixados livres entre a musculatura.

Um apoio à hipótese de aumento na taxa metabólica do GRD de rãs com SNI foi a ocorrência de neurônios sensoriais com acúmulo de mitocôndrias em seu citoplasma,

muitas delas sem alterações em sua morfologia. O mesmo ocorreu no citoplasma das CGSs. Essas mudanças estruturais sugerem maior capacidade de produção de energia por esses tipos celulares do GRD. Em mamíferos, foi sugerido que a preservação da morfologia de mitocôndrias após lesão nervosa periférica é necessário para garantir o atendimento da maior demanda metabólica celular, principalmente de neurônios em processo de apoptose (Oliveira et al., 2001). Como a alteração estava também presente no citoplasma das CGSs, esse resultado sugere que essas células aumentam sua atividade metabólica após SNT em rãs, provavelmente para atender a maior demanda energética gerada por essa condição experimental. O maior número de ribossomos e retículo endoplasmático no citoplasma das CGSs sugere maior capacidade de realização de síntese de proteínas. Nesse contexto, um estudo recente demonstrou que a enzima 3-fosfoglicerato desidrogenase, a qual participa na biossíntese da L-serina, está presente no citoplasma das CGSs (Kiya et al., 2011). Assim, pode-se sugerir que a inexistência de indicadores de mudanças em processos mitóticos nas CGSs se relaciona com o papel metabólico dessas células nessa condição experimental, hipótese que também é sugerida nos estudos em mamíferos (Hanani, 2010b; Liu et al., 2012). Desse modo, parece viável pensar que a interação entre neurônio sensorial e células gliais, no GRD de vertebrados em uma condição dolorosa, praticamente não sofreu modificações ao longo do processo evolutivo. Porém, é clara a necessidade de estudos abordando essa questão para demonstração da viabilidade dessa hipótese.

O terceiro artigo da tese mostrou que a captação de ^{14}C-2-DG foi reduzida quando o lactato foi acrescentado ao meio de incubação do GRD de rãs *Lithobates catesbianus*, independente se a amostra foi obtida de rãs que não sofreram qualquer manipulação cirúrgica, sofreram apenas manipulação no nervo isquiático (animais sham) ou tiveram esse nervo seccionado. Esse resultado mostra que o GRD de rãs pode usar o lactato

como substrato energético, tal como ocorre com outras espécies de vertebrados. Foi demonstrado o uso preferencial de lactato em rotas metabólicas oxidativas em neurônios de aves e mamíferos, inclusive de humanos (Larrabee, 1980; 1982; 1985; 1987; 1995; 1996; Bouzie-Sore et al., 2003a, b; 2006; Pellerin e Magistretti, 2011). Uma possível explicação para o uso de lactato pelo GRD de rãs é a existência de uma menor barreira no gânglio (Matsumoto e Rosenbluth, 1988). Isso permitiria o uso do lactato pelo gânglio tanto nos animais que não sofreram qualquer manipulação cirúrgica como naqueles submetidos à SNI. Essa maior permeabilidade ganglionar também explica a ocorrência de alterações bilaterais na captação de ^{14}C-2-DG. Como a barreira hematoencefálica é maior no sistema nervoso central (Abbott, 2005), essa pode ser a causa para a menor modificação na taxa de captação de ^{14}C-2-DG na medula espinal de rãs sem qualquer manipulação no nervo periférico, quando comparada àquela observada no GRD. Porém, como há um aumento na permeabilidade da barreira hematoencefálica após lesão (Beggs et al., 2010), isso permitiria maior utilização de lactato pelo tecido nervoso, o que pode ser a explicação para a redução na captação de ^{14}C-2-DG pela medula espinal de rãs com nervo isquiático seccionado quando o lactato foi acrescentado ao meio de incubação.

Apesar do uso de lactato pelo tecido nervoso de rãs sem e com SNI, a taxa de conversão de ^{14}C-L-lactato e ^{14}C-glicose a $^{14}CO_2$ não foi modificada após a lesão nervosa periférica. Uma possível explicação para esse resultado pode ser a glicólise presente no tecido nervoso de rãs após a SNI. O aumento na captação de ^{14}C-2-DG, sem mudança significativa na taxa de produção de $^{14}CO_2$ sugere que as células do GRD e medula espinal podem estar produzindo lactato a partir da metabolização da glicose armazenada, o que explica, em parte, a baixa taxa de oxidação da ^{14}C-glicose nesses tecidos. Um apoio a essa hipótese é a presença de moderada reação ao PAS no GRD de

rãs. A maior oxidação de lactato provavelmente se deu devido ao intenso efluxo de lactato impulsionado pela glicólise. Diversos estudos mostraram que os neurônios produzem lactato a partir de glicose, independente da presença de lactato no meio extracelular e de sua simultânea utilização como substrato oxidativo (Bouzie-Sore et al., 2003a, b; 2006; Pellerin e Magistretti, 2011). Como esses estudos foram realizados em mamíferos, novamente se detecta uma similaridade nas respostas de rãs e mamíferos, o que reforça o uso das rãs como modelo experimental para o estudo de diversas situações experimentais que ainda possuem muitas questões em aberto.

O terceiro artigo mostrou ainda que a relação glicose/lactato foi 1,2 no plasma das rãs que não sofreram qualquer manipulação cirúrgica no nervo isquiático, mas mudou para 2,9 após a SNI. A redução na concentração plasmática de lactato provavelmente se relaciona com o procedimento de denervação periférica. Foi demonstrado, em mamíferos, que essa condição experimental reduz a atividade das enzimas succinato e lactato desidrogenases em músculos, reduzindo ainda nesse tecido a expressão de transportadores de monocarboxilados (Wilson et al., 1998; Juel e Halestap, 1999). Essa pode ser também a causa do aumento na relação glicose/lactato no plasma de rãs com SNI. Porém, nas rãs é necessário considerar ainda a hipótese de que o aumento dessa relação seja consequência do efeito de tampão de tecidos mineralizados na condição de acidose láctica. Em anfíbios, foi demonstrado que o esqueleto e tecidos endolinfáticos atuam como tampões em condições de acidose láctica, como a que se observa nas situações de anoxia e exercício físico (Warren e Jackson, 2005). Portanto, não é possível descartar a contribuição desses tecidos na mudança da relação glicose/lactato no plasma de rãs com SNI. Pode-se pensar ainda que a alteração dessa relação se relacione com o uso de lactato devido a maior produção dessa molécula em virtude da anestesia realizada para a intervenção cirúrgica nas rãs. Contudo, foi demonstrado, em sapos, que

a anestesia modifica parâmetros hematológicos e cardiorespiratórios, porém os mesmos são recuperados 24 horas após a cirurgia, e a concentração plasmática de lactato não se altera nessa condição (Andersen e Wang, 2002). Assim, nossos resultados em rãs submetidas à SNI são decorrentes dessa condição e não devido às mudanças provocadas pela anestesia dos animais.

Deste modo, o presente estudo demonstra que as alterações ultraestruturais no GRD de rãs, induzidas pela SNI, são, em sua maioria, similares àquelas descritas em mamíferos. Porém, algumas são peculiares às rãs, o que, por um lado, reforça o uso desses animais como modelo experimental para o estudo de questões ainda em aberto sobre os efeitos da SNI sobre o tecido nervoso, mas, por outro lado, salienta a necessidade de realização de mais estudos para melhor entendimento das respostas peculiares das rãs.

5. Conclusões e Perspectivas

A partir dos resultados do presente trabalho pode-se concluir que o GRD de rãs é ultraestrutural e funcionalmente similar ao de mamíferos. A SNI provoca também nas rãs mudanças estruturais e funcionais no GRD que são similares àquelas descritas nos mamíferos. Porém, diferentemente dos mamíferos, a SNI não provoca alterações no número de CGSs no GRD de rãs três dias após o procedimento cirúrgico. Assim, nosso estudo reforça o uso de rãs como modelo experimental para estudo dos efeitos da SNI, um modelo de dor fantasma, sobre o tecido nervoso, tema que ainda possui muitas questões em aberto. Porém, dada a diferença peculiar ocorrida no GRD de rãs com SNI, nosso estudo deixa evidente a necessidade de um aprofundamento no conhecimento dos efeitos dessa situação experimental nesses animais.

Como perspectivas futuras, sugerimos:

- Demonstrar o efeito das diferentes estações do ano sobre parâmetros funcionais do GRD de rãs com SNI;

- Demonstrar o efeito da SNI sobre a ultraestrutura e parâmetros histoquímicos e imunoistoquímicos no GRD de rãs 7, 15 e 30 dias após o procedimento cirúrgico;

- Demonstrar, mediante imunoistoquímica à caspase e microscopia eletrônica, o padrão temporal de morte neuronal por apoptose no GRD de rãs com SNI.

6. Referências Bibliográficas

Abbott, N.J. Dynamics of CNS barriers: Evolution, differentiation, and modulation. Cell Mol Neurobiol. 2005;25:5-23.

Ahn, S.H., Oh, S.H., Lee, J.S., Jeong, J.M., Lim, D., Lee, D.S., Kim, C.S. Changes of 2-deoxyglucose uptake in the rat auditory pathway after bilateral ablation of the cochea. Hearing Res. 2004;96:33-38.

Andersen, J.B., Wang, A.T. Effects of anaesthesia on blood gases, acid-base status and ions in the thoad *Bufo marinus*. Com Biochem Physiol part A. 2002;131:639-646.

Arkhipova, S.S., Raginov, L.S., Mukhitov, A.R., Chelyshey, Y.A. Satellite cells of sensory neurons after various types of sciatic nerve trauma in the rat. Neurosci Behav Physiol. 2010;40:609-614.

Atlasi, M.A., Mehdizadeh, M., Bahadori, M.H., Joghataei, M.T. Morphological identification of cell death in dorsal root ganglion neurons following peripheral nerve injury and repair in adult rat. Iranian Biomedical J. 2009;13:65-72.

Bałuk, P. Scanning electron microscopic studies of bullfrog sympathetic neurons exposed by enzymatic removal of connective tissue elements and satellite cells. J Neurocytol. 1986;15:85-95.

Basbaum, A.I., Bautista, D.M., Scherrer, G., Julius, D. Cellular and molecular mechanisms of pain. Cell. 2009;139:267-284.

Barros, L.F., Deitmer, J.W. Glucose and lactate supply to the synapse. Brain Research Rev. 2010;63:149-159.

Beccari, N. Neurologia comparata anatomo-funzionale dei vertebrati, compreso l'uomo. Sansoni Edizioni Scientifiche, Firenze, 1943.

Beggs, S., Liu, X.J., Kwan, C., Salter, M.W. Peripheral nerve injury and TRPV1-expressing primary afferent C-fibers cause opening of the blood-brain barrier. Molecular Pain. 2010;6:3-12.

Berrios, I., Castro, C., Kuffer, D.P. Visualization of six unique morphological subpopulations of adult frog dorsal root ganglion neurons at the light microscopic level. P R Health Sci J. 2008;27:55-59.

Berthold, C.H. Ultrastructural appearance of glycogen in the B-neurons of the lumbar spinal ganglia of the frog. J Ultrastructure Res. 1966;14:254-267.

Bouzier-sore, A.K., Serres, S., Canioni, P., Merle, M. Lactate involvement in neuron-glia metabolic interaction: (13)C-NMR spectroscopy contribution. Biochemie. 2003a;85:841-848.

Bouzier-sore, A.K., Voisin, P., Canioni, P., Magistretti, P.J., Pellerin, L. Lactate is a preferential oxidative energy substrate over glucose for neurons in culture. Journal Cerebral Blood Flow Metabolism. 2003b;23:1298-1306.

Bouzier-Sore, A.K., Voisin, P., Bouchaud, V., Bezancon, E., Franconi, J.M. Pellerin, L. Competition between glucose and lactate as oxidative energy substrates in both neurons and astrocytes: a comparative NMR study. European Journal Neurosci. 2006;24:687-694.

Bradman, M.J., Arora, D.K., Morris, R., Thippeswamy, T. How do the satellite glia cells of the dorsal root ganglia respond to stressed neurons? Nitric oxide saga from embryonic development to axonal injury in adulthood. Neuron Glia Biol. 2010;6:11-17.

Brumovsky, P., Watanabe, M., Hökfelt, T. Expression of the vesicular glutamate transporters-1 and -2 in adult mouse dorsal root ganglia and spinal cord and their regulation by nerve injury. Neurosc. 2007;147:469-490.

Brumovsky, P.R., Seroogy, K.B., Lundgren, K.H., Watanable, M., Hökfelt, T., Gebhart, G.F. Some lumbar sympathetic neurons develop a glutamatergic phenotype after

peripheral axotomy with a note on $VGLUT_2$-positive perineuronal baskets. Exp Neurol. 2011;230:258-272.

Butler, A.B, Hodos, W. Comparative Vertebrate Neuroanatomy: evolution and adaptation. 2 ed. Wiley-Liss, Inc, 1996.

Boutilier, R.G., Donohoe, P.H., Tattersall, G.J., West, T.G. Hypometabolic homeostasis in overwintering aquatic amphibians. J Exp Biol. 1997;200:387-400.

Chen, Y., Wang, A.J., Ma, Y.L. Effects of morphine on sensitivities of alpha-adrenoceptors in toad spinal ganglion neurons. Zhongguo Yao Li Xue Bao. 1993;14:417-420.

Chen, N.C., Srinivasan, R.C., Shauver, M.J. A systematic review of outcomes of fasciotomy, aponeurotomy, and collagenase treatments for Dupuytren's contracture. Hand (NY). 2011;6:250-255.

Cheng, J.K., Ji, R.R. Intracellular signaling in primary sensory neurons and persistent pain. Neurochem Res. 2008;33:1970-1978.

Chih, C.P., Lipton, P., Roberts, E.L. Do active cerebral neurons really use lactate rather than glucose? Trends Neurosc. 2001;24:573-578.

Choeiri, C., Staines, W., Messier, C. Immunohistochemical localization and quantification of glucose transporters in the mouse brain. Neurosci. 2002;111:19-34.

Coble, D.J., Taylor, D.K., Mook, D.M. Analgesic effects of meloxicam, morphine sulfate, flunixin meglumine, and xylazine hydrochloride in African-clawed frogs (Xenopus laevis). J Am Assoc Lab Anim Sci. 2011;50:355-360.

Cristino, L., Florenzano, F., Bentivoglio, M., Gugielmotti, V. Nitric oxide synthase expression and cell changes in dorsal root ganglia and spinal dorsal horn of

developing and adult *Rana esculenta* indicate a role of nitric oxide in limb metamorphosis. J Comp Neurol. 2004;472:423-436.

Crowe, M.J., Brown, T.J., Bresnahan, B.M.S. Distribution of NADPH-diaphorase reactivity in the spinal cord of metamorphosing and adult *Xenopus laevis*. Brain Res Dev Brain Res. 1995;86:155-166.

Cury, Y., Picolo, G., Gutierrez, V.P., Ferreira, S.H. Pain and analgesia: The dual effect of nitric oxide in the nociceptive system. Nitric Oxide. 2011;25:243-254.

Delree, P., Martin, D., Sadzot-Delvaux, C., Rogister, B., Leprince, P., Robe, P., Rigo, J.M., Lefebvre, P.P., Malgrange, B., Schoenen, J., Moonen, G. In vitro and in vivo modulation of 5-hydroxytryptamine-, thyrotropin-releasing hormone- and calcitonin-gene related peptide-like immunoreactivities in adult rat sensory neurons. Neurosc. 1992;51:401-410.

Devraj, K., Klinger, M.E., Myers, R.L., Mokashi, A., Hawkins, R.A., Simpson, I.A. GLUT-1 glucose transporters in the blood-brain barrier: differential phosphorylation. J Neurosci Res. 2011;89:1913-1925.

Dienel, G.A. Brain lactate metabolism: the discoveries and the controversies. J Cereb Blood Flow Metab. 2012;32:1107-1138.

Du, F., Zhang, Y., Zhu, X.H., Chen, W. Simultaneous measurement of glucose blood-brain transport constants and metabolic rate in rat brain using in-vivo 1H MRS. J Cereb Blood Flow Metab. 2012;32:1778-1787.

Dublin, P., Hanani, M. Satellite glial cells in sensory ganglia: Their possible contribution to inflammatory pain. Brain Behav Immun. 2007;21:592-598.

Dueli, R., Juschinsky, W. Brain glucose transporters: relationship to local energy demand. News Physiol Sci. 2001;16:71-76.

Feliciano, C., Sosa, I., Reyes, O., Berrios, I., Kuffler, D.P. Morphological characterization of six subpopulations of adult human DRG neurons at the light microscopic level. PR Health Sci J. 2007;26:7-11.

Gandhi, G.K., Cruz, N.F., Ball, K.K., Dienel, G.A. Astrocytes are poised for lactate trafficking and release from activated brain and for supply of glucose to neurons. J Neurochem. 2009;111:522-536.

Garry, E.M., Jones, E., Fleetwood-Walkers, S.M. Nociception in vertebrates: key participating in spinal mechanism of chronic pain in animals. Brain Res Rev. 2004;46:216-224.

Gleeson, T.T. Patterns of metabolic recovery from exercise in amphibians and reptiles. J Exp Biol. 1991;160:187-207.

Gómez, O., Ballester-lurbe, B., Mesoero, J.E., Terrado, J. Glucose transporters GLUT4 and GLUT8 are upregulated after facial nerve axotomy in adult mice. J Anat. 2011;219:525-530.

Guedes, R.P., Marchi, M.I., Viola, G.G., Xavier, L.L., Achaval, M., Partata, W.A. Somatostatin-,calcitonin gene-related peptide, and y-aminobutyric acid-like immunoreactivity in the frog lumbosacral spinal cord:distribution and effects of sciatic nerve transection. Comp Biochem Physiol Part A. 2204a;138:19-28.

Guedes, R.P., Marchi, M.I., Achaval, M., Partata, W.A. Complete sciatic nerve transection induces increase of neuropeptide y-like immunoreactivity in primary sensory neurons and spinal cord of frog. Comp Bioch Physiol Part A. 2004b;139:461-467.

Hamamoto, S., Simone, D.A. Characterization of cutaneous primary afferents fibres by acetic acid in a model of nociception in frogs. J Neuroph. 2003;90:566-577.

Hanani, M., Huang, T.Y., Cherkas, P.S., Ledda, M., Pannese, E. Glial cell plasticity in sensory ganglia induced by nerve damage. Neurosci. 2002;114:279-2283.

Hanani, M. Satellite glial cells in sensory ganglia: from form to function. Brain Res Brain Rev. 2005;48:457-476.

Hanani, M. Satellite glial cells: more than just `rings around the neuron`. Neuron Glia Biology. 2010a;6:1-2.

Hanani, M. Satellite glial cells in sympathetic and parasympathetic ganglia: in search of function. Brain Res Rev. 2010b;64:304-327.

Hansen, N., Uçeyler, N., Palm, F., Zelenka, M., Biko, L., Lesch, K.P., Gerlach, M., Sommer, C. Serotonin transporter deficiency protects mice from mechanical allodynia and heat hyperalgesia in vincristine neuropathy. Neurosci Lett. 2011;495:93-97.

Hart, A.M., Brannstrom, T., Wiberg, M., Terenghi, G. Primary sensory neurons and satellite cells after peripheral axotomy in the rat. 2002;142:308-318.

Hermes-Lima, M., Storey, K.B. Role of antioxidant defenses in the tolerance of severe dehydration by anurans. The case of the leopard frog *Rana pipiens*. Mol Cell Biochem. 1998;189:79-89.

Holz, C.G., Anderson, E.G. The actions of serotonin on frog primary afferent terminals and cell bodies. Comp Biomchem Physiol Part C. 1984;77:13-21.

Hope, B.T., Michael, G.J., Knigge, K.M., Vincent, S.R. Neuronal NADPH-diaphorase is a nitric oxide synthase. Proc Nat Acad Sci USA. 1991;88:2811-2814.

Hoppler, H., Hudlicka, O., Uhlmann, E. Relationship between mitochondria and oxygen consumption in isolated cat muscles. J Physiol. 1987;385:661-675.

Hu, P., McLachlan, E.M. Long-term changes in the distribution of galanin in dorsal root ganglia after sciatic or spinal nerve transection in rats. Neurosc. 2001;103:1059-1071.

Hu, P., McLachlan, E.M. Selective reactions of cutaneous and muscle afferent neurons to peripheral nerve transection in rats. J Neurosci. 2003;23:10559-10567.

Huang, Tian-Y., Cherkas, P.S., Rosenthal, D.W., Hanani, M. Dye coupling among satellite glial cells in mammalian dorsal root ganglia. Brain Res. 2005;1036:42-49.

Humbertson, A.Jr., Zimmermann, E., Leedy, M.A. chronological study of mitotic activity in satellite cell hyperplasia associated with chromatolytic neurons. Z Zellforsch Mikrosk Anat. 1969;100:507-515.

Hunt, C.C., Nelson, P.G. Structural and functional changes in the frog sympathetic ganglion following cutting of the presynaptic nerve fibres. J Physiol. 1965;177:1-20.

Juel, C., Halestrap, A.P. Lactate transport in skeketal muscle – role and regulation of the monocarboxylate transporter. J Physiol. 1999;517:633-642.

Kardong, K.V. Vertebrates: comparative anatomy, function, evolution. 2 ed. McGraw-Hill, New York, 1997.

Keilhoff, G., Fansa, H., Wolf, G. Nitric oxide synthase, an essential factor in peripheral nerve regeration. Cell Mol Biol. 2003;49:885-97.

Kiya, T., Kawamata, T., Namiki, A., Yamakage, M. Role of satellite cell-derived L-serine in the dorsal root ganglion in paclitaxel-induced painful peripheralneuropathy. Neurosc. 2011;174:190-199.

Kiss, A.C.I., Carvalho, J.E., Navas, C.A., Gomes, F.R. Seasonal metabolic changes in a year-round reproductively active subtropical tree-frog (*Hypsiboas prasinus*). Comp. Biochem. Physiol ;Part A. 2009;152:182-188.

Klusálová, I., Dubový, P. Experimental models of peripheral neurophatic pain based on traumatic nerve injuries – An anatomical perspective. Ann Anat. 2009;191:248-259.

Ko, J.H., Strafella, A.P. Dopaminergic neurotransmission in the human brain: new lessons from perturbation and imaging. Neuroscientist. 2012;18:149-168.

Koskela, P., Pasanen, S. Effect of thermal acclimation on seasonal liver and muscle glycogen content in the common frog, *Rana temporaria* L. Comp Biochem Physiol Part A. 1975;50:723-727.

Kreutzberg, G.W., Emmert, H. Glucose utilization of motor nuclei during regeneration: A [^{14}C] 2-Deoxyglucose Study. Exp Neurol. 1980;70:712-716.

Larrabee, M.G. Metabolic disposition of glucose carbon by sensory ganglia of 15-day-old chicken embryos, with new dynamic models of carbohydrate metabolism. J Neuroch. 1980;35:210-231.

Larrabee, M.G. [14]Glucose metabolism in sympathetic ganglia of chicken embryos and in primary cultures of neurons and of others cells from these ganglia. J Neuroch. 1982;38:215-232.

Larrabee, M.G. Ontogeny of glucose metabolism in sympathetic ganglia of chickens. Changes in the carbon fluxes to CO_2, lactate, and tissue constituents from 8 to 19 days of embryonic age. J Neuroch. 1985;45:1193-1200.

Larrabee, M.G. Ontogeny of glucose and lipd metabolism in dorsal root ganglia of chickens. Similarities and contrasts with sympathetic ganglia. J Neuroch. 1987;49:393-398.

Larrabee, M.G. Lactate metabolism and its effects on glucose metabolism in an excised neural tissue. J Neuroch. 1995;64:1734-1741.

Larrabee, M.G. Partitioning of CO_2 production between glucose and lactate in excised sympathetic ganglia, with implication for brain. J Neuroch. 1996;67:1726-1734.

Ledda, M., De Palo, S., Pannese, E. Ratios between number of neuroglial cells and number and volume of nerve cells in the spinal ganglia of two species of reptiles and three species of mammals. Tissue & Cell 2004;36:55-62.

Leech, R.W. Changes in satellite cell of rat dorsal root ganglia during central chromatolysis. Neurol. 1967;17:349-358.

Lesch, K.P., Waider, J. Serotonin in the modulation of neural plasticity and networks: implications for developmental disorders. Neuron. 2012;76:175-91.

Li, S., Liu, Q., Wang, Y., Gu, Y., Liu, D., Wang, C., Ding, G., Chen, J., Liu, J., Gu, X. Differential gene expression profiling and biological process analysis in proximal nerve segments after sciatic nerve transection. PLOS One. 2013;8:1-10.

Liu, F.Y., Sun, Y.N., Wang, F.T., Li, Q., Su, L., Zhao, Z.F., Meng, X.L., Zhao, H., Wu, X., Sun, Q., Xing, G.G., Wan, Y. Activation of satellite glial cells in lumbar dorsal root ganglia contributes to neuropathic pain after spinal nerve ligation. Brain Res. 2012;1427:65-77.

Lukácová, N., Cízková, D., Krizanová, O., Pavel, J., Marsala, M., Marsala, J. Peripheral axotomy affects nicotinamide adenine dinucleotide phosphate diaphorase and nitric oxide synthases in the spinal cord of the rabbit. J Neurosc Res. 2003;71:300-313.

Ma, W., Bisby, M.A. Partial sciatic nerve transection induced tyrosine hydroxidase immunoreactive axon sprouting around both injured and spared dorsal root ganglion neurons which project to the gracile nucleus in middle-aged rats. Neurosc Lett. 1999;275:117-120.

McDougal, D.B., Holowach, J., Howe, M.C., Jones, E.M., Thomas, C.A. The effects of anoxia upon energy sources and selected metabolic intermediates in the brains of fish, frog and turtle. J Neurochem.1968;15:577-588.

Machado, V.L.A., Wassermann, G.F., Marques, M. In vitro effect of insulin on the uptake of glucose and α-Aminoisobutyric acid in the thyroid gland of the turtle (*Chrysemys dorbigni*). General and Comparative Endocrinology 1991;82:8-13.

Mao, J., Mayer, D.J., Hayes, R.L., Price, D.D. Spatial patterns of increased spinal cord membrane-bound protein kinase C and their relation to increases in ^{14}C-2-deoxyglucose metabolic activity in rats with painful peripheral mononeuropathy. J Neurophysiol. 1993;70:470-481.

Matsumoto, M., Rosenbluth, J. Structure of the satellite cell sheath around the cell body, axon hillock, and initial segment of frog dorsal root ganglion cells. The Anatomical Record. 1986;215:182-191.

Matsumoto, E., Rosenbluth, J. Freeze-fracture study of the perineurium around frog dorsal root ganglia. Journal Neur. 1988;17:425-432.

Maruhashi, J., Mizuguchi, K., Tasaki, I. Action currents in single afferents nerve fibres elicited by stimulation of the skin of the toad and the cat. J Physiol. 1952;117:129-151.

Mizell, S. Seasonal changes in energy reserves in the common frog *Rana pipiens.* J. Cell Comp Physiol. 1965;66:251-258.

Moran, L.B. Graeber, M.B. The facial nerve axotomy model. Brain Res Rev. 2004;44:154-178.

Moreno-Flores, M.T., Olazábal, U.E., Kreutzberg, G.W. Axotomy increases the expression of glucose-regulated protein 78 kDa in rat facial nucleus. Exp Neurol. 1997;146:10-16.

Nascimento, R.S., Santiago, M.F., Marques, S.A., Allodi, S., Martinez, A.M.B. Diversity among satellite glial cells in dorsal root ganglia of the rat. Braz J Med Biol Res. 2008;41:1011-1017.

Nickel, F.T., Seifert, F., Lanz, S., Maihöfner, C. Mechanisms of neuropathic pain. European Neuropsycopharmacology 2012;22:81-91.

Ohara, P.T., Vit, J.P., Bhargava, A., Romero, M., Sundberg, C., Charles, A.C., Jasmin, L. Gliopathic pain: when satellite glial cells go bad. Neurosci. 2009;15:450-463.

Ohtori, S. Takahashi, K., Moriya, H., Myers, R.R. TNF-alfa and TNF-alfa receptor type 1 upregulation in glia and neurons after peripheral nerve injury: studies in murine DRG and spinal cord. Spine 2004;29:1082-1088.

Ohkita, M., Saito, S., Imagawa, T., Takahashi, K., Tominaga, M., Ohta, T. Molecular cloning and functional characterization of *Xenopus tropicalis* frog transient receptor potential vanilloid 1 reveal its functional evolution for heat, acid, and capsaicin sensitivities in terrestrial vertebrates. J Biol Chem. 2012;287:2388-2397.

Oliveira, A.L. Apoptosis of sensory neurons and satellite cells after sciatic nerve transection in C57BL/6J mice. Braz J Med Biol Res. 2001;34:375-380.

Pasanen, S., Koskela, P. Seasonal and age variation in the metabolism of the common frog, *Rana temporaria* L. in northern finland. Comp Biochem Physiol Part A. 1974;47:635-654.

Pannese, E. Number and structure of perisomatic satellite cells of spinal ganglia under normal conditions or during axon regeneration and neuronal hypertrophy. Z. Zellforsch. 1964;63:568-592.

Pannese, E. The satellite cells of the sensory ganglia. Adv Anat Embryol Cell Biol. 1981;65:1-111.

Pannese, E., Ledda, M., Cherkas, P.S., Huang, T.Y., Hanani, M. Satellite cell reaction to axon injury of sensory ganglion neurons: Increase in number of gap junctions and formation of bridges connecting previously separate perineuronal sheaths. Anat Embryol. 2003;206:337-347.

Pannese, E. The structure of the perineuronal sheath of satellite glial cells (SGCs) in sensory ganglia. Neuron Glia Biology. 2010;6:3-10.

Partata, W.A., Cerveira, J.F., Xavier, L.L., Viola, G.G., Achaval, M. Sciatic nerve transection decrease P immunoreactivity in the lumbosacral spinal cord of the (*Rana catesbeiana*). Comp Biochem Physiol Part B. 2002;131:807-814.

Pellerin, L., Magistretti, P.J. Sweet sixteen for ANLS. Journal of Cerebral Blood Flow & Metabolism 2011;32:1152-1166.

Pfeiffer, B., Buse, E., Meyermann, R., Hamprecht, B. Immunocytochemical localization of glycogen phosphorylase in primary sensory ganglia of the peripheral nervous system of the rat. Histochem. 1995;103:69-74.

Philippi, M., Vyklický, L., Kuffler, D.P., Orkan, R.K. Serotonin- and proton-induced and modified ionic currents in frog sensory neurons. J Neurosci Res. 1995;40:387-395.

Price, D.D., Mao, J., HAVES, R.L. Regional changes in spinal cord glucose metabolism in a rat model of painful neuropathy. Brain Research. 1991;564:314-318.

Rocha, P.L., Branco, L.G. As mudanças sazonais nas respostas cardiovasculares, respiratórias e metabólicas à temperatura e hipóxia na rã-touro *Rana catesbeiana*. J Exp Biol. 1998;201:761-768.

Saito, S., Nakatsuka, K., Takahashi, K., Fukuta, N., Imagawa, T., Ohta, T., Tominaga, M. Analysis of transient receptor potential ankyrin 1 (TRPA1) in frogs and lizards illuminates both nociceptive heat and chemical sensitivities and coexpression with

TRP vanilloid 1 (TRPV1) in ancestral vertebrates. J Biol Chem. 2012;287:30743-30754.

Singer, P., Mehler, S. 2-Deoxy [^{14}C]glucose uptake in the rat hypoglossal nucleus after nerve transection. Exp Neurol. 1980;69:617-626.

Scapin, S., Giuseppe, G.D. Glycogen phosphorylase activity in the liver of the frog *Rana esculenta*. Comp Biochem Physiol Part B. 1993;105:401-407.

Scapin, S., Giuseppe, G.D. Seasonal variations of glycogen synthase and phosphorylase activities in the liver of the frog *Rana esculenta*. Comp Biochem Physiol Part B. 1994;107:189-195.

Schaible, H.G., Richter, F. Pathophysiology of pain. Langenbecks Arch Surg. 2004;389:237-43.

Shinder, V., Govrin-Lippmann, R., Cohen, S., Belenky, M., Ilin, O., Fried, K., Wilkinson, H.A., Devor, M. Structural basis of sympathetic-sensory coupling in rat and human dorsal root ganglia following peripheral nerve injury. J. Neurocytol. 1999;28:743-761.

Schurr, A., Payne, R.S., Miller, J.J. Study of Cerebral Energy Metabolism Using the Rat Hippocampal Slice Preparation. Methods. 1999;18:117-126.

Schurr, A., Payne, R.S. Lactate, not pyruvate, is neuronal aerobic glycolysis end product: an in vitro electrophysiological study. Neurosc. 2007;147:613-619.

Schurr, A., Gozal, E. Aerobic production and utilization of lactate satisfy increased energy demand and support neuronal activation in hippocampal slices and provide neuroprotection against oxidative stress. Frontiers in Pharmacology 2012;2:1-15.

Siemionow, K., Weinstein, J.N., McLain, R.F. Support and satellite cells within the rabbit dorsal root ganglia. Spine 2006;31:1882-1887.

Smith, C.L. Environmental temperature and the glycogen content of the frog`s liver (*Rana temporaria*). Nature 1952;170:74-75.

Soares, H.D., Chen, S.C., Morgan, J.I. Differential and prolonged expression of Fos-lacZ and jun-lacZ in neurons, glia and muscle following sciatic nerve damage. Exp Neurol. 2001;167:1-14.

Stark, B., Carlstedt, T., Cullheim, S., Marten, R. Developmental and lesion-induced changes in the distribution of the glucose transporter Glut-1 in the central and peripheral nervous system. Exp Brain Res. 2000;131:74-84.

Stebbins, R.C., Cohen, N.M. A natural history of amphibians. 1997. Princeton, USA, 316p.

Stevens, C.W. Opioid research in amphibians: an alternative pain model yielding insights on the evolution of opioid receptors. Brain Res Rev. 2004;46:204-215.

Stevens, C.W., Brasel, C.M., Mohan, S. Cloning and bioinformatics of amphibian mu, delta, kappa, and nociceptin opioid receptors expressed in brain tissue: evidence for opioid receptor divergence in mammals. Neurosci Lett. 2007;419:189-194.

Stevens, C.W., Martin, K.K., Stahlheber, B.W. Nociceptin produces antinociception after spinal administration in amphibians. Pharmacol Biochem Behav. 2009;91:436-440.

Storey, K.B., Storey, J.M. Biochemical adaptation for freezing tolerance in the wood frog *Rana sylvatica*. J Comp Physiol. 1984;155:29-36.

Tabernero, A., Medina, J.M., Giaume, C. Glucose metabolism and proliferation in glia: role of astrocytic gap junctions. J Neurochem. 2006;99:1049-1061.

Tolleson, C., Claassen, D. The function of tyrosine hydroxylase in the normal and Parkinsonian brain. CNS Neurol Disord Drug Targets. 2012;11:381-386.

Voituron, Y., Paaschburg, L., Holmstrup, M., Barré,H., Ramlos, H. Survival and metabolism of *Rana arvalis* during freezing. J Comp Physiol Part B. 2009;179:223-230.

Von Hehn, C.A., Baron, R., Woolf, C.J. Deconstructing the neuropathic pain phenotype to reveal neural mechanisms. Neuron. 2012;73:638-52.

Yamamoto, T. The fine strucutre of the sympathetic ganglion of the frog. Anat Rec. 1962;142:293.

Yamamoto, T. Some observations on the fine structure of the sympathetic ganglion of bullfrog. J Cell Biol. 1963;16:159-170.

Yun, J., Jakobsen, J. Different apoptotic reactions of dorsal root ganglia A- and B-cells after sciatic nerve axotomy: effect of p75 neurotrophin receptor. Chinese Medical Journal 2010;123:2695-2700.

Wall, P.D., Devor, M., Inbal, R., Scadding, J.W., Schonfeld, D., Seltzer, Z., Tomkiewicz, M.M. Autotomy following peripheral nerve lesions:experimental anesthesia dolorosa. Pain 1979;7:103-113.

Warren, D.E., Jackson, D.C. The role of mineralized tissue in the buffering of lactic acid during anoxia and exercise in the leopard frog *Rana pipiens*. Journal Experimental Biology 2005;208:1117-1124.

Wilson, M.C., Jackson, V.N., Heddle, C., Price, N.T., Pilegaard, H., Juel, C., Bonen, A., Montgomery, I., hutter, O.F., Halestrap, A.P. Lactic acid efflux from white skeletal muscle is catalyzed by the monocarboxylate transporter isoform MCT3. J Biol Chem. 1998;273:15920-15926.

Xia, C.M., Colomb, D.G.Jr., Akbarali H.I., Qiao, L.I. Prolonged sympathtic innervation of sensory neurons in rat thoracolumbar dorsal root ganglia during chronic colitis. Neurogastroenterol Motil. 2011;23:801-339.